G.S. Mityurich
J. Motylewski, J. Ranachowski

MODERN PHOTOACOUSTIC SPECTROSCOPY PROBLEMS THEORY AND EXPERIMENT (A REVIEW)

41/1993

WARSZAWA 1993

ISSN 0208-5658

Praca wpłynęła do Redakcji dnia 10 grudnia 1993 r.

Na prawach rękopisu

Instytut Podstawowych Problemów Techniki PAN
Nakład 100 egz. Ark.wyd. 8,20 Ark.druk.10,9
Oddano do drukarni w grudniu 1993 r.

Wydawnictwo Spółdzielcze sp. z o.o.
Warszawa, ul.Jasna 1

G. S. Mityurich

Gomel State University, Dept. of Physics
Gomel, Rep. of Byelorus

J. Motylewski, J. Ranachowski

Polish Academy of Sciences
Institute of Fundamental Technological Research
Warsaw, Poland

MODERN PHOTOACOUSTIC SPECTROSCOPY PROBLEMS - THEORY AND EXPERIMENT (A REVIEW)

ABSTRACT

The review presents investigation of photoacoustic transformation in condensed media , including naturally gyrotropic and magnetoactive substances. The analysis is performed on numerous theoretical models of as well linear as nonlinear sound generation mechanism . Sound wave excitation is assumed to be amplitude- or polarisation-modulated light beam. The potentiality of linear and circular dichroism parameters determination by means of photoacoustic and photodeflectional spectroscopy is evaluated. The experimental stands for subsequent gyrotropic media investigation in IFTR are described.

Supported by Polish Committee for Scientific Research (KBN) research project No. 7 1018 91 01.

CONTENTS

4.2. Method of polarized modulation in photoacoustic spectroscopy of gyrotropic crystals.

4.3. Photoacoustic transformation in crystals of rombic singony.

5. PIEZOPHOTOACOUSTIC SPECTROSCOPY OF GYROTROPIC CRYSTALS.

5.1. Piezophotoacoustic crystal spectroscopy of higher and middle singonies.

5.2. Formation of photoacoustic response in nonlinear piezoelectric crystals.

5.3. Photoacoustic transformation in layered piezoelectric structures.

6. PHOTOACOUSTIC SPECTROSCOPY OF CHOLESTERIC LIQUID CRYSTALS.

6.1. Photoacoustic interaction in cholesteric liquid crystals. Eigenmodes circular polarization rates.

6.2. Photoacoustic response in the CLC samples. Bragg-reflection region.

6.3. Influence of temperature on the CLC structure in the PA transformation process.

7. PHOTOACOUSTIC SPECTROSCOPY IN NONLINEAR GYROTROPIC CRYSTALS.

7.1. Photoacoustic transformation in nonlinear gyrotropic crystals of selenite type. Approximation of given field.

7.2. Thermooptical sound excitation at generation of higher harmonics in piezocrystals.

7.3. Photoacoustic spectroscopy in nonlinear crystals with centrosymmetrical paramagnetical phase.

THEORETICAL ASPECTS OF PHOTOACOUSTIC SPECTROSCOPY OF GYROTROPIC MEDIA

INTRODUCTION

Method of photoacoustic spectroscopy has been broadly applicable lately for the investigation of interaction between electromagnetic radiation and substance. The use of laser sources in photoacoustics permitted to make a transition to qualitatively higher level of measurement and to increase substantially sensitivity of the method. High efficiency of the photoacoustic method has been demonstrated at investigation of media in different aggregative states in wide spectral range from ultraviolet to infrared, exhibiting absorption both strong $\sim 10^{5} sm^{-1}$ and very weak $\sim 10^{-10} sm^{-1}$ [1,2].

An advanced method of PA spectroscopy along with conventional methods is applied at investigation of dissipative, thermal and nonlinear characteristics of naturally gyrotropic and magnetoactive media.

As is known [3,4], absorption of electromagnetic waves by gyrotropic media has a characteristic peculiarity connected with the availability of circular dichroism, phenomenon of different absorption of electromagnetic waves with clockwise and counterclockwise polarization. Substantional dependence of circular dichroism on the slightest structural changes of media has become the basis for creation of powerful method for investigation of biological and chemical chyral structures enabling to get a valuable information about delicate details of inner structure of substance, symmetry of its electronic states etc [5,6].

The development of modern photoacoustics occurs on the boun-

dary of the several fields of physics - optics, acoustics, thermal physics and presumes correspondingly the solution of three problems: optical, thermal and acoustic. Until recently primary attention has been drawn to solution of the problems on laser thermooptical sound generation in condensed matters for determining energetic characteristics of acoustic fields, direction diagrams of optoacoustic sources and development of methods for parameter control, what has been represented in recent papers [7,8]. It is necessary for the investigation of photoacoustic transformation in gyrotropic media to have particular reference to optical and dissipative effects which noticeably influence the mechanism of photoacoustic signal generation (see e.g.[9]).

Just from this point of view problems of photoacoustic transformation in media with different types of gyrotropy will be discussed below. Before particular representation of theoretical aspects of photoacoustic spectroscopy let us discuss some electrodynamic problems of absorbing gyrotropic media.

1. FUNDAMENTALS OF PHENOMENOLOGICAL OPTICS OF ABSORBING GYROTROPIC MEDIA.

In phenomenological optics phenomenon of gyrotropy is specified by introduction into linear material equations, connecting electric $\underline{D}$ and magnetic $\underline{B}$ inductions with intensities of electric field $\underline{E}$ and magnetic field $\underline{H}$, of the terms which are first order spatial derivatives of $\underline{E}$ and $\underline{H}$ [3,10]

$$\begin{aligned} D_i &= \varepsilon_{ij} E_j + \alpha_{ijk} \nabla_j E_k, \\ B_i &= \mu_{ij} H_j + \beta_{ijk} \nabla_j H_k, \end{aligned} \qquad (1.1)$$

where $\varepsilon_{i,j}$ and $\mu_{i,j}$ are tensors of dielectric and magnetic permeability, $\alpha_{i,j,k}$, $\beta_{i,j,k}$ are tensors of the third rank responsible for gyrotropy.

From the law of energy conservation the tensors of material constants of gyrotropic medium are restricted by the condition [3,11]

$$\varepsilon = \tilde{\varepsilon}, \quad \mu = \tilde{\mu}, \quad \alpha\tilde{\mu} = \varepsilon\tilde{\beta},$$

(sign ~ stands for transpose operation), with the regard to which and Maxwell equations ratios (1.1) will take the form

$$\begin{aligned} \underline{D} &= \varepsilon \underline{E} - \frac{\alpha}{c} \frac{d\underline{B}}{dt} \\ \underline{B} &= \mu \underline{H} + \frac{\tilde{\alpha}}{c} \frac{d\underline{E}}{dt} \end{aligned} \qquad (1.2)$$

The advantage of (1.2) over material equations (1.1) is in introduction of one tensor α instead of two, providing for gyrotropy.

It is necessary for explanation of characteristics of absorbing gyrotropic medium in (1.2) to place ε, μ, α tensors in complex.

From three classes of limitations [3,10] put for tensors of material constants of medium, mostly general ones follow from the symmetry principle of Onzaher-Kazimir kinetic coefficients [3,10], which is also applicable for absorbing crystals of arbitrary symmetry. The principle in question gives following limitations for absorbing gyrotropic media

$$\varepsilon=\tilde{\varepsilon},\ \mu=\tilde{\mu},\ \gamma=-\tilde{\gamma},\ \gamma=\frac{\omega}{c}\alpha,$$

with the regard to those, material equations for fourier-component will take the form

$$\underline{D} = \varepsilon\underline{E} + i\gamma\underline{H},$$

$$\underline{B} = \mu\underline{H} - i\tilde{\gamma}\underline{E}, \qquad (1.3)$$

where $\gamma=\gamma'+i\gamma''$, γ' describes specific rotation of a polarization plane of light got through gyrotropic medium, and imaginary part of γ, $Im(\gamma)=\gamma''$ parameter is responsible for circular dichroism.

If $\mu=1$ is put in (1.3), what is valid [10] for optical range of wavelengths, and besides antisymmetric part of ε tensor is extracted into separate component we will have [12]

$$\underline{D} = \varepsilon_0\underline{E} + ig_m^x\underline{E} + i\gamma\underline{H},$$

$$\underline{B} = \underline{E} - i\tilde{\gamma}\underline{E} \qquad (1.4)$$

Here g_m^x is antisymmetric complex tensor of the second rank and it is dual to magnetic gyration vector [3]. The second component in the right-hand side of an equation for electric induction describes magnetic gyrotropy connected with the presence of external magnetic field. Real part of g_m^x tensor causes the rotation of polarization plane, which is induced by magnetic field, and imaginary part $Im(g_m^x)$ is responsible for magnetic circular dichroism.

Neglecting in (1.4) the parameter of natural optical activity ($\gamma=0$), we come to coupling equations

$$\underline{D} = \varepsilon_0 \underline{E} + i g_m^{\times} \underline{E}, \qquad \underline{B} = \underline{H}, \tag{1.5}$$

characterizing magnetoactive media. In some cases one can better use material equations in equivalent form [3]

$$\underline{E} = (\frac{1}{\varepsilon} + i \underline{G}^{\times}) \underline{D}, \qquad \underline{H} = \underline{B}, \tag{1.6}$$

where $\underline{G}^{\times}$ is a tensor connected with $g_m^{\times}$ by ratio $\underline{G}^{\times} = -\varepsilon_0^{-1} g_m^{\times}$.

Further the discussion concerns energetic ratios in gyrotropic media. From Maxwell equations one can get ratio

$$\underline{E} \frac{d\underline{D}}{dt} + \underline{H} \frac{d\underline{B}}{dt} = -c\nabla[\underline{E}\ \underline{H}],$$

expressing law of conservation of energy in the form of continuity equation

$$div \underline{S} = \frac{dU}{dt},$$

where $\underline{S} = \frac{c}{4\pi} [\underline{E}\ \underline{H}]$ is a density vector of electromagnetic energy and

$$\frac{dU}{dt} = \frac{1}{4\pi} \left(\underline{E} \frac{d\underline{D}}{dt} + \underline{H} \frac{d\underline{B}}{dt} \right) \tag{1.7}$$

is the sum for energy change of electromagnetic field and extracted heat referred to the unit of time [13]. As was noted in [10,13] division (1.7) in separate components responsible for change of field energy and dissipation is not possible as it leads to appearance in (1.7) of terms with different nature, which can't be interpreted unambiguously from the physical point of view. In this connection first we will discuss the case of nonabsorbing medium in which quasi-monochromatic radiation propa-

gates. Keeping account in (1.3) of frequency dependence of ε,μ,γ tensors and expression for quasi-monochromatic waves [10]

$$\underline{E} = \underline{E}_0(t)exp(-i\omega t),\ \underline{H} = \underline{H}_0(t)exp(-i\omega t),$$

where $\underline{E}_0(t)$ and $\underline{H}_0(t)$ are more slowly oscillated time functions in comparison with exponential factor; ratio (1.7) averaged over time can be presented in the form [4]

$$\overline{\frac{dU}{dt}} = \frac{1}{4\pi}\overline{\left[Re\underline{E}\ Re\dot{\underline{D}} + Re\underline{H}\ Re\dot{\underline{B}} \right]} = \frac{1}{16\pi}\left[\underline{E}\frac{d\underline{D}^*}{dt} + \underline{H}\frac{d\underline{B}^*}{dt} + к.с. \right]. \tag{1.8}$$

For absorbing media obtained expression (1.8) presents by itself velocity of energy dissipation $Q=\frac{dU}{dt}$ in units of substance volume. Using material equations (1.3) convert (1.8) into [4]

$$Q = \frac{\omega}{8\pi}\left[\underline{E}^*\varepsilon''\underline{E} + \underline{H}^*\mu''\underline{H} + i(\underline{E}^*\gamma''\underline{E} - \underline{E}\ \gamma''\underline{H}^*) \right]. \tag{1.9}$$

Regarding medium to be nonmagnetic and isotropic we will find velocity for energy dissipation of circular polarized eigenwaves

$$Q_{\pm} = \frac{\omega}{8\pi}\left[\varepsilon''|\underline{E}_{\pm}|^2 + i\gamma''(\underline{E}^*_{\pm}\underline{H}_{\pm} - к.с.) \right], \tag{1.10}$$

which is completely determined by imaginary part ε and by γ'' parameter of circular dichroism. For magnetoactive media $Q_{\pm}$ is determined by the expression

$$Q_{\pm} = \frac{\omega}{8\pi}\cdot\left[\frac{\varepsilon_0''}{\varepsilon_0'^2 + \varepsilon_0''^2}|\underline{D}_{\pm}|^2 - i\underline{G}''[\underline{D}_{\pm}\underline{D}^*_{\pm}] \right], \tag{1.11}$$

obtained from (1.8),(1.6). In media with Faraday effect vectors $\underline{D}$ and $\underline{H}$ are connected [3]

$$\underline{D}_{\pm} = \pm i n_{\pm}\underline{H}_{\pm}, \tag{1.12}$$

where $\underline{n}_{\pm} = n'_{\pm} + in''_{\pm} = (\varepsilon_o^{-1} \pm G_z)^{-1/2}$ are complex indices of refraction of isonormal waves. Taking into account (1.12) for $Q_{\pm}$ one can put down

$$Q_{\pm} = \frac{\omega|n_{\pm}|^2}{8\pi} \left(\frac{\varepsilon''_o}{\varepsilon'^2_o + \varepsilon''^2_o} |H_{\pm}|^2 - i\underline{G}''[\underline{H}_{\pm}\underline{H}^*_{\pm}] \right), \qquad (1.13)$$

As it follows from (1.10),(1.11).(1.13) definition for explicit form $Q_{\pm}$ of naturally gyrotropic and magnetoactive media demands finding expressions for intensities of electric field $\underline{E}_{\pm}$ and magnetic field $\underline{H}_{\pm}$ from the solution of corresponding boundary electrodynamic tasks.

Let us note that for anisotropic gyrotropic crystals at evaluation of energy dissipation one must proceed from the general expression (1.9) and account of tensor character of values ε and γ. In the case, if electromagnetic wave is normally incident on the surface of a plane-parallel crystal plate cut from uniaxial absorbing gyrotropic crystal in parallel with optical axis ($\underline{n} \perp \underline{c}$), velocity of energy dissipation $Q_{o,e}$ for ordinary and extraordinary waves may be presented in the form [14]

$$Q_{o,e} = \frac{\omega|\underline{E}|^2\tau_{o,e}}{8\pi(1+\tau^2)R} [\underline{o}\,\underline{n}]\varepsilon''[\underline{o}\,\underline{n}] exp\left(\frac{2\omega}{o} n''_{o,e} d\right) \qquad (1.14)$$

Here $R=(1+k'^2-k''^2)^2+4k'^2k''^2$, $\underline{k}=\underline{r}n_o=\underline{r}n_e$, $\underline{r}=\frac{\underline{n}\,\underline{g}}{(\varepsilon_e-\varepsilon_o)}$, $\underline{g}=(Sp\gamma-\tilde{\gamma})\underline{n}$ is a complex vector of gyration, $Sp\gamma$ is a γ tensor track, τ is elliptiocity of an incident light wave, $\tau_o=1-2\tau k''+\tau^2|k|^2$, $\tau_e=\tau-2\tau k''+|k|^2$, $n_{o,e}=n'_{o,e}+in''_{o,e}$ are refractive indices of isonormal waves, not depending on gyration parameters accurate up to terms of the first order to γ inclusively.

Basing on the general expression (1.9) and the corresponding

solution of boundary tasks it will not be difficult to calculate velocities of energy dissipation and for media with more strong combination of gyrotropy and anisotropy effects, e.g., for the crystals of lower singonies as well as for the crystals with cholesteric structure of anisotropy. The value of energy dissipation, as is known, is a density of thermal source power of thermal conductivity equation, the solution of which allows to get distribution of thermal fields in the specimen under investigation and later to determine characteristics of PA response. That is why one of the main problems in photoacoustic spectroscopy consists in finding precise solutions of nonuniform differential equation of the second order in special derivatives that is not always possible because of the complexity of expressions for thermal sources. However, the approach to solution of photoacoustic transformation tasks in view of the solution of electrodynamics boundary tasks and further calculation of the velocity of energy dissipation change, from our point of view, is more preferable to conventionally accepted one in photoacoustics [1], as it allows when necessary to account of boundary and diffraction effects, multibeam interference in the layer and etc. In essence we make an attempt to look at problems in photoacoustics by eyes of optician and to draw additional information to that already obtained from acoustical point of view [7,8].

Subsequent parts review a theoretical description of photoacoustic transformation in condensed matters exhibiting different types of gyrotropy and anisotropy as well as their combination.

2. PHOTOACOUSTIC SPECTROSCOPY OF NATURALLY GYROTROPIC MEDIA.

2.1. Brief review of experimental methods of photoacoustic spectroscopy of gyrotropic media.

In the year 1978 in France A.Boccara, D.Badoz, D.Fourier started experimental investigation of gyrotropic media by method of photoacoustic spectroscopy. Conventional methods of optical spectroscopy for determining optical parameters seemed to have limited application for strongly absorbing crystals as well as for samples with imperfect surface. Optical methods are not convenient for investigation of strongly dissipative media, powders, biological and chyral structures, chemical compounds and living tissues. Optical spectroscopy has essential limitations at analysis of tracking numbers of atoms and molecules in gas and condensed matter with samples of small volume and low concentrations.

Method of photoacoustic and thermoacoustic spectroscopy based on the phenomenon of generation of thermoacoustic fields in media absorbing modulated electromagnetic radiation has a number of peculiarities [1], which compare favourably it with the methods of optical and acoustic spectroscopy. Thermooptical excitation of elastic and thermal oscillations affected by modulated radiation includes a number of physical processes, optical pumping of medium, nonradiative relaxation of particles from the excited levels, nonstationary thermal warming of the sample accompanied by radiation of thermoelastic waves are the principle ones. Specificity of energy transformation of electromagnetic wave makes this method of photoacoustic spectroscopy most effective for investigation of media with nonradiative canal of relaxation of absorbed light energy considered to be principal. Ta-

king into account high sensitivity and high speed of measurement, possibility to carry out investigations in wide frequency range, it may be argued that method of laser photoacoustical spectroscopy turned into one of the powerful up-to-date noncontact methods for analysis of the state and characteristics of condensed matter. Wide application of the method of PA spectroscopy at investigation of absorbing gyrotropic media with strips of linear and circular dichroism, in general case of anisotropic crystals with ones of elliptical dichroism corroborates this [14-23].

In above mentioned paper [15] two-beam photoacoustic set-up with registration of resultant signal by gas-microphone method has been developed. Linearly polarized light from continuous dye laser consistently was transforming into clockwise and counterclockwise polarized radiation with the help of electrooptical modulator. In its turn circular polarized wave was transformed into orthogonal linear polarized modes by means of achromatic quarter-wavelength plate. Besides polarized modulation application of polarizer permitted to get light beam modulation by intensity. Thus, measurements of normalized coefficient of absorption for spectra of linear and circular dichroism can be conducted.

Experiments were conducted with strongly absorbing samples of $NdMoO_4$ monocrystal 2mm thick with the power of laser radiation in front of PA cell being ~100 mW. Spectra of axial absorption and magnetic circular dichroism (MCD) have been obtained. MCD spectrum taken at room temperature can be accounted for Zeeman splitting for principal and excited states.

As follows from Rosenzweig-Gersho theory phase of PA signal

has to be linear function of thermal diffusion length μ_s and optical absorption length μ_β ratio $\Phi \sim f\left(\frac{\mu_s}{\mu_\beta}\right)$ for small values $R=\frac{\mu_s}{\mu_\beta}$, as above $R=0,5$ level saturation of signal occurs. In frequency range of $300\text{-}3\cdot10^3$Hz it was shown that $R\sim0,4$ at 3kHz for most intensive bandwidth of absorption spectrum. For indicated value phase and amplitude of PA signal according to [15] remained proportional to optical absorption with approximately 10 percent nonlinearity error.

In the next work made by a group of french physicists [16] it was stated that measurement of absorption coefficient and parameters of linear and circular dichroism with application of spectroscopy of photothermal deflection (mirage-effect) on the basis of Fourier transformation is 3 orders more sensitive than conventional PA spectroscopy gives. In this case it was used not laser but broad band noncoherent continuous source - 250W quartz halogen lamp. Application of Fourier spectroscopy permitted, as was noted in [16] to get great capacity, high resolution, accurate calibration of spectral wave numbers and possibility of multiplex processing of measurement data.

In [16] absorption spectrum and spectrum of linear dichroism of $CAWO_4/Nd^{+3}$ (1%) monocrystal were obtained, and spectrum of circular dichroism of $NiSO_4\cdot6H_2O$ crystal in the near infrared range was evaluated. It was noted that method of photothermodeflectional fourier-spectroscopy is very useful at investigation of volume and especially surface absorption and it surpasses method of photoacoustic detection in sensitivity.

The research of photoinduced dichroism in *DODCI* and *DQOCI* dye-stuffs in methanol solution has been conducted in [17] by

method of impulse spectroscopy of photothermal deflection. Experimental diagram is shown in Fig.1.

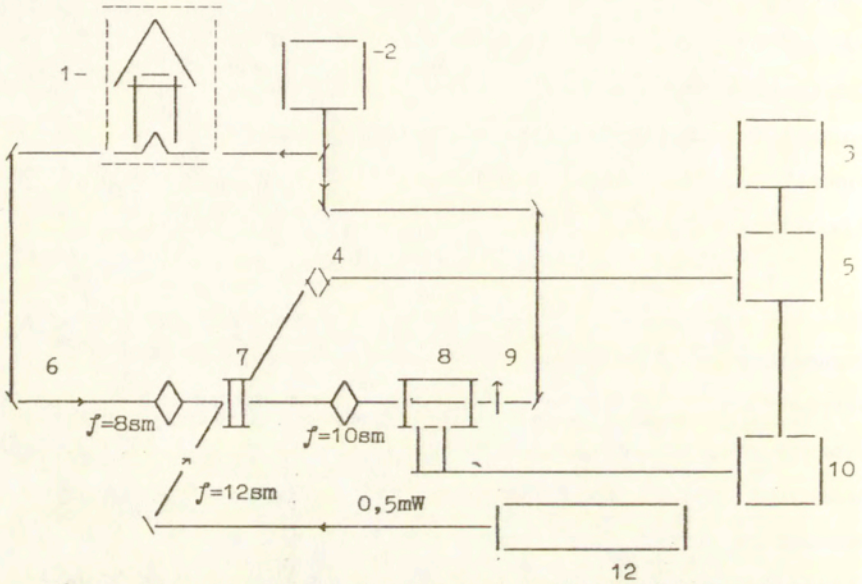

Fig.1. Diagram of experimental set-up for photothermodeflection spectroscopy [17].

1. Optical delay line.
2. Dye laser operating in mode synchronization.
3. Register.
4. Positional detector.
5. Phase detector.
6. Pumping radiation - 60mW.
7. Sample.
8. Probing beam - 8mW.
9. Polarizer.
10. Impulse generator.
11. Pokkels cell.
12. *He-Ne* laser.

Excitation of photothermal signal occurs by picosecond impulses being approximately 5ps long with power of 1,5nJ at repetition frequency of 228mHz, what is equivalent to 4,2ps interval between impulses. Average power was 300mW. Propagating in two opposite directions light-striking and probing beams met in the specimen, moreover their average powers were near 10 mW. Photothermal deflection was observed by *He-Ne* laser with the power of 0,5mW, which was measured by silicon positioning detector (*Silicon Detector Corporation SD-380-23-21-051*) and the signal obtained was proportional to the value of induced dichroism.

As is shown in the work it follows from the signal-to-noise ratio that minimum detectable angle of deflection is estimated $\alpha_{min} \sim 3{,}3 \cdot 10^{-8}$ rad for the following typical values: $\frac{dn}{dT} = 4{,}1 \cdot 10^{-4}$, $\rho c = 2 \cdot 10^{6} J \cdot m^{-3}$, $P = 10^{-2} W$, $\omega = 10 Hz$.

Minimum angle of deflection in conventional photodeflection spectroscopy is of the order of 10^{-9}rad that in sensitivity by some orders of magnitude greater than the result obtained in [17]. The authors account this difference for turbulent convectional flow in the sample, connected with the absorption of a light-striking beam, inducing dichroism.

The next step in the development of experimental methods of PA spectroscopy of gyrotropic media was made by american investigators [18,19] who developed supersensitive cross-light spectropolarimeter of circular dichroism (Fig.2) on thermal lens.

Argon laser with operating wavelength of 514,5nm was used in [18] as a source of excitation of thermooptical signal. Laser beam transmitting Glan-Thompson prism (3) was transformed into linearly polarized one and was splitted by the splitter (5) into

2 linear orthogonal polarized beams of equal intensity modulated by harmonic law. Fresnel's rhomb (3) was used for the transformation of these beams into left and right circular polarized radiation. Thermal energy generated by modulated beams with left and right circular polarization was registered at absorbing the probing beam of *He-Ne* laser (2), intensity change of which was fixed by photodiode *PD*-2, and intensity of circular polarized modes was measured by photodiode *PD*-1 placed behind the sample.

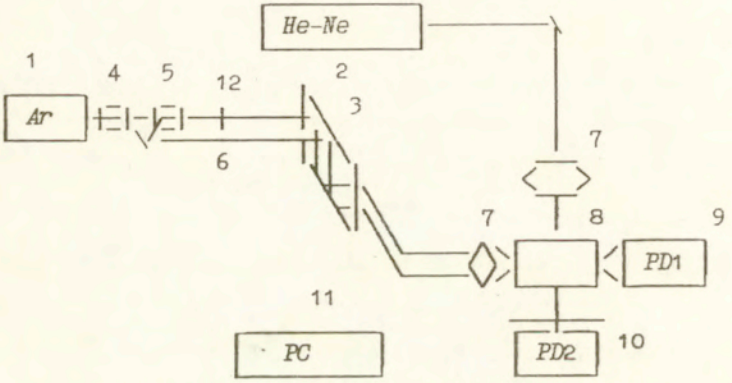

Fig.2. Diagram of spectropolarimeter of circular dichroism [18].

1. Argon laser.
2. *He-Ne* laser.
3. Fresnel's rhomb.
4. Polarizer prism.
5. Polarizer beam splitter.
6. Mechanical attenuator.
7. Lenses.
8. Sample.
9,10. Photodiodes.

The authors of [18] demonstrated the possibility of measuring circular dichroism in optically active composite compounds $Co(en)_3$; being in supersmall concentrations and volumes approximately on the level of nanogram and microliter. Further improvements of the method for measuring circular dichroism on the basis of spectropolarimeter with thermal lens were obtained in [19]. To increase selectivity and sensitivity double-wave spectrometer thermal lens was developed in which a sample was excited in turn on two wave lengths emitted by argon-ion laser operating in multimode mode. Compared with one-wave method [18] the advantage of two-wave spectrometer except higher selectivity lies in the possibility of investigation of binary mixtures, as well as determination of solution pH_s at very low indicator concentrations decreasing to 10^{-9}M. Detection limit of optically active composite compounds $[Co(en)_3]^{3+}$with the help of circular dichroism spectrometer was 5ng in the volume of 8µl at laser excitation power of 37mWt, λ=514,5nm and modulation frequency of the beam 1,1kHz [19].

Elaborated in [19] a universal method of thermal lens solves as well inverse problems on determining the values of temperature gradient of refraction index $\frac{dn}{dT}$ and thermal conductivity coefficient k.

It should be noted that combination of two methods: thermal lens and circular dichroism not only makes them most sensitive and selective among spectroscopy methods of chemical analyses as it follows from carried out research in [18,19]; but also opens wide out looks for noncontact research of chemical and stereochemical structures, biological objects, determination of kinetics

of high-speed chemical reactions, concentrations of multicomponent mixtures and etc.

Research works [20,21] are devoted to investigation of natural circular dichroism of some optically active crystal complexes. In [22] there is a report about possibility to measure anisotropy of optothermal infrared signal for determining characteristics of dichroic crystal minerals.

In conclusion it should be emphasized that in spite of comparatively small number of experimental research in the field of PA spectroscopy of gyrotropic media this method is considered to be very promising for investigation of considered wide range optically active materials. Experimental techniques are realized only for the cases of gas-microphone registration and measuring angles of deflection (mirage-effect, thermal lens), though there are not less effective and sometimes more sensitive methods of registration of resulting signal, for example detection of PA response with the help of piezopiroelectric sensor or registration of PA signal within the scope of piezophotoacoustic spectroscopy, when the sample under investigation is concurrently a detector.

The subject of the investigation in the near-term outlook will become absorbing gyrotropic crystals of medium and low singonies. Combination in low symmetrical crystals of optical anisotropy and gyrotropy effects plus anisotropy on thermal and acoustic parameters have to result in very complex regularities demanding the development of approximate methods of calculation and the improvement of experimental instrument base.

The solution of such difficult problems demands deepened

development of theoretical statements in PA spectroscopy of gyrotropic media.

Further we will consider different theoretical model of PA transformation in media with natural and stimulated (Faraday effect) optical and acoustic gyrotropy.

2.2. Photoacoustic effect in isotropic-gyrotropic medium.

Consider gas-microphone method of photoacoustic signal registration in isotropic medium or cubic crystal, exhibiting natural optical activity.

Suppose elliptically polarized beam with the amplitude modulation frequency Ω is normally incident on the input window of PA cell (Fig.3), containing gyrotropic-isotropic sample of length l, detector gas and backing. Due to [3] in optically active isotropic absorbing medium in any direction two circular polarized electromagnetic waves propagate with different phase velocities and absorption coefficients, and the difference of the latter results in circular dichroism. Thermal sources formed inside absorbing sample due to energy transformation of eigenwaves into thermal energy cause modulated thermoelastic tension giving rise to the appearance of thermal and acoustic waves forming the resulting phoacoustic signal.

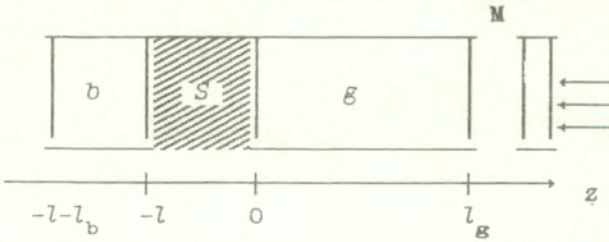

Fig.3. Diagram of PA cell.

For determination of exess pressure value in detector gas of the changing part a set of thermal conduction equations should be used

$$\nabla^2 T - \frac{1}{\beta_j}\frac{dT}{dt} = \begin{cases} 0, & 0 \leqslant z \leqslant l_g \\ \dfrac{Q}{2k_s}(1+e^{i\Omega t}), & -l \leqslant z \leqslant 0, \\ 0, & -l-l_b \leqslant z \leqslant -l, \end{cases} \qquad (2.2.1)$$

Where T is the temperature, β is the thermal diffusivity coefficient, index j takes values g,s,l correspondingly for gas, sample and backing, k_j is the thermal conductivity coefficient, $\beta_j = k_j/\rho_j C_j$, ρ_j, C_j is the density and thermal conductivity of j-material, Ω is the frequency of light modulation, $Q = Q_+ + Q_-$ is the energy dissipation of circular polarized waves in the sample defining by ratio [23]

$$Q_{\pm} = \frac{c}{4\pi}\,|\underline{E}_{\pm}|^2 \left[\varepsilon'' + 2\sqrt{\frac{\varepsilon' + \sqrt{\varepsilon'^2 + \varepsilon''^2}}{2}}\right], \qquad (2.2.2)$$

and sign "+" corresponds to the wave with right polarization, and sign "-" to the wave with left circular polarization. In (2.2.2) $\underline{E}_{\pm}$ are the vectors of electric field intensity of eigenwaves with circular polarization, ε'' is the imaginary part of dielectric permeability, γ'' is the parameter of circular dichroism, c is the velocity of light, λ is radiation wavelength. Basing on the expressions for the fields [4] (the case for the semiinfinite medium is considered), energy dissipation with gaussian intensity distribution $Q_{\pm}$ may be thought of markedly dependent on ellipticity τ [23].

$$Q_{\pm}=\frac{cn_1^2|E|^2(1\pm\tau)^2}{2\lambda|n_0+n_1|^2(1+\tau^2)}\exp(-\frac{2r^2}{w_0^2})\left[\varepsilon''+2\sqrt{\frac{\varepsilon'+\sqrt{\varepsilon'^2+\varepsilon''^2}}{2}}\right]\exp(\alpha_{\pm}z) \tag{2.2.3}$$

Here $\alpha_{\pm}=\frac{4\pi}{\lambda}(\frac{\varepsilon''}{2\sqrt{\varepsilon'}}\pm\gamma'')=k_0(1\pm\alpha_0^{-1}\gamma'')$, $k_0=a_0\alpha_0$, $a_0=\frac{4\pi}{\lambda}$, $\alpha_0=\frac{\varepsilon''}{2\sqrt{\varepsilon'}}$, $n_0=\frac{1}{2}(n_++n_-)$, $n_{\pm}=\sqrt{\varepsilon}\pm\gamma$ are complex refractive indexes of eigenwaves, $r^2=x^2+y^2$, w_0 is the radius of Gaussian beam, n_1 is the refractive index of detector gas.

If we use Hankel transformation [24] over special coordinate z

$$\tilde{T}(p,z)=\int_0^{\infty}T(r,z)rJ_0(pr)dr, \tag{2.2.4}$$

conditions of continuity of temperature and temperature gradient on the boundaries of photoacoustic cell regions as well as requirement of value finiteness $\tilde{T}(p,z)$, $T(r,z)$ for $z\to\pm\infty$, temperature field distribution in volume of detector gas column may be described by ratio

$$T_g^{\pm}(r,z)=\int_0^{\infty}\tilde{T}_g^{\pm}(p,0)\exp\left[-z\sqrt{p^2+\sigma_g^2}\right]pJ_0(pr)dp, \tag{2.2.5}$$

In (2.2.5) $J_0(pr)$ is Bessel function of the first rank, $\sigma_g=(1+i)\sqrt{\frac{\Omega}{2\beta_g}}=(1+i)a_g$, a_g is the thermal diffusion coefficient of detector gas,

$$\tilde{T}_g^{\pm}(p,0)=\frac{A_{\pm}w_0^2}{8k_s}\,\frac{2b-(b-1)\exp\left[l\sqrt{p^2+\sigma_s^2}\right]-(b+1)\exp\left[-l\sqrt{p^2+\sigma_s^2}\right]}{(b+1)(g+1)\exp\left[l\sqrt{p^2+\sigma_s^2}\right]-(b-1)(g-1)\exp\left[l\sqrt{p^2+\sigma_s^2}\right]}\times$$

$$\times \frac{exp(-p^2w_0^2)}{p^2+\sigma_s^2} \qquad (2.2.6)$$

is the temperature image on the detector gas - sample boundary surface,

$$A_{\pm} = \frac{c\sqrt{\varepsilon'}n_2^2|E|^2(1\pm\tau)^2}{2\lambda|n_0+n_1|^2(1+\tau^2)}, \quad g = \frac{k_g\sqrt{p^2+\sigma_g^2}}{k_s\sqrt{p^2+\sigma_s^2}},$$

$$b = \frac{k_b\sqrt{p^2+\sigma_b^2}}{k_s\sqrt{p^2+\sigma_s^2}}, \quad \sigma_{b,s} = (1+i)a_{b,s},$$

$a_{b,s}$ are the thermal diffusion coefficients of a backing and gyrotropic sample. Having fulfilled averaging (2.2.5) over spatial coordinate z and radius of PA cell r

$$\left\langle T_g^{\pm}(r,z)\right\rangle = \int_0^{\infty}\int_0^{l_y}\int_0^{\infty}\tilde{T}_g^{\pm}(p,0)exp\left[-z\sqrt{p^2+\sigma_g^2}\right]rJ_0(pr)pdpdrdz,$$

taking into account, that $\int_0^{\infty} rJ_0(pr)dr = \frac{1}{p}\delta(p)$, a $\int_{-\infty}^{+\infty} f(z)\delta(z)dz = \frac{1}{2}f(0)$, and basing on adiabat equation within the scope of "acoustic piston" model [1], for the excess of pressure in PA cell one may write

$$\Delta P(t) = \frac{\gamma_0 P_0 \theta_0}{4\sqrt{2}T_0 l_g a_g}\,\frac{(1-e^{-y})}{k_s\sigma_s^2 y}\left[1-exp(e^{-y}-1)\right]exp\left(i\left(\Omega t - \frac{\pi}{4}\right)\right), \qquad (2.2.7)$$

where $\theta_0 = \left\langle T_g\right\rangle = \left\langle T_g^{+}\right\rangle + \left\langle T_g^{-}\right\rangle$, $y = \frac{2r^2}{w_0^2}$,

$$\left\langle T_{\underline{g}}^{+}\right\rangle = \frac{A_{\underline{+}} w_0^2}{4k_s\sigma_s^2} \frac{2b-(b-1)exp(\sigma_s l) - (b-1)exp(-\sigma_s l)}{(b+1)(g+1)exp(\sigma_s l) - (b-1)(g-1)exp(-\sigma_s l)} \qquad (2.2.8)$$

The expression (2.2.8) is given in approximation $exp(-\sigma_{\underline{g}} l_{\underline{g}}) \tilde{-} 1-\sigma_{\underline{g}} l_{\underline{g}}$.

The problem solution on calculation the value of occurring pressure in PA cell can be found by some other way, which was proposed for the first time in the history by Rosenzweig and Gersho [1]. In this case the expression for complex amplitude of temperature field on gyrotropic sample - detector gas boundary has the form in the general case [23]

$$\theta_0 = \frac{(L-G)(b+1)exp(\sigma_s l) - (L+G)(b-1) + 2H}{(b+1)(g+1)exp(\sigma_s l) - (b-1)(g-1)exp(-\sigma_s l)}, \qquad (2.2.9)$$

where $(L\underline{+}G)=h_+(r_+\underline{+}1)+h_-(r_-\underline{+}1)$, $r_{\underline{+}}=(1-t)\alpha_{\underline{+}}/2\alpha_s$,

$H=h_+(b-r_+)exp(-\alpha_+ l)+h_-(b-r_-)exp(-\alpha_- l)$, $h_{\underline{+}}=A_{\underline{+}}/\alpha_{\underline{+}}^2-\sigma_s^2$,

$$A_{\underline{+}}=A_0\frac{(1\underline{+}\tau)^2}{(1+\tau^2)}\alpha_{\underline{+}}, \qquad A_0=\frac{c\sqrt{\varepsilon'}n_1^2|\underline{E}|^2}{2k_s\lambda|n_0+n_1|^2}$$

Ratio (2.2.9) is similar to the above given (2.2.8), but it is more general and complete, what is connected with the absence of adopted at derivation (2.2.8) approximations of temperature finiteness on the boundaries of PA cell for $z\to\infty$.

As it follows from (2.2.9), PA signal value is determined by thermal characteristics of cell materials, ε'' and γ'' parameters, ellipticity of incident light τ, modulation frequency Ω and by radius of the beam w_0, as well as by geometry of PA cell.

Considering practically most interesting case when sample width l is smaller than optical absorption length $\mu_{\alpha\underline{+}}=\alpha_{\underline{+}}^{-1}$ and

larger than thermal diffusion length $\mu_s=\alpha_s^{-1}$, and $exp(-\alpha_{\pm} l)\simeq 0$, $exp(-\sigma_s l)\simeq 0$, we arrive to noticeable simplification (2.2.9):

$$\theta_0 = \frac{A_0}{(g+1)(1+\tau^2)}\left[\frac{(1+\tau)^2(r_+ +1)}{\alpha_+^2+\sigma_s^2}\alpha_+ + \frac{(1-\tau)^2(r_- -1)}{\alpha_-^2-\sigma_s^2}\alpha_-\right]. \quad (2.2.10)$$

In the dependence on ellipticity of incident light ($\tau=0$ is the linear polarization, $\tau=\pm 1$ is the circular polarization) from (2.2.10) it follows:

$$\theta_0^{\text{лин.}} = \frac{A_0}{(g+1)}\left[\frac{(r_+ -1)}{\alpha_+^2-\sigma_s^2}\alpha_+ + \frac{(r_- -1)}{\alpha_-^2-\sigma_s^2}\alpha_-\right] \quad (2.2.11)$$

and

$$\theta_{0\pm} = \frac{2A_0}{g+1}\,\frac{r_{\pm}-1}{\alpha_{\pm}^2-\sigma_s^2}\,\alpha_{\pm} \quad (2.2.12)$$

Experimentally obtainable value of PA signal is determined by relation

$$\theta = \frac{\gamma_0 P_0 \theta_0}{\sqrt{2}\, a_g\, l_g\, T_0} f(y) = q\, exp(-i\psi), \quad (2.2.13)$$

where $f(y)=\dfrac{1-e^{y}}{k_s\sigma_s^2 y}\left[1-exp(e^{-y}-1)\right]$, $g=|\theta|=\sqrt{(Re\theta)^2+(Im\theta)^2}$ (2.2.14)

is the amplitude,

and $\psi=arctg(Im\theta/Re\theta)$ (2.2.15)

is the phase of resulting signal.

In connection with (2.2.11), (2.2.13), (2.2.14) it is simple to show that resulting pressure in the cell for linear polarization of an incident wave does not depend on γ'' accurate up to terms of the second order by γ'' parameter, and is defined by the ratio of values k_0 and Q_s, incident light characteristics and modulation frequency Ω.

For circular polarized incident light in conformity with (2.2.12), (2.2.14) we have [23]

$$q_{\pm} = \frac{A\alpha_{\pm}}{\sqrt{2}a_s(\alpha_{\pm}^4+4a_s^4)}\,(\alpha_{\pm}^6+\beta_{\pm}+8a_s^6)^{1/2}, \qquad (2.2.16)$$

$$A = 2\gamma_0 P_0 A_0/a_g l_g T_0(g+1),\ \beta_{\pm} = -2a_g a_{\pm}(\alpha_{\pm}^4-a_s\alpha_{\pm}^3-2a_s^3\alpha_{\pm}+4a_s^4). \qquad (2.2.17)$$

Representing $\alpha_{\pm}^n$ in the form of polynomials $\alpha_{\pm}^n = k_0^n(1\pm n\alpha_0^{-1}\gamma'')$ and imposing constraints on linear expansion terms by γ'' we will find using (2.2.16) explicit expression of the circular dichroism parameter in terms of PA amplitude signal ratio

$$\gamma'' = \frac{1}{4}\,\frac{k_0}{a_0 a_s}\,\frac{q_- - q_+}{q_-} f(k_0,a_s), \qquad (2.2.18)$$

where $f(k_0,a_s)$ is the function of optical and thermal parameters of the medium which obtainable from (2.2.16). Using the dependence of thermal diffusion coefficient a_s on modulation frequency Ω, by changing of the latter, we may strive for the fulfillment of the condition $k_0=a_s$, i.e. make average optical absorption and thermal diffusion length equal. Then $f(k_0,a_s)\simeq 10k_0/3$ and formula (2.2.18) will take the form

$$\gamma'' = \frac{5}{6}\,a_0\left[1-\left(\frac{q_+}{q_-}\right)\right]. \qquad (2.2.19)$$

From the formula presented (2.2.18), (2.2.19) it follows that for the determination of circular dichroism γ'' parameter it is enough to get PA spectra of isotropic-gyrotropic medium corresponding to the left and right circular polarization of the incident light.

2.3. Influence of multiray interference on the PA response.

The above considered analysis of PA transformation has been

made for the case of semiinfinite medium. Further we shall go on to the investigation of the influence of boundary surfaces of the examined sample on the type of photoacoustic spectra. With that aim in view for defining energy dissipation in the sample we shall make use of accurate solution of the boundary problem on passing a light beam through the crystal isotropic plate, cut from a cubic naturally gyrotropic absorbing crystal. Then the complex amplitude of excess pressure in the PA cell will look like [25]:

$$\theta = \theta_+ + \theta_-$$

$$\theta_{\pm} = \frac{Y\alpha_{\pm}\theta_0}{k_s a_g(\alpha_{\pm}^2-\sigma_s^2)}\,(N_1T_{\pm}R_{1\pm}+N_2T_{\mp}R_{2\pm}), \qquad (2.3.1)$$

where

$$R_{1\pm}=\Delta[(r_{\pm}-1)(b+1)exp(\sigma_s l)-(r_{\pm}+1)(b-1)exp(-\sigma_s l)+2(b-r_{\pm})exp(-\alpha_{\pm} l)],$$

$$\Delta=[(b+1)(g+1)exp(\sigma_s l)-(b-1)(g-1)exp(-\sigma_s l)]^{-1},$$

$$R_{2\pm}=\Delta[(r_{\pm}-1)(b-1)exp(-\sigma_s l)-(r_{\pm}+1)(b+1)exp(\sigma_s l)+2(b+r_{\pm})exp(\alpha_{\pm} l)],$$

$$Y=\gamma_0 P_0/\sqrt{2}a_g l_g T_0, \quad T_{\pm}=(1\pm\tau)^2/(1+\tau^2), \quad \alpha_{\pm}=\frac{4\pi}{\lambda}(n_0''\pm\gamma''),$$

$$N_1=|n_0|^2+n_2^2+2n_2n_0', \quad N_2=(|n_0|^2+n_2^2-2n_2n_0')exp(-\alpha\text{æ}l), \quad \text{æ}=\frac{4\pi}{\lambda}n_0'',$$

$$n_0''=\frac{\varepsilon''}{2\sqrt{\varepsilon'}}, \quad \theta_0=\frac{cn_0'n_1^2E^2}{4\pi|\xi|^2},$$

$$|\xi|^2=\xi_1+[\xi_2 sin(\beta l)+\xi_3 cos(\beta l)]exp(-\text{æ}l)++\xi_4 exp(-2\text{æ}l),$$

$$\xi_1=|n_0+n_1|^2|n_0+n_2|^2, \quad \xi_2=4n_0''(n_1+n_2)(|n_0|^2-n_1n_2),$$

$$\xi_3=8n_1n_2n_0''^2-2(|n_0|^2-n_1^2)(|n_0|^2-n_2^2), \quad \xi_4=|n_0-n_1|^2|n_0-n_2|^2,$$

$$\beta=\frac{4\pi}{\lambda}n_0'.$$

The second item in (2.3.1) corresponds to contribution of wave reflected from the lower border of the layer (2.2.12). If it is neglected, what is possible when $\alpha l \gg 1$, then we receive the above mentioned expression (2.2.9). If the condition $d \gg d_{\alpha}$, $d_{\alpha}=\lambda(\varepsilon'+\sqrt{\varepsilon'^2+\varepsilon''^2})^{1/2}/2\sqrt{2}\pi\varepsilon''$ is fulfilled, optical interference in the layer can be neglected, what is true when $d \gg (50/\pi)\lambda$, if to accept values for $\varepsilon' \sim 1$, $\varepsilon'' \sim 10^{-2}$.

As the obtained expression (2.2.12) is awkward, let us make its numerical analysis. As the ellipticity τ grows the velocity of energy dissipation in the layer increases with the growth of γ''. This is true for absolute and difference $q'=|q_+-q_-|$ values of PA signals amplitude (Fig.4). The dependence $q'(\tau)$ is near to linear only when τ are small, which corresponds to the case of light polarization near to the linear one.

The influence of optical and thermal waves interference on PA signals formation is given in Fig.5. One can see that thermal processes are the main ones. Optical interference is not displayed in the given graphs and can be registered only by sensitive measurements. Parameter growth $b=(k_b/k_s)/(\rho_s/\rho_b)^{1/2}$, characterizing thermophysical peculiarities of the sample and the backing leads to an increase of thermal interference influence on PA spectrum, the influence of interference processes on the value of difference PA signal displaying more vividly. Hence follows, that it is expedient to take measurements of the values of circular dichroism at values of parameter, for which interference of thermal waves within the layer is displayed more essentially.

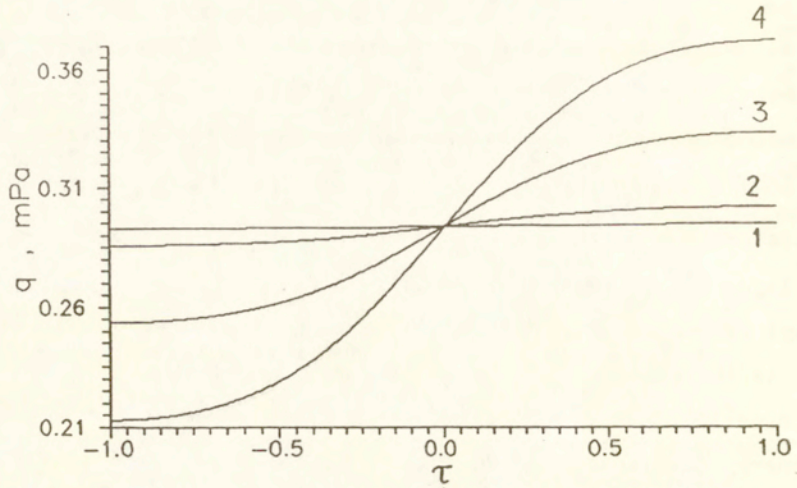

Fig.4. Dependence of PA signal amplitude q on ellipticity τ when $\gamma''=10^{-6}$(1); 10^{-5}(2); $5\cdot10^{-5}$(3); 10^{-4}(4); Ω=100Hz; l=10μm; $\varepsilon''=10^{-3}$; b=1.

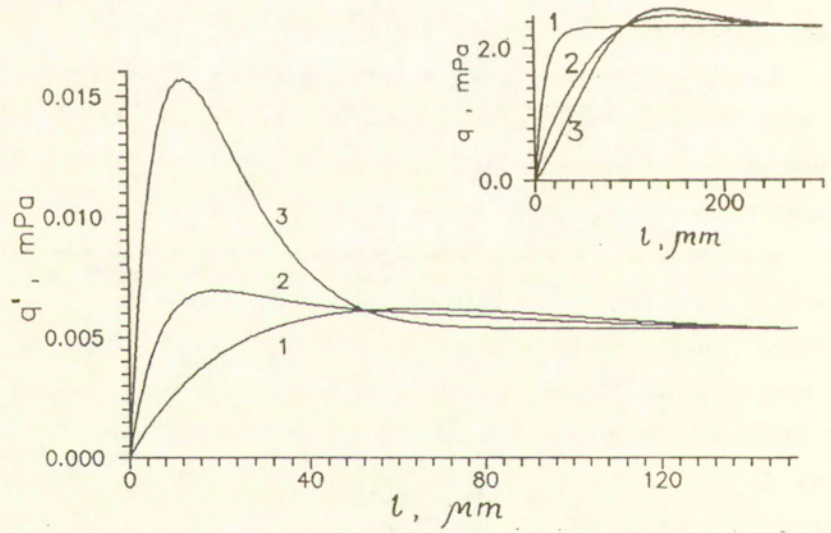

Fig.5. Dependence of PA signal amplitude q', q on the layer thickness l when b=1(1,4); 3(2,5); 10(3,6); Ω=150Hz; $\gamma''=3\cdot10^{-5}$; $\varepsilon''=10^{-2}$; τ=1.

2.4. Piezoelectric detection of PA signal.

The method of piesoelectric detection of PA signal implies immediate detecting acoustic modes and belongs to one of the simplest and at the same time very sensitive ways of measuring responses of a medium phonon subsystem on external influence.

PA effect in nongyrotropic media with subsequent piezoelectric detection of PA signal has been investigated by a number of scientists [26-31], who have established boundaries of using application for the given method taking into account dissipative characteristics of the samples under examination [28], and who have taken advantages of the piezoelectric method of registration before a gas-microphone [1].

We shall consider the peculiarities of piesoelectric detection of PA signal in isotropic-gyrotropic media. Let an intensity modulated and elliptically polarized laser beam with Gaussian distribution of intensity normally falls on the surface of the optically active absorbing sample contacting with a piezoelectric detector.

Description of the field of temperature distribution in a gyrotropic sample can be achieved on the basis of the equation:

$$\nabla^2 T - \frac{1}{\beta_s}\frac{dT}{dt} = \frac{(A_+ exp(-\alpha_+ z)+A_- exp(-\alpha_- z))}{2k_s}(1+exp(i\Omega t))\times$$

$$\times exp(-2r^2/w_0^2), \qquad (2.4.1)$$

$$w^2=w_0^2(1+z^2/z_0^2),\ z_0=\pi w_0^2/\lambda,\ r^2=x^2+y^2,$$

w_0- the radius of cross-section of of beam. The solution of this equation can be found with the help of Hankel integral transformation [32]

$$T(r,z) = T_+(r,z) + T_-(r,z),$$

$$T_{\pm}(r,z) = \int_0^{\infty} p[C_{\pm}(p)exp(-\alpha_{\pm}z) + A_{\pm}(p)exp(\xi z) + B_{\pm}(p)exp(-\xi z)] \times$$

$$\times J_0(pz)dp$$

where $\xi^2=p^2+\sigma_s^2$, p is Hankel transformation parameter. Proceeding from the demands of temperature continuity and temperature flows at the sample boundaries it is easy to represent the solution for (2.4.1) as [32]

$$T_{\pm}(r,z) = \int_0^{\infty} \frac{R(p)J_0(pz)pdp}{(\alpha_{\pm}^2-\sigma_s^2-p^2)D(\xi)} \Big\{(r_{\pm}+g)[(b-1)exp((z-l)\xi)-$$

$$(b+1)exp(-(z-l)\xi)]A_{\pm}^0(0) + [(1+g)exp(\xi z)+(1-g)exp(-\xi z)]$$

$$(r_{\pm}-b+a(\xi))A_{\pm}^0(l)exp(-\alpha_{\pm}l) + [(1+g)(1+b)exp(\xi z)$$

$$-(1-g)(1-b)exp(-\xi z)]A_{\pm}^0(z)exp(-\alpha_{\pm}l)\Big\}, \qquad (2.4.2)$$

where $D(\xi)=(1+g)(1+b)exp(\xi z)-(1-g)(1-b)exp(-\xi z)$

The energy of a of beam absorbed by a gyrotropic sample is transformed into energy of elastic oscillations, detected by a piezoelectric, the characteristics of which can be described on the basis of Dugamel-Neuman correlations:

$$\sigma_{ij}=c_{ijkl}^E U_{kl}-e_{ijk}E_k,$$

$$D_i=e_{ijk}U_{kl}+\varepsilon_{ik}^s E_k. \qquad (2.4.3)$$

Here c_{ijkl}^E is the a tensor of coefficients of elasticity for $E=const$, connecting tensors of tensions σ_{ij} and deformations U_{kl}, e_{ijk} and ε_{ik}^s are correspondingly the tensors of piezoelectric co-

efficients and dielectric permeability.

Considering that the sample surface is free from tensions and the piezoelectric is thin enough, to let $\sigma_{zz}=\sigma_{xz}=\sigma_{yz}=0$, and the components of the electric field E_x and E_y equal 0 (light propagates along the axis z) in the paper [27], and proceeding from (2.4.3), an expression was obtained for potential difference, which in the considering case looks like

$$V_{\pm} \simeq \text{æ}(1+\nu)[\langle T_{\pm}\rangle+(z-l/2)\langle\tau_{\pm}\rangle]_{z=0,l} \qquad (2.4.4)$$

where $\text{æ}=e_{31}^{p}L\alpha_t/\varepsilon_{33}^{p}S$, $e_{31}^{p}=e_{31}-e_{33}c_{31}/c_{33}$, $\varepsilon_{33}^{p}=\varepsilon_{33}^{s}+e_{33}^{2}/c_{33}$ (numerical designations are used for writing down tensor components c_{ijkl} and e_{ijk} [33]), L and S are thickness and the detector's area, α_t is the coefficient of the piezocrystal thermal expansion, ν is Puasson's coefficient, signs "+" ("-") belong to the left and right circular polarized incident wave.

$T_{\pm}=1/c\int T_{\pm}(r,z)dz$ is averaged temperature by z, $\tau_{\pm}=12/c^{3}\int(z-l/2)T_{\pm}(r,z)dz$ is the temperature gradient by z, brackets $\langle f(r)\rangle$ mean $2\pi\int rf(r)dr$.

Performing the substitution (2.4.2) into (2.4.4) and having integrated, we shall receive the following expression for the piezophotoacoustic signal $V=V_{+}+V_{-}$ induced in the detector for $z=0$ and for $z=l$ correspondingly [32]:

$$V_{\pm}=-k_{\pm}(3J_{\pm}-J_{\pm}^{0}), \qquad (2.4.5)$$

(frontal location of the detector)

$$V_{\pm}= k_{\pm}(3J_{\pm}-2J_{\pm}^{0}), \qquad (2.4.6)$$

(back location of the piezotransformer).

In (2.4.5),(2.4.6) the following designations are introduced

$$J_{\pm}=(g+r_{\pm})[(b-1)F(\sigma_s l)exp(-\sigma_s l)+(b+1)F(-\sigma_s l)exp(\sigma_s l)]+$$

$$+(r_{\pm}-b)exp(-\alpha_{\pm}l)[(1+g)F(\sigma_s l)-(1-g)F(-\sigma_s l)]-D\sigma_s F(-\alpha_{\pm}l)/\alpha_{\pm},$$

$$J^{o}_{\pm}=(g+r_{\pm})[(b-1)F^{o}(-\sigma_s l)+(b+1)F^{o}(\sigma_s l)]+$$

$$+(r_{\pm}-b)exp(-\alpha_{\pm}l)[(1-g)F^{o}(-\sigma_s l)-(1+g)F^{o}(\sigma_s l)]+Dr_{\pm}^{-1}F^{o}(-\alpha_{\pm}l),$$

$$D=(1+g)(1+b)exp(\sigma_s l)-(1-g)(1-b)exp(-\sigma_s l),$$

$$F(p)=exp(p)-\frac{1}{p}(exp(p)-1),\ F^{o}(p)=1-exp(p),\ r_{\pm}=\alpha_{\pm}/\sigma_s,$$

$$K_{\pm}=\Phi_{\pm}(\tau)B_{\pm},\ \Phi_{\pm}(\tau)=\frac{A_o w_o^2 \pi e_{31}^{p} L a_t (1\pm\tau^2)}{2k_s \varepsilon_{33}^{p} S(1+^2)},$$

$$B_{\pm}=\frac{\alpha_{\pm}}{D(\alpha_{\pm}^2-\sigma_s^2)\sigma_s l},\ g=\frac{k_1}{k_s\sigma_s},\ b=\frac{k_2}{k_s\sigma_s},$$

k_1 and k_2 are coefficients of heat conductivity on the front and back surfaces of the sample.

The received expressions let us state that the value of PA signal is defined by the absorption parameters ε'' and dichroism γ'', elastic, thermal and piezoelectric constants of the detector, ellipticity τ, modulation frequency Ω and the radius of the cross-section w_o the incident light of beam, as well as geometric parameters of the sample and piezodetector.

Awkwardness of the correlations (2.4.5),(2.4.6) creates difficulties in their analysis, therefore let us start the investigations of some particular cases. Consider the frontal location of the piezoelectric sensor (z=0) in relation to the sample under investigation which is optically thin ($exp(-\alpha_{\pm}l)\tilde{}1-\alpha_{\pm}l$)and analyze dependence of the PA response value on the ellipticity of the incident light τ in boundary cases of characteristic lengths

l, $\mu_s=\alpha_s^{-1}$, $\mu_{\alpha\pm}=\alpha_\pm^{-1}$.

If the incident light is linearly polarized ($\tau=0$), and the length of thermal diffusion is less then that one of the sample and much more less than the length of the optical absorption (the sample is thermally thick $exp(-\sigma_s l)\simeq 0$, $|r_\pm|\ll 1$), then from (2.4.5) we have

$$q=\frac{8\pi\Phi_\pm(0)\varepsilon''}{\lambda\alpha_s^2\sqrt{\varepsilon'}}\sim\Omega^{-1}, \qquad (2.4.7)$$

i.e. PA signal amplitude is inversely proportional to the frequency of the amplitude modulation and does not depend on dichroic properties of the medium in linear γ'' approximation.

Considering the case of circular polarization of the incident light ($\tau=\pm 1$) for thermally thick sample, according to (2.4.5), we receive the expression

$$q_\pm=\frac{2\alpha_\pm\Phi_\pm(\pm 1)}{\alpha_s^2-}, \qquad (2.4.8)$$

hence. follows hyperbolic dependence of PA response value on Ω. Defining the difference of PA signals amplitudes $\Delta q=|q_+-q_-|$ and considering, that $\alpha_+^2-\alpha_-^2\sim 4k_0\alpha_0\gamma''$, $\alpha_0=4\pi/\lambda$, $k_0=\alpha_0\varepsilon''/2\sqrt{\varepsilon'}$, in accordance with (2.4.8) we come to the possibility of explict expressing the parameter of circular dichroism γ'' in terms of Δq

$$\gamma''=\frac{\lambda\alpha_s^2}{16\pi\Phi_\pm(\pm 1)}\Delta q. \qquad (2.4.9)$$

It is worth noting, that formulas (2.4.7)-(2.4.9), received for $z=0$, remain true for the case of the piezodetector location on the back surface of the sample under investigation ($z=l$), only constant multiplier being different 1/2.

On the basis (2.4.7), (2.4.9) we can conclude that measuring PA signals amplitude for different polarization of the incident radiation lets us fully solve the problem of defining parameters, responsible for the absorption and dichroism of the gyrotropic medium.

2.5. Combined method of PA signal registration.

As is known [1,26], two ways of registering the resulting signal are more often used in the photoacoustic spectroscopy of condensed media: gas-microphone and piezoelectric one. In using the first method the main role is played by the processes of heat transformation from the examined sample to the detector gas, elastic deformations in sample volumes being usually neglected. Calculation of oscillations of the sample surface in the limits of the combined piston model was investigated in [34,35], it is shown there that the given model is true for a particular case of poorly absorbing media ($\alpha<1 sm^{-2}$) for modulation frequency of incident radiation >1kHz. Method for piezoelectric detection of PA signal is based, as it was stated in section 2.4, on the calculation of thermo-elastic oscillations induced in the sample by a modulated absorption of the incident light beam. In this case one neglects heat exchange with the surroundings. As a matter of fact in using any method part of the information is inevitably lost, therefore working out new or additional methods in addition to the existing ones for PA signals registration in condensed media is of great interest.

In investigating nonradiative relaxation and electronic transitions in semiconductor crystals of *n*-type *CdS* by the scien-

tists [36] a combined method of photoacoustic and photoconductive spectroscopy was used. In the papers [37,38] a noncontact optico-acoustic method was proposed, in which a thermal mechanism of PA signal forming with its subsequent piezoelectric registration was realized. Studying homogeneities of electronic characteristics along semiconductors surface by combined photoacoustic method was carried out in [39]. Following paper [40] the aim of the section is to investigate the possibility of the combined method for PA signal registration in gyrotropic media taking into account the kinetics of processes connected on the one hand with heat transmission from the surface of the examined sample into detector gas, on the other hand with its volumetric elastic deformations. For realization of the scheme of the combined method for PA signal registration it is necessary to modify PA cell putting the examined sample on a piezoelectric detector of longitudinal elastic oscillations instead of the backing. From the solution of the system of thermal conductivity equations for the gyrotropic sample and wave equations for longitudinal shifts in the sample and the piezotransformer under boundary conditions

$$U_s(l_1)=U_p(l_1),\ \sigma_s(l_1)=\sigma_p(l_1),\ \sigma_s(0)=0,\ \sigma_p(l_2)=0$$

we obtain expressions for potential differences developed by the piezodetector (compare with [40,41]) in the case of circular polarized incident light:

$$V_{\pm}=\frac{2h}{\varkappa}\sin^2\frac{k_1\Delta l}{2}\,(P_{\pm}\cos k_0 l_1+N_{\pm}k_0c^T\sin k_0 l_1-F_{\pm}). \qquad (2.5.1)$$

The following designations are used here:

$$N_{\pm}=\eta\alpha_t(a_{\pm}\exp(\sigma_s l_1)-b_{\pm}\exp(-\sigma_s l_1)+c_{\pm}\exp(-\alpha_{\pm} l_1)),$$

$$P_{\pm}=[\eta\alpha_t c^T(\sigma_s a_{\pm}exp(\sigma_s l_1)+\sigma_s b_{\pm}exp(-\sigma_s l_1)-\alpha_{\pm}c_{\pm}exp(-\alpha_{\pm}l_1))-$$

$$-B\alpha_t(U_{\pm}exp(\sigma_s l_1)+V_{\pm}exp(-\sigma_s l_1)-E_{\pm}exp(-\alpha_{\pm}l_1))],$$

$$F_{\pm}=[\eta\alpha_t c^T(\sigma_s a_{\pm}+\sigma_s b_{\pm}-\alpha_{\pm}c_{\pm})-B\alpha_t(U_{\pm}+V_{\pm}-E_{\pm})],$$

$$U_{\pm}=\frac{E_{\pm}}{2sh\sigma_s l_1}[(exp(-\alpha_{\pm}l_1)+W_0)-(\theta_0+1)exp(-\sigma_s l_1)], \qquad (2.5.2)$$

$$V_{\pm}=\frac{E_{\pm}}{2sh\sigma_s l_1}[(exp(-\alpha_{\pm}l_1)+W_0)-(\theta_0+1)exp(\sigma_s l_1)],$$

$$a_{\pm}=\frac{\sigma_s U_{\pm}}{\sigma_s^2+k_0^2},\ b_{\pm}=\frac{\sigma_s V_{\pm}}{\sigma_s^2+k_0^2},\ c_{\pm}=\frac{\alpha_{\pm}E_{\pm}}{\alpha_{\pm}^2+k_0^2},$$

$$E_{\pm}=\frac{\alpha_{\pm}A}{\alpha_{\pm}^2-\sigma_s^2},\ A=\frac{c\sqrt{\varepsilon'}n_1^2|E|^2}{\sqrt{2}k_s|n_0+n_1|^2},\ \alpha_{\pm}=\frac{4\pi}{\lambda}\left(\frac{\varepsilon''}{2\sqrt{\varepsilon'}}\pm\gamma''\right),$$

$$\varkappa=k_0c^T sink_0l_1 cosk_1\Delta l+k_1c^P cosk_0l_1 sink_1\Delta l,$$

$\Delta l=l_2-l_1$, l_2 and l_1 are respectively the lengths of the examined sample and the piezodetector. In (2.31) $\theta_{\pm}=E_{\pm}\theta_0$, $W_{\pm}=E_{\pm}W_0$ are complex amplitudes of temperature fields on the border of gyrotropic sample - detector gas and the gyrotropic sample - piezotransducer defined from the solution of the system of equations for heat conductivity for PA cell regions

$$\theta_{\pm}=\frac{E_{\pm}}{\chi}[exp(-\alpha_{\pm}l_1)(p-r_{\pm})-sh\sigma_s l_1(1-pr_{\pm})+ch\sigma_s l_1(r_{\pm}-p)], \qquad (2.5.3)$$

$$W_{\pm}=\frac{E_{\pm}}{\chi}[(r_{\pm}+q)-exp(-\alpha_{\pm}l_1)(sh\sigma_s l_1(1+r_{\pm}q)+ch\sigma_s l_1(r_{\pm}+q)], \qquad (2.5.4)$$

where $\chi=sh\sigma_s l_1(1+pq)+ch\sigma_s l_1(p+q)$, $p=(\sigma_p k_p)/(\sigma_s k_s)$, $r_{\pm}=(1-i)\alpha_{\pm}/\alpha_s$.

The rest of the designations correspond to the adopted in [23,41].

Potential difference developed in the gas-microphone method is proportional to Rosenzwaig pressure $V_g=k\Delta P_{\pm}$ where K is the microphone sensitivity, $\Delta P_{\pm}\sim\theta_{\pm}$.

Thus, part of the energy of incident radiation is spent on exciting a signal in the detector gas column, and the other one is transformed into energy of the piezoelectric elastic oscillations. By the way potential difference detected by the piezotransducer, as follows from (2.5.1), is influenced by amplitude changes of temperature fields on border $x=l_1$ and $x=l_2$.

Numerical analysis of expressions for PA signals amplitudes in a particular case of a thermally thick sample as arosult of this in (2.5.3), (2.5.4) $W_{\pm}=0$, $P=0$, shows that on a fixed frequency of modulation of incident radiation at a certain thickness of a sample PA signals amplitudes V_q and V_p as follows from Fig.6 can be compared in length. On the diagram of dependencies $V_{q,p}=f_{1,2}(l_1)$ there are characteristic extremums which can be accounted for thermal waves interference, what was stated for example in [42].

The region of modulation frequencies $\Delta\Omega$ in which graphs of dependencies $V_q=f_1(\Omega)$ and $V_p=f_2(\Omega)$ intersect (Fig.7) depends first of all on the microphone sensitivity, value $h=l/\xi^2$, defining piezoelectric characteristics of the detector as well as geometrical parameters of the sample, the piezodetector in the region occupied by the detector gas. Decrease of the length of the gas layer in the cell, at $l_1=const$, $l_2=const$ leads to increase of PA signal amplitude and considerable shift of the point of

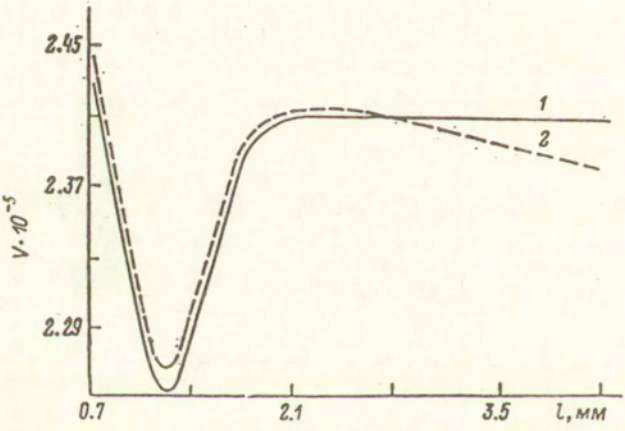

Fig.6. Dependence of PA signal amplitude (1- gas-microphone method of registration, 2- piezoelectric) on the length of the sample l_1 (absorption coefficient $\alpha=10^3 m^{-1}$, $\beta_s=0.5\cdot10^{-3}$ m^2/s, coefficient of temperature expansion $\alpha_t=2.3\cdot10^{-6}K^{-1}$, $V_s=9.8\cdot10^3 m/s$, $\Omega=2121Hz$, $E=0.01V/m$).

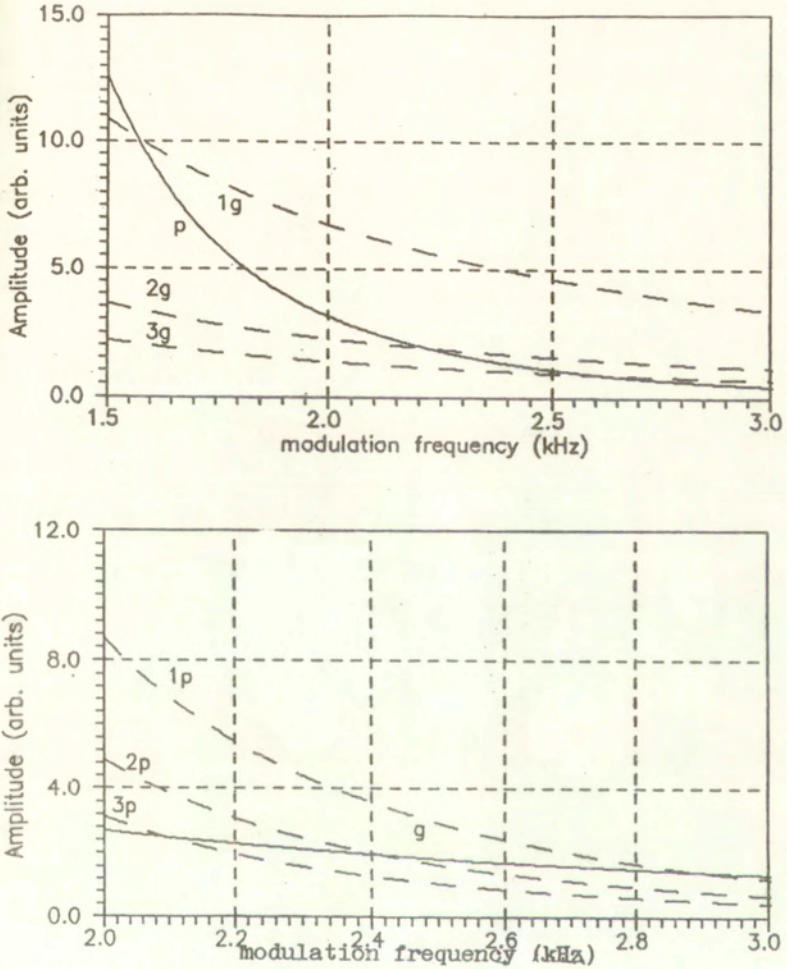

Fig.7. Dependence of PA signal amplitude on modulation frequencies of the incident emission: a) at different lengths of the gas pillar (1g-2mm, 2g-6mm, 3g-10mm); b) at different thickness of the piezodetector ($LiNbO_3$, $h=0.5\cdot10^{10}$V/m, $V_p=7.3\cdot10^3$m/s, 1p-3mm, 2p-4mm, 3p-5mm).

graphs intersection ($\Delta\Omega \tilde{}$1000Hz) (Fig.7a). Variations of the piezotransducer thickness at l_g=*const*, l_1=*const* still more greatly influences (two times as much) the examined field of modulation frequencies (Fig.7b).

Thus, as shown above, the calculation of volumetric elastic oscillations of the examined sample in gas-microphone method for defining modulation frequencies range are principally necessary. The combined method of PA signal detection will on the one hand let us receive simultaneously more full information about dichroic, optical, acoustic, thermophysical properties of the examined sample and on the other hand carry out investigations in a broad interval of modulation frequencies without traditional change of elements of the registration system of amplitude and phase characteristics of PA signal.

2.6. PA transformation at the contrary interaction of light waves.

A number or interesting phenomena which can find practical application arise at the contrary interaction of light waves in absorbing media. In reference [43], for example, a phenomenon of passing light through in strongly absorbing metal films of titanium have been experimentally investigated at the interaction of two contrary light beams. It was shown that owing to interference redistribution of energy the transparency coefficient value essentially depends on energy and polarization characteristics of contrary light beams, dissipative peculiarities of the films under investigation.

As it will be shown further, the calculation of a sample

gyrotropic peculiarities in the process of waves contrary interaction may essentially change volume interference of interacting waves.

Let us turn to a case of a gas-microphone method of PA signal registration. Let two plane electromagnetic waves of arbitrary polarization propagating "towards" each other fall normally on isotropy-gyrotropy layer (Fig.8), placed in PA cell [44]. A combined solution of the system of equations of thermal conductivity for each region of PA cell, with regard to the expression for energy dissipation velocity $Q_{\pm}(z)$ [9] and boundary conditions

$$T_0\left(-\frac{d}{2}\right) = T_s\left(-\frac{d}{2}\right);$$

$$k_0\frac{dT_0}{dz}\left(-\frac{d}{2}\right) = k_s\frac{dT_s}{dz}\left(-\frac{d}{2}\right) + Q_+\left(-\frac{d}{2}\right) + Q_-\left(-\frac{d}{2}\right);$$

$$T_s\left(\frac{d}{2}\right) = T_1\left(\frac{d}{2}\right);$$

$$k_1\frac{dT_1}{dz}\left(\frac{d}{2}\right) = k_s\frac{dT_s}{dz}\left(\frac{d}{2}\right) + Q_+\left(\frac{d}{2}\right) + Q_-\left(\frac{d}{2}\right);$$

lets us define complex amplitude of temperature field on the border $z=d/2$ [9]:

$$\theta = \frac{2}{\Delta}\left[sh(\sigma_s d)(F_3 - S_0(F_4+Q_1)) + ch(\sigma_s d)[S_0F_3 - F_4 - Q_2] - \right. \quad (2.6.1)$$

$$\left. - S_0F_3 - F_4 - Q_2\right]$$

where

$$\Delta = (s_1+1)(s_0+1)exp(\sigma_s d) - (s_1-1)(s_0-1)exp(-\sigma_s d)$$

$$F_1 = -E_1^+ e^{\alpha_+ d/2} - E_1^- e^{\alpha_- d/2} - E_2^+ e^{-\alpha_+ d/2} - E_2^- e^{-\alpha_- d/2}$$

$$F_2 = r_+E_1^+ e^{\alpha_+ d/2} + r_-E_1^- e^{\alpha_- d/2} - r_+E_2^+ e^{-\alpha_+ d/2} - r_-E_2^- e^{-\alpha_- d/2}$$

$$F_3 = - E_1^+ e^{-\alpha_+ d/2} - E_1^- e^{-\alpha_- d/2} - E_2^+ e^{\alpha_+ d/2} - E_2^- e^{\alpha_- d/2}$$

$$F_4 = r_+ E_1^+ e^{-\alpha_+ d/2} + r_- E_1^- e^{-\alpha_- d/2} - r_+ E_2^+ e^{\alpha_+ d/2} - r_- E_2^- e^{\alpha_- d/2}$$

$$U_1^{\pm} = \frac{A^{\pm}}{\alpha_{\pm}^2 - \sigma_s^2}, \quad U_2^{\pm} = \frac{B^{\pm}}{\alpha_{\pm}^2 - \sigma_s^2}, \quad s_0 = \frac{k_0 \sigma_0}{k_s \sigma_s}, \quad s_1 = \frac{k_1 \sigma_1}{k_s \sigma_s},$$

the rest of notation is given in [9].

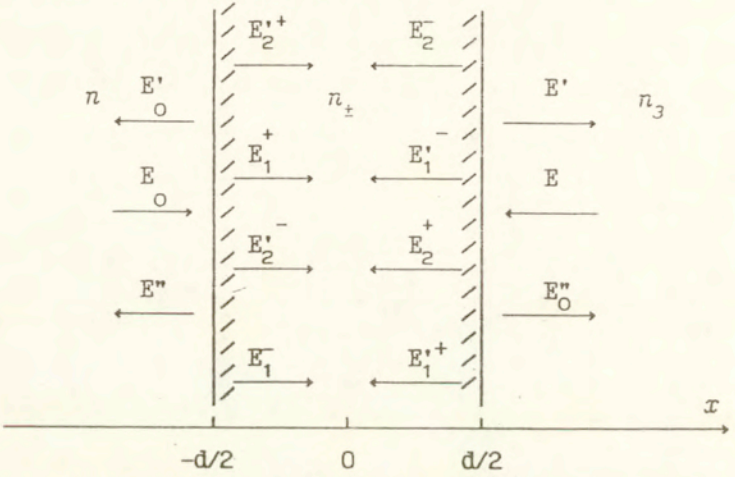

Fig.8. Geometry of interaction of two contrary light waves in an isotropic-gyrotropic sample.

Numerical analysis of the obtained expression (2.6.1) showed that in the region of the examined sample thicknesses $d \gg 1$mm PA response amplitude essentially depends on γ' parameter which defines specific rotation of a polarization plane and its value may increase by some orders depending on correlations of the parameter characteristics $(\Delta\varphi, \tau = 0, \pm 1, \Omega)$. The highest increase of the PA signal amplitude displaying at the interaction of two of the same plane linear polarized light waves which have difference of ini-

tial phases $\Delta\varphi=\varphi_o-\varphi=\pi/2$ at low modulation frequencies ($\Omega<10^3$) (Fig.9). A given circumstance lets us speak about "a photoacoustic analog of Josephson effect". The higher the sample absorption the wider is a range of changes of PA signal amplitude, this thing taking place only at the contrary interaction of light waves. In a case of absorption of two circular polarized interacting waves a changes $\Delta\varphi$ results in displacing of PA response amplitude maximum without an increase of absolution value. Thus, influence on the amplitude and phase characteristics value of PA signal may be caused by a choice of difference of initial phases of interacting waves and their polarization. The presence of gyrotropy in an examined sample may also bring about an essential change PA response amplitude and phase (Fig.10).

Analysis of dependence of PA signal amplitude on the parameter of circular dichroism brought about a characteristic extremum (Fig.11), the position of which essentially depends on difference values of initial phases. The maximum presense is defined, on the one hand, by velocity of changing energy volume dissipation, on the other hand, by redistribution of dissipated energy due to multibeam interference of interacting modes.

Concluding we state that gyrotropic characteristics of the examined sample essentially influence PA signal forming mechanism. The change of a γ' parameter, responsible for specific rotation of a light polarization plane lets us increase PA signal amplitude by several orders waves does not change. Placing a sample into the PA cell, which is in external magnetic field and changing its value one can influence interference redistribution of energy dissipation, which lets us propose a way of effective

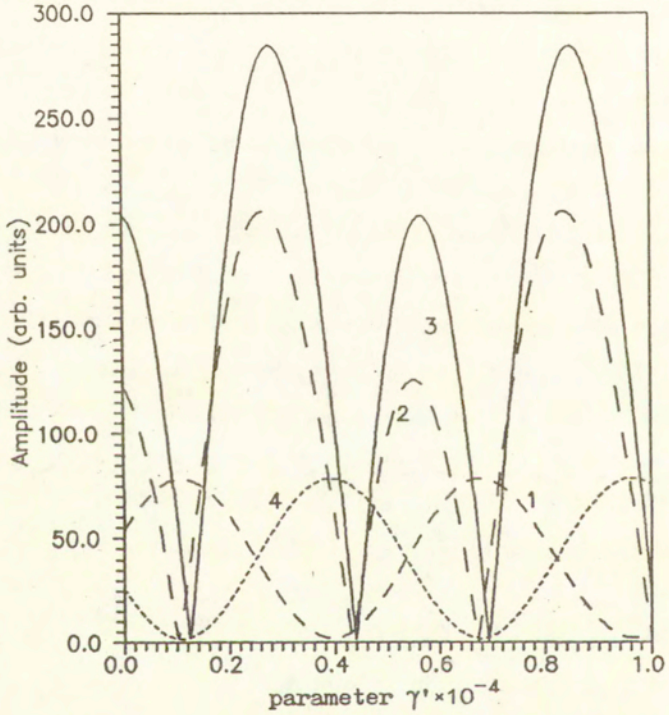

Fig.9. Dependence of PA signal amplitude q on γ' parameter value at different values of initial phases difference ($\Delta\varphi=\varphi_o-\varphi$, rad): 1-0, 2-$\pi/4$, 3-$\pi/2$, 4-$\pi$.

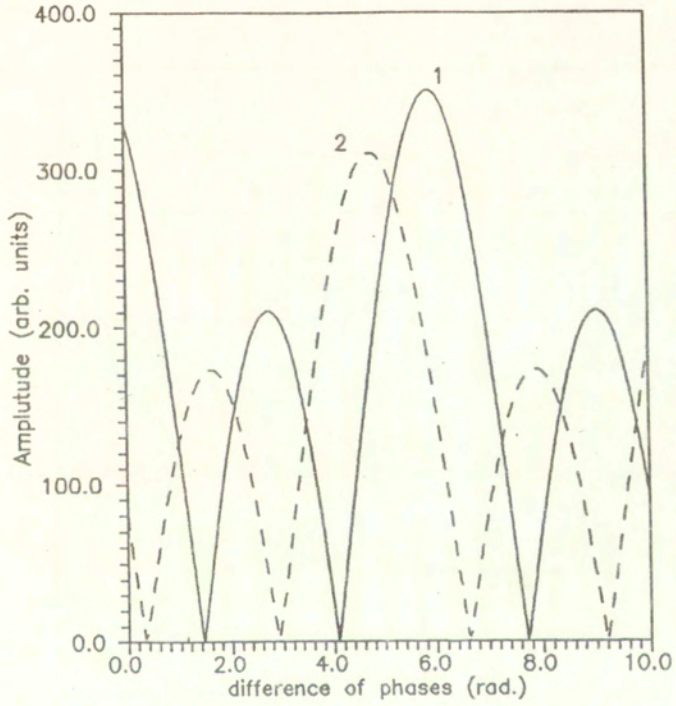

Fig.10. Dependence of PA response amplitude on difference of phases $\Delta\varphi=\varphi_0-\varphi$ (Ω=500Hz, d=1mm):

1- with regard to gyrotropy ($\gamma'=10^{-4}$, $\gamma''=10^{-5}$);

2- without regard to sample gyrotropic characteristics.

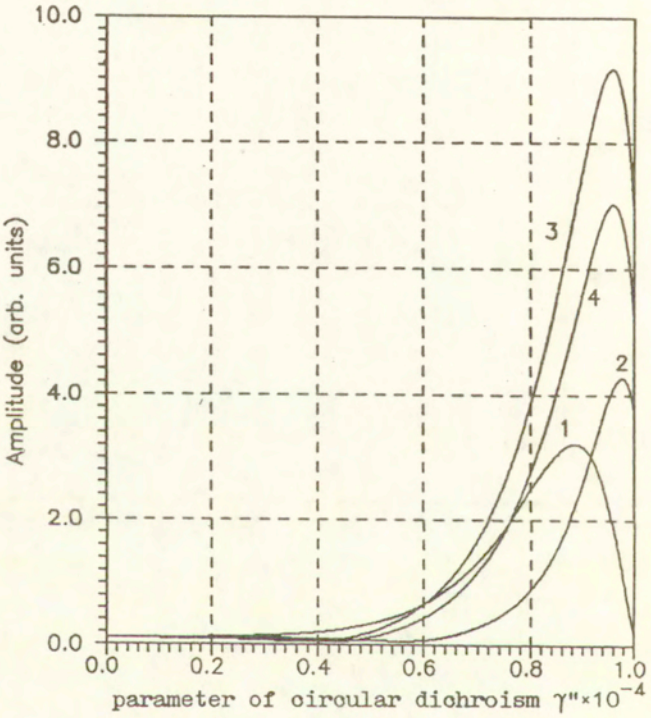

Fig.11. Dependence of PA signal amplitude q on value of γ"parameter of circular dichroism at different values of the phase difference: ($\Delta\varphi=\varphi_o-\varphi$, rad): 1-0, 2-$\pi/4$, 3-$\pi/2$, 4-$\pi$.

controlling amplitude and phase characteristics of a generating PA signal.

2.7. Photoacoustic response of the two-layer sample.

Possessing high inform, sensitivity and quickness PA method finds application in studying multilayer media [45-47], thin films sputtered on dielectric and conducting backings [48,49], in investigating optically and thermally homogeneous solids [42,50]. Many elements of modern electronic techniques include, as is known, multilayer structures containing backings made of natural gyrotropic and magnetoactive crystals such as quartz, bismuth germanate, bismuth silicate,lithium iodate and others. Until now investigation of layer samples have been carried out with the help of PA method without taking into consideration gyrotropy effects [45,50] (for details see references in [51]). Note, that unlike non-gyrotropic samples PA signal formation in the media having spatial dispersion is more complex and has characteristic properties [14,9], connected with circular and linear dichroism display.

In this section amplitude and phase characteristics of PA signal in natural gyrotropic two-layer absorbing sample have been investigated taking into consideration multibeam interference within the layers.

Energy Dissipation.

Solution of the problem stated will be fulfilled within the limits of the method of gas-microphone registration of PA signal. Let a plane electromagnetic wave having amplitude modulation frequency Ω normally fall on the surface of two-layer isotropic-

gyrotropic absorbing sample which had been put in PA cell. For calculation of energy dissipation in a unit of a sample volume we shall solve a boundary problem in geometry shown at Fig.12.

Basing on Makswell's equations for plane monochromatic waves $\underline{D}=-[\underline{m}\ \underline{E}]$, $\underline{B}=[\underline{m}\ \underline{H}]$ ($\underline{m}$ - vector of refraction [3]), material equations for gyrotropic media, as well as on conditions of circular polarization $\underline{E}_{\mp}=\mp i[\underline{n}\ \underline{E}_{\mp}]$, $\underline{H}_{\mp}=\mp i[\underline{n}\ \underline{H}_{\mp}]$ [3] and demands of continuity of tangential components of electromagnetic fields on borders of media partition, we shall obtain the system of 12 scalar equations in relation to unknown complex amplitudes $E'_{\mp}$, $E_{1,2\mp}$, $E'_{1,2\mp}$ the solution of which is represented as:

$$E_{1\mp} = BCE_{\mp},\quad E'_{1\mp} = CE_{\mp},$$

$$E_{2\mp} = exp[-i(\varphi_{2\mp}+\varphi_{1\mp})]DE_{\mp}, \qquad (2.7.1)$$

$$E'_{2\mp} = exp[-i(\varphi_{2\mp}+\varphi_{1\mp})]DE_{\mp}/A,$$

where

$$A = \frac{n_{20}+n_3}{n_{20}-n_3}\,exp[-i(\varphi_{3+}+\varphi_{3-})],\quad \varphi_{3\mp} = -\frac{2\pi}{\lambda}n_{2\mp}d_2,$$

$$B = \frac{A(n_{10}+n_{20})+(n_{10}-n_{20})exp[-i(\varphi_{2+}+\varphi_{2-})]}{A(n_{10}-n_{20})+(n_{10}+n_{20})exp[-i(\varphi_{2+}+\varphi_{2-})]}\,exp[-i(\varphi_{1+}+\varphi_{1-})],$$

$$C = \frac{2n_1}{B(n_1+n_{10})+(n_1+n_{10})},\quad \varphi_{1,2\mp} = -\frac{2\pi}{\lambda}n_{1,2\mp}d_1,$$

$$D = \frac{(n_{10}+n_{20})BC-(n_{10}-n_{20})(BC+C-1)exp[-i(\varphi_{1+}+\varphi_{1-})]}{2n_{20}exp[-i(\varphi_{1+}+\varphi_{1-})]},$$

$$n_{10} = (n_{1+}+n_{1-})/2,\quad n_{20} = (n_{2+}+n_{2-})/2,$$

$$n_{t\pm} = \sqrt{\varepsilon_t} \pm \gamma_t, \quad t=1, \quad E_{\pm} = \frac{1}{\sqrt{2}} \cdot \frac{1 \pm \tau}{\sqrt{1+\tau^2}} E,$$

τ, E is ellipticity and tension of the electric field of an incident light wave; d_1, d_2 - thickness of layers.

Dissipation of energy in each layer according to [4] is defined by correlations

$$Q_{1+} = \frac{cn'_{10}}{2\lambda} |\underline{E}^1_{\pm}|^2 \left(\frac{\varepsilon''_1}{2\sqrt{\varepsilon'_1}} \pm \gamma''_1 \right), \qquad (2.7.2)$$

$$Q_{2+} = \frac{cn'_{20}}{2\lambda} |\underline{E}^2_{\pm}|^2 \left(\frac{\varepsilon''_2}{2\sqrt{\varepsilon'_2}} \pm \gamma''_2 \right),$$

where $\underline{E}^1_{\pm} = \underline{E}_{1\pm} + \underline{E}'_{1\pm}$; $\underline{E}^2_{\pm} = \underline{E}_{2\pm} + \underline{E}'_{2\pm}$. It is worth to note that polarization of electric field tension vectors while solving a boundary problem was given in explict form [4]: $\underline{E} = E\underline{e}$, $\underline{e} = (\underline{a} + i\tau\underline{b})/\sqrt{1+\tau^2}$ is elliptic polarization vector, $\underline{a}$ and $\underline{b}$ are unit vectors of main axes of a polarization ellipses or $\underline{E} = E_+\underline{e}_+ + E_-\underline{e}_-$, $\underline{e}_{\pm} = (\underline{a} \pm i\underline{b})/\sqrt{2}$ are circular polarization vectors.

Using the results of solution of a boundary problem (2.7.1) and taking into consideration (2.7.2) we can obtain for $Q_{\pm}$ following expressions, which obviously depend on ellipticity of the incident light wave τ:

$$Q_{1\pm} = A^1_{\pm} exp(-\alpha_{\pm} x) + A^2_{\pm} exp(\alpha_{\pm} x), \qquad (2.7.3)$$

$$Q_{2\pm} = B^1_{\pm} exp(-\beta_{\pm} x) + B^2_{\pm} exp(\beta_{\pm} x).$$

In (2.7.3) following designations are used

$$A^1_{\pm} = \frac{cn'_{10}}{2\lambda} \left(\frac{\varepsilon''_1}{2\sqrt{\varepsilon'_1}} \pm \gamma''_1 \right) Q_{\pm}, \quad A^2_{\pm} = \frac{cn'_{10}}{2\lambda} \left(\frac{\varepsilon''_1}{2\sqrt{\varepsilon'_1}} \pm \gamma''_1 \right) R_{\pm},$$

$$B^1_{\pm} = \frac{cn'_{20}}{2\lambda}\left[\frac{\varepsilon''_2}{2\sqrt{\varepsilon'_2}} \pm \gamma''_2\right] Y_{\pm},\quad B^2_{\pm} = \frac{cn'_{20}}{2\lambda}\left[\frac{\varepsilon''_2}{2\sqrt{\varepsilon'_2}} \pm \gamma''_2\right] Z_{\pm},$$

$$Q_{\pm} = |BCE_{\pm}|^2,\quad R_{\pm} = |CE_{\pm}|^2,\quad Y_{\pm} = |DE_{\pm}|^2 X_{\pm},$$

$$Z_{\pm} = |DE_{\pm}|^2 X_{\mp}/|A|^2,\quad X_{\pm} = exp[-(4\pi/\lambda)d_1(n''_{2\pm}+n''_{1\mp})],$$

$$\alpha_{\pm} = (4\pi/\lambda)n''_{1\pm},\quad \beta_{\pm} = (4\pi/\lambda)n''_{2\pm}.$$

The given correlations (2.7.3) have been received with accuracy to the first order including gyrotropy parameters and have summands responsible for multibeam interference inside the layer sample.

Amplitude and Phase characteristics

Distribution of temperature fields in PA cell is defined by the correlation of optical, thermophysical and geometric parameters of gyrotropic samples, the backing and detector gas. A joint solution of the system of equations for heat conductivity taking into consideration (2.7.3) for every PA cell region under condition on borders of temperature continuity and temperature gradient on borders of regions partition lets us find a complex amplitude of the temperature field on the border of gyrotropic sample - detector gas [52]

$$\theta = \frac{1}{\Delta}\left(G_+ æ^1_+ + G_- æ^1_- + H_+ æ^2_+ + H_- æ^2_-\right), \qquad (2.7.4)$$

where

$$G_{\pm} = (A^1_{\pm}+A^2_{\pm})/2k_{s1}(\alpha^2_{\pm}-\sigma^2_{s1}),$$

$$H_{\pm} = (B^1_{\pm}+B^2_{\pm})exp(-\beta_{\pm}d_1)/2k_{s2}(\beta^2_{\pm}-\sigma^2_{s2}),$$

$$\Delta = (s-1)[(b+1)(1-g)\xi_1^{-1}\xi_2+(b-1)(1+g)\xi_1\xi_2^{-1}] +$$

$$+ (s+1)[(b+1)(1+g)\xi_1\xi_2+(b-1)(1-g)\xi_1^{-1}\xi_2^{-1}];$$

$$\text{æ}^1_{\pm} = (r^1_{\pm}-1)(b-1)(s-1)\xi_1\xi_2^{-1} - (r^1_{\pm}+1)(b-1)(s+1)\xi_1\xi_2 +$$
$$+ (r^1_{\pm}+1)(b+1)(s-1)\xi_1^{-1}\xi_2 - (r^1_{\pm}-1)(b+1)(s+1)\xi_1\xi_2 +$$
$$+ 2(b-1)(s+r^1_{\pm})\xi_2\eta^1_{\pm} + 2(b+1)(s-r^1_{\pm})\xi_2\eta^1_{\pm};$$
$$\text{æ}^2_{\pm} = 4s(b-r^2_{\pm})\eta^2_{\pm} - 2s(b-1)(1+r^2_{\pm})\xi_2^{-1} - 2s(b-1)(1-r^2_{\pm})\xi_2;$$
$$g = k_g\sigma_g/k_{s1}\sigma_{s1};\ b = k_b\sigma_b/k_{s2}\sigma_{s2};\ \eta^1_{\pm} = exp(-\alpha_{\pm}d_1);$$
$$r^1_{\pm} = \alpha_{\pm}/\sigma_{s1};\ r^2_{\pm} = \beta_{\pm}/\sigma_{s2};\ \eta^2_{\pm} = exp(-\beta_{\pm}d_1);$$
$$s = k_{s2}\sigma_{s2}/k_{s1}\sigma_{s1};\ \xi_i = exp(\sigma_{si}d_{si}),\quad i=1,2;$$

$\sigma_{si}=(1+i)\alpha_{si}$; $\alpha_{si}=\sqrt{\Omega/2\beta_{si}}$ is coefficient of thermal diffusion i-th layer, β_{si} is coefficient temperature conductivity of i-th layer. If in the obtained for θ expression one neglects parameters of circular dichroism layers γ_1'', γ_2'' and multipliers responsible for multibeam interference and to take $\tau=0$ (a case of linear polarization of incident light wave), then from (2.7.4) follows a result, coinciding with the accuracy to a constant multiplier with given one above in [47] for non-gyrotropic samples.

Further we shall use numerical and graphic methods of analysis. With the help of correlations (2.7.4) dependence of amplitude and the phase of PA signal on modulation frequency of the incident light Ω and thicknesses of the layer sample d_1, d_2 has been analyzed at an arbitrary value of ellipticity of the incident light beam τ. We shall mention here most interesting in our new results.

Complex oscillation dependence (Fig.13) of PA response value on the thickness of the first layer d_1 ($d_1=0\div3\cdot10^{-4}$m) at $d_2=const$, conditioned by interference effects inside the two-

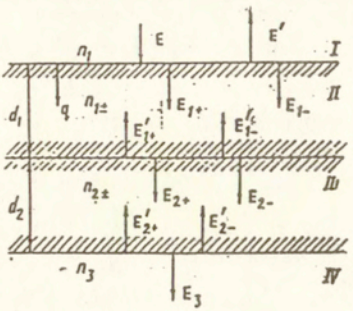

Fig.12. Transversing by plane electromagnetic wave gyrotropic two-layer sample

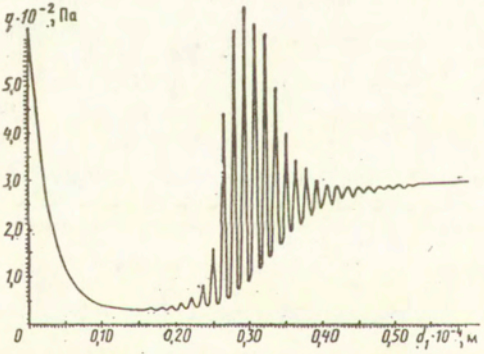

Fig.13. Dependence of PA signal amplitude on the thickness of the first layer; Ω=150Hz, $E=1\cdot10^{-3}$V/m, $\lambda=5.5\cdot10^{-7}$m, $\varepsilon_1''=5.6\cdot10^{-2}$, $\gamma_1''\sim1\cdot10^{-5}$, $\beta_{s1}=0.628$W/m·K, $\varepsilon_2''=1\cdot10^{-2}$, $\gamma_2''\sim1\cdot10^{-5}$, $\beta_{s2}=0.46\cdot10^{2}$W/m·K, $d_2=0.1\cdot10^{-2}$m.

layer sample. As follows from the graph, on the increase of the thickness of the first layer smoothing out of oscillations and saturation of PA signal amplitude is observed, i.e. a case of PA opacity is realized, appearing when the length of thermal diffusion $\mu_{s1}=\alpha_{s1}^{-1}$ and thickness of the layer d_1 coincide.

It is shown that at the region of the low modulation frequencies (up to 200Hz) dependence of PA signal amplitude q on modulation frequency has a distinctly expressed minimum (Fig.14,a) for which are responsible contributions of the waves reflected from the borders inside the layer sample. It is characteristic that PA signal phase by π ($\Omega\tilde{}$49Hz) experiences a leap at this moment (Fig.14,b).

If reflection from the borders of the layer medium is neglected then dependence $q=f(\Omega)$ becomes traditional for PA spectroscopy of single-layer media, near to exponential.

Note, that in some particular cases expression (2.7.4) is essentially simplified and its analytical investigation becomes possible. We shall examine, for example, a layer sample for which the first layer is optically clear and thermally thick ($\mu_{a\pm}>d_1$, $\mu_{s1}<d_1$, $\mu_{s1}\ll\mu_{a\pm}$, $\mu_{a\pm}=\alpha_{\pm}^{-1}$ is the length of optic absorption for clockwise and counterclockwise circular polarization of the incident light wave), and the second one is optically opaque and thermally thick ($\mu_{s2}\ll d_2$, $\mu_{s2}\ll\mu_{\beta\pm}$, $\mu_{\beta\pm}=\beta^{-1}\ll d_2$). When $\eta_{\pm}^1\tilde{}1-\alpha_{\pm}d_1$, $\eta_{\pm}^2=0$, $\xi_{1,2}^1=0$ and from (2.7.4) one can obtain

$$\theta = \frac{1}{1+g}\left[\frac{r_+^1-1}{\alpha_+^2-\sigma_{s1}^2}E_+^0 + \frac{r_-^1-1}{\alpha_-^2-\sigma_{s1}^2}E_-^0\right] \qquad (2.7.5)$$

$$E_{\pm}^0 = 1/2k_{s1}(A_{\pm}^1 + A_{\pm}^2).$$

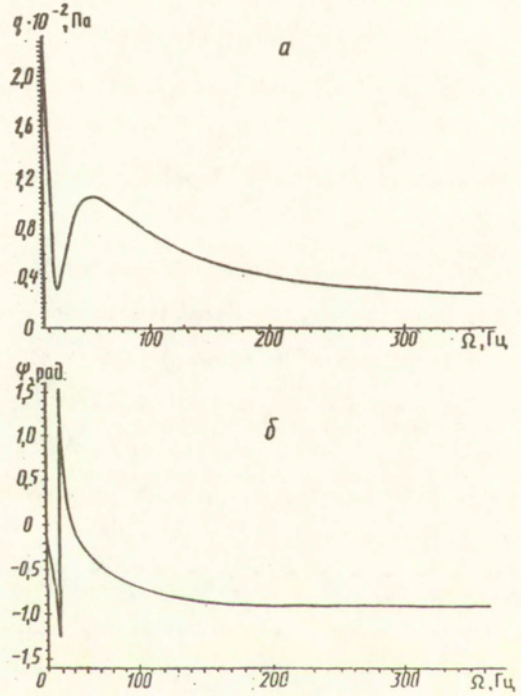

Fig.14. Dependence of the amplitude (a) and phase (b) of PA signal on modulation frequency: $E=1\cdot10^{-3}$V/m, $\lambda=5.5\cdot10^{-7}$m, $\varepsilon_1''=5.6\cdot10^{-2}$, $\gamma_1''\sim1\cdot10^{-5}$, $\beta_{s1}=0.628$W/m·K, $d_1=0.3\cdot10^{-3}$m, $\varepsilon_2''=1\cdot10^{-2}$, $\gamma_2''\sim1\cdot10^{-5}$, $\beta_{s2}=0.46\cdot10^{2}$W/m·K, $d_2=0.5\cdot10^{-2}$ m.

Considering further a case of circular polarization of the incident radiation ($\tau=\pm 1$) we obtain for PA signal amplitude and phase the following expressions:

$$q_{\pm} = \frac{cn'_{10}\varkappa'_0\sqrt{\beta_g}|CE|^2}{4\lambda\rho_{s1}c_{s1}\Omega^{3/2}}\left[\frac{\varepsilon''_1}{2\sqrt{\varepsilon'_1}}(|B|^2+1) \pm \gamma''_1(|B|^2-1)\right], \qquad (2.7.6)$$

$$\Psi_{\pm} = \frac{\pi}{4} + arctg\,\frac{1-(a_{\pm}/2a_{s1})+(a_{\pm}^3/4a_{s1}^3)}{1-(a_{\pm}/a_{s1})+(a_{\pm}^2/2a_{s1}^2)}, \qquad (2.7.7)$$

where ρ_{s1}, c_{s1} are density and specific heat resistance of the first layer, β_g is coefficient of temperature conductivity of the detector gas, $\chi'_0=\sqrt{2a_g}\chi_0$.

From (2.7.6), (2.7.7) follows, that the resulting signal changes depending on amplitude modulation frequency according to the law $\Omega^{-3/2}$, and the phase shift within the limits $a_{s1}\gg a_{\pm}$ and tends to a constant value, equal to $\pi/2$.

Having calculated the difference of absolute values q_+ and q_- on the basis of (2.7.6) we find

$$\Delta q = \frac{cn'_{10}\varkappa'_0\sqrt{\beta_g}|CE|^2(|B|^2-1)}{2\lambda\rho_{s1}c_{s1}\Omega^{3/2}}\gamma''_1,$$

i.e. for defining the parameter of circular dichroism of the first layer γ''_1 in the given particular case it is enough the measure differences of PA signals, responsible for the left and right circular polarization of the incident light.

3. PHOTOACOUSTIC TRANSFORMATION IN MAGNETOACTIVE MEDIA.

Cubic crystal, placed in external magnetic field, behaves relatively many optic characteristics similarly to isotropic medium with natural optical activity. It exhibits in the rotation of light wave polarization plane, having gone through the crystal, and the appearance of magnetic circular dichroism in absorption strip [53]. However, certain differences exist in exhibiting magnetic and natural gyrotropy phenomenon, which are connected in the first place with appearance of noninvertibility effects in limited magnetoactive media [12,54,55]. Besides, the appearance of circular dichroism in magnetoactive medium is also possible at real gyration parameter, while in naturally gyrotropic gyrotropic media similar effect is absent [54]. In development of optical characteristics of more complex magnetic structures, for example, absorbing antiferromagnetic crystals, nonlinear dissipative effects can appear, i.e. along with linear, quadric in field $\underline{H}$, magnetic circular dichroism [56], whose spectra contain extra information about principle and excited energetic states of antiferromagnetic.

In this connection it will be interesting to study PA transformation in media with Faraday effect.

3.1. Amplitude-phase characteristics of PA signal in magnetoactive media.

Intensity modulated elliptically polarized incident light wave causes thermoelastic oscillations in absorbing magnetoactive medium, the value of which is proportional the velocity of energy dissipation $Q=Q_{+}+Q_{-}$ [57]

$$Q_{\pm} = \frac{cn^2(|n_{\pm}|^2)^2(1\pm\tau)^2}{4\lambda|n_{\pm}+n|^2(1+\tau^2)}\,|H_0|^2(\varkappa_0''\mp G_z'')\exp(-\alpha_{\pm}z), \quad (3.1.1)$$

where $G_z''=\underline{n}\,\underline{G}''$ is the projection of complex vector imaginary part of magnetic gyration $\underline{G}$ on the direction of wave normal $\underline{n}$, $\alpha_{\pm}=(4\pi/\lambda)\cdot n_{\pm}''$, $n_{\pm}''\approx 1/2\varepsilon_0'\sqrt{\varepsilon_0'}\alpha_{\pm}^0$, $\alpha_{\pm}^0=\varkappa_{\pm}''\mp G_z''$, $\varkappa_0''=\varepsilon_0''/\varepsilon_0'^2$. Expression (3.1.1) is given for the case of semiinfinite medium. Making use of standard boundary conditions and following the method of calculation of PA signal (gas-microphone method of registration) [1], taking into account (3.1.1), we may write for amplitude of resulting pressure of detector gas the following expression [57]

$$\theta = \frac{cn^2A_0|H_0|}{8\lambda k_s(1+\tau^2)}\left[\frac{(r_+-1)(1+\tau)^2}{\alpha_+^2-\sigma_s^2}\,a_+ + \frac{(r_--1)(1-\tau)^2}{\alpha_-^2-\sigma_s^2}\,a_-\right], \quad (3.1.2)$$

where $Q_{\pm}=a_{\pm}^0\alpha_{\pm}^0$, $a_{\pm}^0=(|n_{\pm}|^2)^2/|n_{\pm}+n|^2$, $A_0=\gamma_0P_0/\sqrt{2}a_g\,lgT_0(g+1)$.

As it follows from (3.1.2) the value of PA signal essentially depends on the value and orientation of external magnetic field and the state of polarization of light incident on the sample under investigation.

In the case of circular polarization of incident light ($\tau=\pm1$) for difference in amplitudes of PA signals we can write down [58]

$$\Delta q = \frac{\sqrt{2}\pi A_0a_0G_z''}{(\varkappa^4+4a_s^4)^2}\cdot\frac{\varkappa^9+\beta_1+16a_s^9}{(\varkappa^6+\beta_2+8a_s^6)^{1/2}}, \quad (3.1.3)$$

$$a_0=(\varepsilon_0'^2+\varepsilon_0''^2)/(\sqrt{\varepsilon_0'^2+\varepsilon_0''^2}+2n\sqrt{\varepsilon_0'}+n^2),\ \varkappa=4\pi/\lambda\varkappa_0'',$$

$$\beta_1=-a_s\varkappa(3\varkappa^7-4a_s\varkappa^6+16a_s^4\varkappa^3-16a_s^5\varkappa^2+16a_s^7),$$

$$\beta_2=-2a_s\varkappa(\varkappa^4-a_s\varkappa^3-2a_s^3\varkappa+4a_s^4).$$

Received expression (3.1.3) we will analyze in two limiting

cases of relationship between lengths of optical absorption $\mu_{\alpha}=\alpha^{-1}$ and thermal diffusion $\mu_s=a_s^{-1}$.

1. If the optical absorption length is much less than thermodiffusion length ($\mu_{\alpha} \ll \mu_s$), what occurs in strongly absorbing crystals, we will derive from (3.1.3)

$$\Delta q = \frac{\Delta a_0}{\alpha^2} G''_z \qquad (3.1.4)$$

whence hyperbolic amplitude dependence of difference PA signal on incident light frequency modulation follows $\Delta q \sim \Omega^{-1/2}$.

2. In the case of crystals with slight absorption, when value $\mu_{\alpha} \gg \mu_s$, in conformity with (3.1.3), is determined by expression

$$\Delta q = \frac{\Delta a_0}{\sqrt{2} a_s^2} G''_z \qquad (3.1.5)$$

and is proportional to $\Omega^{-3/2}$. Note, that received dependencies of PA signal on incident light modulation frequency in magnetoactive semiinfinite crystals, as one would expect, coinside with quoted before in [59] for medium with natural optical activity. As it also follows from (3.1.3)-(3.1.5) that experimental amplitude measurement of difference PA signal allows to determine magnetic circular dichroism parameter G''_z.

3.2. PA transformation in magnetoactive ε-isotropic crystals.

In this section we will consider PA transformation in magnetoactive crystals with traversing dispersion curves of principle tensor values of dielectric permeability. As a result of this, possibility of linear dichroism at $\varepsilon'_e-\varepsilon'_o=0$ will be taken into

account, what is implemented when relationship is satisfied $\varepsilon_e=\varepsilon_o(1+2i\Delta)$, $\Delta=\varepsilon_e''/2\varepsilon_o'$ [60].

The solution of the problem formulated can be realized in the scope of gas-microphone method for PA signal registration. We will proceed from material equations [3]

$$\underline{E} = \left[\varepsilon^{-1} + i(g)^{\times}\right]\underline{D}, \qquad \underline{B} = \underline{H}, \quad (\mu = 1), \tag{3.2.1}$$

where $g^{\times}$ is the antisymmetric complex tensor of the second rank, dual to magnetic gyration vector g, real part g'of which is responsible for specific rotation of polarization plane, and g" describes magnetic circular dichroism.

The density of thermal sources power in thermal conduction equation determined by (3.21) and the results of [60] can be presented in the form $Q=Q_+ + Q_-$

$$Q_{\pm} = \frac{\omega}{4\pi} |A_{\pm}|^2 \frac{(1+|\underline{n}\,\underline{G}|^2}{n_o} n_z'' \exp(-\alpha_{\pm} z) \tag{3.2.2}$$

where $\alpha_{\pm}=2\omega n_{\pm}''/c$, $n_{\pm}''=n_o(\Delta \sin^2\chi \pm \sqrt{r}\sin(\varphi/2))/2$, χ is the angle between optical axis of the crystal and the direction of wave vector $\underline{n}$, $n_o=\sqrt{\varepsilon_o}$, $\Delta=\varepsilon_e''/2\varepsilon_o'$, $r=\sqrt{a^2+b^2}$, $\cos\varphi=a/r$, $\sin\varphi=b/r$, $a=\varepsilon_o^2(\underline{ng}')^2-(\underline{ng}'')^2-\Delta^2\sin^4\chi$, $b=2\varepsilon_o^2(\underline{ng}')^2(\underline{ng}'')^2$, $A_{\pm}=(1+\tau^2)H_o[\alpha_{\pm}(1\pm\tau\tau_o)+i(\tau_o\pm\tau)\alpha_{\mp}]^{-1}$, $\alpha_+=\cos\psi_o$, $\alpha_-=\sin\psi_o$, τ, ψ_o are ellipticity and azimuth of the major axis of isonormal wave polarization ellipse, H_o, τ_o are intensity and ellipticity of incident light wave.

Joint solution of a set of thermal conduction equations for each region of PA cell taking into account (3.22) allows to find an amplitude of temperature field θ on magnetoactive sample -

detector gas boundary. An expression for θ in case of thermally thick and optically transparent sample ($\tau_0=\pm 1$, incident light is circular polarized) has the form

$$\theta_{\pm}=\frac{R_{\pm}}{g+1}\,\frac{r_{\pm}-1}{a_{\pm}^2-\sigma_s^2}, \qquad (3.2.3)$$

where $r_{\pm}=(1-i)a_{\pm}/2a_s$, $R_{\pm}=\omega(2\pi n_0)^{-1}|A_{\pm}|^2(1+|n\underline{g}|^2)n''_{\pm}$. Due to (3.2.3) it is easy to determine amplitude and phase of PA signal [61]

$$q_{\pm}=\frac{\varkappa_0 A_0\varepsilon_0^2(n\underline{g}')(n\underline{g}'')}{\sqrt{\varepsilon_0^2[(n\underline{g}')^2-(n\underline{g}'')^2]-\Delta^2 sin^4\chi}} \qquad (3.2.4)$$

$$\Phi_{\pm}=\frac{\pi}{4}-arctg\frac{1-2\mu_{a\pm}^2\mu_s^{-2}(1-2\mu_{a\pm}\mu_s^{-1})}{1-2\mu_{a\pm}\mu_s^{-1}(1-\mu_{a\pm}\mu_s^{-1})} \qquad (3.2.5)$$

Here $\varkappa_0=\gamma_0 P_0/\sqrt{2}lg\alpha_g T_0$ is the standard factor in PA spectroscopy (notations see e.g., in [52]), $A_0=(1-\tau)^2|H_0|^2$, $\mu_{a\pm}$, μ_s are the lengths of optical absorption and thermal diffusion correspondingly.

As it follows from (3.2.4) for magnetoactive crystals with high dielectric permeability $\varepsilon\sim 10^4$–10^5, e.g., in segnetoelectrics, there is possibility to express in the explicit form magnetic circular dichroism parameter G'' by means of the difference of PA signal amplitude $\Delta q=|q_+-q_-|$

$$\Delta q=\frac{4\pi}{\lambda}\varkappa_0\varepsilon_0^{3/2}(n\underline{g}''),$$

what is true generally saying at small enough angle values χ.

Evaluation of PA signal phase with respect to (3.2.5) allows in magnetoactive crystals with ε-isotropic point of linear birefringence to find linear dichroism Δ parameter.

3.3. Nonreciprocal effects in PA spectroscopy of magnetoactive media.

As is known [62-64], optical nonreciprocal effects occur in gyrotropic crystals under the influence of external magnetic field. Noninvertibity of light propagation depends on the difference of phase velocities of isonormal waves in opposite directions. There is also polarizing nonreciprocity of direct and approaching waves [64], connected with different ellipticity of eigenwaves. If gyrotropic crystal placed in external field, can absorb, one more similar effect - dichroic nonreciprocity of direct and approaching waves, caused by different absorption of orthogonally polarized isonormal waves, is likely to appear.

Further we investigate possibility of using PA spectroscopy method for measuring the value of dichroic nonreciprocity in gyrotropic media.

Let us proceed from material equations [62]

$$\underline{D} = \left[\varepsilon + i(\gamma\underline{h})^{\times}\right]\underline{E} + i\alpha\underline{H}, \qquad (3.3.1)$$

$$\underline{B} = \underline{H} - i\alpha\underline{E}, \quad (\mu = 1),$$

describing naturally active medium placed in external magnetic field. In (3.3.1) $(\gamma\underline{h})^{\times}$ is the antisymmetric tensor of the second rank dual to vector of magnetic gyration $(\gamma\underline{h})$, the imaginary part of which γ'' describes magnetic circular dichroism, $\alpha=\alpha'+i\alpha''$, where α'' is the intensity of external magnetic field.

The solution for the equation of normals for plane waves (3.3.1) and Maxwell equations $\underline{m}^{\times}\underline{E}=\underline{B}$, $\underline{m}^{\times}\underline{H}=-\underline{D}$, allows to get for the refractive indexes of circular polarized waves expressions [62]

$$n_{\pm} = \sqrt{\varepsilon_0} \pm (\alpha_0 + \frac{\gamma_0}{\sqrt{\varepsilon_0}} \underline{n}\,\underline{h}), \qquad (3.3.2)$$

where $\underline{n}$ is the unit vector of wave normal, and the parameters ε_0, α_0, γ_0 correspond to isotropic media without center of symmetry. If we single out imaginary part in (3.3.2) accurate to the first order by gyration parameter, we will get

$$n''_{\pm} = \frac{\varepsilon''_0}{2\sqrt{\varepsilon'_0}} \pm \left[\alpha''_0 + \frac{\gamma''_0 \sqrt{\varepsilon'_0}}{2(\varepsilon'_0 + (\varepsilon''^2_0/4\varepsilon'_0))} \underline{n}\,\underline{h}\right]. \qquad (3.3.3)$$

In the case in question the investigated sample is placed into gas-microphone rotating cell for measurement in the conditions of capacity [44], the cell being in external magnetic field h. Having chosen optimal case for the investigation of thermally thick and optically transparent sample, we can write an expression for amplitude of PA signal [65]

$$\theta_{\pm} = \frac{\text{æ}J\alpha_{\pm}}{(g+1)2k_s} \cdot \frac{(r_{\pm}-1)}{(\alpha^2_{\pm}-\sigma^2_s)}, \qquad (3.3.4)$$

whence it follows

$$q_{\pm} = A \frac{1}{\Omega\,\alpha_{\pm}},$$

where $\alpha_{\pm} = 4\pi n''_{\pm}/\lambda$, Ω is the modulation frequency of the incident light beam, A is the value, determined by the parameters of medium and geometry of PA cell. Then

$$\delta q = \frac{\alpha_+ - \alpha_-}{\alpha_+ \alpha_-} \cdot \frac{A}{\Omega}.$$

Substituting (3.3.3) in (3.3.4) we will have

$$\delta q_{1,2} \sim 2\alpha''_0 \pm \gamma''_0\,\underline{n}\,\underline{h},$$

whence it follows that the difference of PA signal amplitudes measured in direct and opposite directions differs on value, proportional to double value of magnetic circular dichroism γ''_0. It is not difficult also the show that the difference of PA signal phases for the waves with right and left cirular polarizations $\Delta\phi=|\phi_+-\phi_-|=arctg((x-y)/(1+xy))$ (where $x=1-2\ae_+^2(1-2\ae_+)$, $y=1-2\ae_-(1-2\ae_-)$, $\ae_\pm=a_s/a_\pm$), measured in opposite directions differs on the value $2\gamma''_0$, magnified into $f(\ae_\pm)$-function of optical and thermal parameters of the medium, determined by the relation

$$f(\ae_\pm)=\frac{4(\ae_++\ae_-)[(\ae_++\ae_-)-1]+8\ae_+^2\ae_-^2(1-(\ae_++\ae_-)/(\ae_+\ae_-))-2}{(1+2\ae_+(1-\ae_+))(1-2\ae_-(1-\ae_-))},$$

a_s is the coefficient of thermal diffusion of the sample.

In such a manner the measurement of amplitude and phase characteristics of PA signal, corresponding to circular polarization of incident light, allows to determine, as was shown above, the value of dichroic nonreciprocity of gyrotropic media.

4. PHOTOACOUSTIC TRANSFORMATION IN ANISOTROPIC GYROTROPIC CRYSTALS.

The study of PA transformation in natural gyrotropic and magnetoactive absorbing media has been conducted in previous sections without taking into account the influence of anisotropic properties of objects under investigation. In formulating theory of PA interaction in uniaxial crystals in common case one must take into account anisotropy of optical as well as thermal and acoustical properties of gyrotropic samples, which is a very complicated task in finding analytical solution for related system of photothermoacoustical equations.

Thermal effects in media with continuous change of optical and thermal properties have been studied on the basis of vector and matrix formalism in [66].

Investigation of photothermal waves propagation in anisotropic media using a related system of three-dimensional thermoacoustical equations have been conducted by authors of [67]. In [68] was shown possibility of describing thermal anisotropy by way of transforming heat conductivity equation in a normalized coordinate system in which heat conductivity equation corresponds in form to isotropic medium, anisotropy effect being included into a thermal source density value. Basing on Green function method [68] one gets a solution to heat conductivity equation with anisotropic source, describing linearized distribution of temperature field in crystallic medium.

Little atention was paid to investigation of PA transformation in crystals with regard to optical anisotropy effects, not saying about gyrotropy.

In this connection we examine possibilities of PA spectroscopy method for defining optical parameters of absorbing gyrotropic uniaxial crystals.

4.1 PA Effect in Uniaxial Gyrotropic Crystals.

Let a modulated Ω frequency electromagnetic monochromatic wave fall normally on the surface of plane parallel crystal plate cut from uniaxial absorbing gyrotropic crystal parallel to optical axis ($\underline{n}, \underline{c}$, $\underline{n}$ and $\underline{c}$ - unit vectors of wave and optical normals respectively) and placed in a PA cell. Description of PA transformation can be attained on the basis of heat conductivity equation

$$k_{ij}\nabla_i\nabla_j T - \rho_c C_s \frac{dT}{dt} = \frac{1}{2} Q(1+exp(i\Omega t)), \qquad (4.1.1)$$

where $Q=Q_o+Q_e$, Q_o, Q_e is energy dissipation with odinary and extraordinary waves, k_{ij} is thermal conductivity tensor. Accurate solution (4.1.1) involves great mathematical difficulties, therefore for the purpose of simplification calculation of PA effect will be done in plane wave approximation. Taking in a view thermal conductivity tensor k_{ij} symmetry, as well as an adopted geometry of interaction (light propagates along the axis z), one can neglect dependence of temperature on coordinates x and y. Then (4.1.1) will take the form

$$\frac{d^2T}{dz^2} - \frac{1}{\beta}\frac{dT}{dt} = \frac{1}{2k} Q(1+exp(i\Omega t)) \qquad (4.1.2)$$

Basing on the results of solution of boundary problem [4] and correlations for energy dissipation we can write [14]

$$Q_{o,e} = \frac{\omega|E|^2\tau_{o,e}}{8\pi(1+\tau^2)G} [\underline{c}\,\underline{n}]\varepsilon''[\underline{c}\,\underline{n}] exp(-\frac{2\omega}{c} n''_{o,e} d), \qquad (4.1.3)$$

where $n_{o,e}=n'_{o,e}+in''_{o,e}$ are indexes of isonormal waves refraction independent of gyration parameters in the first approximation on γ, $G=(1+k'^2-k''^2)+4k'^2k''^2$, $\underline{k}\sim\underline{r}n_o\sim\underline{r}n_e$, $\underline{r}=\underline{n}g/(\varepsilon_e-\varepsilon_o)$, $g=(Sp\gamma-\tilde{\gamma})\underline{n}$ is complex gyration vector, $\gamma=\gamma'+i\gamma''$- pseudotensor of optical activity, τ is ellipticity, $\tau_o=1-2\tau k''+\tau^2|k|^2$, $\tau_e=\tau-2\tau k''+|k|^2$, E, ω are electric field tension and angular frequency of a light wave, d is thickness of a crystal plate.

Calculation of PA signal for a gas - microphone method for registration gives Rosenowaig expression

$$\Delta P(t) = \theta_o exp[i(\Omega t-\pi/4)],$$

where complex amplitude of temperature field θ_o on the gyrotropy crystal-detector gas edges is defined by the expression [14]

$$\theta_o = \frac{N}{1+\tau^2}\left[\frac{r_o-1}{\alpha_o^2-\sigma_s^2}\tau_o + \frac{r_e-1}{\alpha_e^2-\sigma_s^2}\tau_e\right], \qquad (4.1.4)$$

$$N = c|E|^2 æ_o[\underline{o}\,\underline{n}]\varepsilon''[\underline{o}\,\underline{n}]/4\lambda k_s(1+g)G,$$

$$r_{o,e}= (1-i)\alpha_{o,e}/2\alpha_s,\ \alpha_{o,e}= (4\pi/\lambda)n''_{o,e}.$$

The rest of notation is common, see,for example [1,4,22]. Note, that (4.1.4) is given for most interesting case for analysis of thermally thick ($exp(-\sigma_s l)\sim 0$) but optically transparent sample ($exp(-\alpha_{\pm} l)\sim 1-\alpha_{\pm} l$).

As follows from (4.1.4) a resulting signal value is defined by parameters ε'', k'', which characterise absorption anisotropy and dichroism as well as by thermophysical constants of material of a cell, insident light wave elliptisity τ and its modulation frequency Ω.

Evident dependence of θ_o on ellipticity τ lets us consider some particular cases of incident radiaton polarization, quadra-

tic summands by k being neglected as k-value is usually small ($k \sim 10^{-2}-10^{-3}$).

Let incident light wave be linearly polarised and the vector of electric field tension oscillate parallel ($\tau=0$) or perpendicular to ($\tau=\infty$) of a crystal main plane. Then from (4.1.4) follows

$$\theta_{\parallel,\perp} = N(r_{0,e}^{-1})/(\alpha_{0,e}^2-\sigma_s^2). \qquad (4.1.5)$$

In case of circularly polarised incident light ($\tau=\pm 1$) a resulting signal according (4.4) is defined by correlation

$$\theta_{\pm} = \frac{1}{2}N(1\mp k'')\left[\frac{r_0^{-1}}{\alpha_0^2-\sigma_s^2}\tau_0 + \frac{r_e^{-1}}{\alpha_e^2-\sigma_s^2}\tau_e\right], \qquad (4.1.6)$$

The obtained expressions (4.1.5), (4.1.6) let us find PA signals amplitudes and phases. For the purpose of concretizing calculation we shall consider crystals of middle singony classes 32, 422, 622 for which tensors ε and γ in covariant presentation look like [3]

$$\varepsilon = \varepsilon_0-(\varepsilon_e-\varepsilon_0)\underline{o}\,\underline{o}, \quad \gamma = \gamma_1+\gamma_2\underline{o}\,\underline{o},$$

where $\underline{o}\cdot\underline{o}$ is diad, and k''- within the frame of adopted approximation will be represented as follows

$$k'' = n'_e\frac{\underline{n}\cdot\underline{g}''(\varepsilon'_e-\varepsilon'_0)-\underline{n}\cdot\underline{g}'(\varepsilon''_e-\varepsilon''_0)}{(\varepsilon'_e-\varepsilon'_0)^2+(\varepsilon''_e-\varepsilon''_0)^2}. \qquad (4.1.7)$$

Basing on expressions (4.1.5) and correlations $q=[(Re\theta)^2+(Im\theta)^2]^{1/2}$, $\Psi=arctg(Im\theta/Re\theta)$, of PA signals amplitudes and phases we will have [14]

$$q = (N/2a_s)\,[(Re\theta_{\parallel,\perp})^2 + (Im\theta_{\parallel,\perp})^2]^{1/2}, \qquad (4.1.8)$$

$$\Psi_{\parallel,\perp} = -\,arctg\frac{1-(2a_s^2/\alpha_{0,e}^2)(1-2a_s/\alpha_{0,e})}{1-(2a_s/\alpha_{0,e})(1-a_s/\alpha_{0,e})} \qquad (4.1.9)$$

where real and imaginary parts $\theta_{\parallel,\perp}$ are defined as

$$Re\theta_{\parallel,\perp} = (\alpha^3_{0,e}+2\alpha_{0,e}\alpha^2_s-2\alpha^2_{0,e}\alpha_s)/(\alpha^4_{0,e}+4\alpha^4_s)$$

$$Im\theta_{\parallel,\perp} = -(\alpha^3_{0,e}-2\alpha_{0,e}\alpha^2_s+4\alpha^3_s)/(\alpha^4_{0,e}+4\alpha^4_s)$$

In accordance with (4.1.9) calculations of signals phases difference for incident light orthogonal polarisation $\Delta\Phi=|\Phi_\parallel-\Phi_\perp|$ shows that $\Delta\Phi$ is proportional to linear dichroism value $\delta\varkappa=n''_e-n''_o$

$$\Delta\Phi = arctg\left[f(\alpha_s/\alpha_{0,e})\,\frac{\omega}{c}\,\delta\varkappa\right] \qquad (4.1.10)$$

where $f(\alpha_s/\alpha_{0,e})$ are functions of optical and thermal parameters of medium defined from (4.1.9).

If incident wave is circularly polarised then

$$q_{\pm} = (N/4\alpha_s)(1\mp 2k")[(Re\theta_\parallel+Re\theta_\perp)^2 + (Im\theta_\parallel+Im\theta_\perp)^2]^{1/2} \qquad (4.1.11)$$

and as follows from (4.1.11) $k"$ value is defined through relation of module of semidifference of PA signals amplitudes $\Delta q=|q_+-q_-|$ to their sum

$$k" = \Delta q/2(q_++q_-). \qquad (4.1.12)$$

PA signal registered in this case depends in a complicated way on a correlation of birefrigence parameters, optical activity and linear and circular dichroism. But in cases when linear dichroism is much less then birefrigence

$$|\varepsilon''_e-\varepsilon''_o| \ll |\varepsilon'_e-\varepsilon'_o|,$$

and $\alpha'=ng'$ and $\alpha"=ng"$ are of the same order (a situation which is realised, for example, for benzyl crystal in a definite range of waves lengths [69]), $q_{\pm}$ value is proportional to circular dichroism

$$k'' \approx n'_e \alpha''/(\varepsilon'_e - \varepsilon'_o). \qquad (4.1.13)$$

Thus PA signals amplitudes measurements let us find according (4.1.12), (4.1.13) parameters α'' of a circular dichroism, when birefrigence $\varepsilon'_e - \varepsilon'_o$ is known.

In other cases in order to define circular dichroism it is necessary to conduct additional measurements, in particular, real part of α gyration parameter by a method proposed, for example, in [69].

Let us note that absorbing gyrotropic crystals can experience ε-isotropy of linear dichroism and linear birefrigence [69], cross-section points of dispersion curves of tensors real and imaginary parts do not coincide as a rule [69]. We shall further consider these cases.

Let a crystal for the given wave length ε-isotropic by linear dichroism, i.e. $\varepsilon''_e - \varepsilon''_o = 0$. Then from (4.12) follows correlations [14]

$$\alpha'' = \frac{\Delta\varepsilon'}{2n'_e} \cdot \frac{\Delta q}{(q_+ + q_-)}, \qquad (4.1.14)$$

$$\Delta\varepsilon' = N_o^{-1} (2\pi/\lambda)^2 (q_\perp - q_\parallel), \qquad (4.1.15)$$

immediately correlating a circular dichroism parameter with PA signal relative value and anisotropy crystals with amplitudes difference of PA signals, measured respectively at modulation frequencies Ω_1 (vector of $\underline{E}$ incident light wave which is parallel to the crystal main plane) and Ω_2 (vector $\underline{E}$ is perpendicular to a crystal main plane).

If a crystal is ε-isotropic by linear birefrigence $\varepsilon'_e - \varepsilon'_o = 0$ then formulae corresponding to this case are as follows [14]

$$\alpha' = \frac{\Delta\varepsilon''}{2n'_e} \cdot \frac{\Delta q}{(q_+ + q_-)}, \qquad (4.1.16)$$

$$\Delta\varepsilon'' = N_0^{-1}(2\pi/\lambda)^2 \frac{\varepsilon''_e}{\varepsilon'_0}(q_\parallel - q_\perp), \qquad (4.1.17)$$

Thus, experimental measurements of PA signals amplitudes $q_{\mp}$, $q_{\parallel,\perp}$ and their phases $\Phi_{\parallel,\perp}$ for different polarizations of incident light lets us find from (4.1.8)-(4.1.17) the optical parameters of absorbing gyrotropic unaxial crystals near ε-isotropic by linear birefrigence and linear dichroism of points as well as for investigation of dispersionof values δn and k''. It has been found that linear dichroism value can be calculated on the basis PA signals phase difference, wich correspond to orthogonal linear polarization of incident radiation or with the help of PA signals amplitudes difference $q_\parallel$, $q_\perp$ measured at different modulation frequencies.

A registered signal for circular polarization of incident light is a complex function of dichroism and birefrigence linear and circular effects, which makes difficulties in defining circular dichroism in evident view as it was in the case with cubic crystals or with uniaxial crystals along the direction of optical axis. But however, in the case of poorly absorbing crystals whose values α' and α'' are comparable in order it is shown that relative PA signal value is directly proportional to circular dichroism parameter.

4.2 Method of Polarized Modulation in PA Spectroscopy of Gyrotropic Crystals.

Thermal mechanism of exciting thermoelastic waves is based

on modular absorption of incident optical radiation by a medium. The most effective and widely spread is a method of amplitude and amplitude-polarized modulation of a light beam. Investigation of PA transformation in gyrotropic uniaxial crystals with amplitude modulation of absorbing polarized radiation has been conducted in [14] where it is shown that registed PA signal in common cases depends in a complicated way on correlation of a samples optical and themophysical properties. The parameter of circular dichroism can be expressed in explicit form through the amplitude of a relative PA signal only in some particular cases.

As it will be shown further the use of incident radiation polarization modulation lets us simplify solution of a problem on defining optical parameters of absorbing gyrotropic crystals by PA method.

Note, that in [15] PA spectra of linear and magnetic circular dichroism g_{KD} of monocrystal $NdMoO_4$ were received with the help of incident light beam modulation along orthogonal polarizations, threshold sensitivity g_{KD} reaching 10^{-7} value for magnetic field induction 0,7T and polarized modulation frequency 3kHz.

Conduction of PA precise measurements with incident radiation modulation is suppozed to use laser sources having various types of modulaters, linear and circular polarizers. In total such sistems may posess depolarizing properties. An analysis of laser systems polarization states, containing electrical and magnetooptical modulators with partial polarizers hase been made, for example, in [70].

Consider PA transformation in absorbing gyrotropic uniaxial

crystals with the use of polarized modulation*) of partially polarized radiation falling on a crystal sample. Let a partially polarized light beam with polarized modulation frequency Ω normally fall on the surface of absorbing uniaxial gyrotropic crystal, cut parallel to optical axis and located in a PA cell. Volume dissipation of energy at a unit of time which is defined as an intensity difference of passed and reflected beam on the basis of [71] can be presented as follows

$$Q = I_0(1-R)[1-exp(-(\delta''))(ch\Delta''+Psh\Delta''cos2\beta_0 cos\alpha_0+ \qquad (4.2.1)$$
$$+2Pk''(-ch\Delta''+cos\Delta')cos2\beta_0 sin2\alpha_0-2sin2\beta_0(k''sin\Delta'+k'sh\Delta'')],$$

where $\Delta'=(\omega/c)(n_2'-n_1')d$, $\Delta''=(\omega/c)(n_2''-n_1'')d=(\omega/c)\delta æd$, $\delta æ$ - linear dichroism $\delta''=\omega(n_1''+n_2'')d/c$, R is coefficient of reflection, β_0, α_0 is ellipticity and asimuth of a light beam polarized component, P is degree of incident radiation polarization, $k=k'+ik''=n_2\tilde{r}n_1 r$, $r=\underline{n}g/(\varepsilon_e-\varepsilon_0)$, $g=(Sp\gamma-\tilde{\gamma})\underline{n}$ is gyration complex vector, $\underline{n}$ is unit vector of wave gyration, $\gamma=\gamma'+i\gamma''$ is complex pseudotensor of gyration, d is thickness of a plate.

Periodical constant of a temperature field on gyrotropic crystal-detector gas boundary which is responsible for PA signal formation on polarized modulation frequency appears due to dissipation difference of eigenwaves of orthogonal polarizations. Main contribution into a constant component connected with temperature rise in a PA cell to a value of $T_0+\Delta T=const$ (T_0- initial temperature) is defined by absorption of a light beam non- pola-

*) Here and further modulation of polarized component light beam is meant.

rised component. For thermal sources density an equation of crystal sample thermal conductivity for linear ($\beta_0=0$, $\alpha_0=0$, $\pi/2$) or circular ($\beta_0=\pi/4$) polarization of incident radiation polarized component in accordance with (4.2.1) may be written as follows:

$$\Delta Q^{L} = 2I_0(1-R)P\exp(-\delta'')\sin\Delta'', \qquad (4.2.2)$$

$$\Delta Q^{C} = 4I_0(1-R)P\exp(-\delta'')(k''\sin\Delta'+k'\sin\Delta''). \qquad (4.2.3)$$

Supposing that a medium is weakly dichroic and taking into account according to [71] that for crystals of middle syngonies of 32, 422, 622 classes approximated correlations are true $\sin\Delta''\simeq\Delta''(\omega/c)\delta$æd, $k''\sin\Delta'+k'\sin\Delta''\simeq(\omega/c)\alpha''$d ($\alpha''$ is a parameter of circular dichroism) thermal conductivity equation for two particular cases of incident light polarization will be presented as follows

a) linear polarization

$$\nabla^2 T - (1/\Delta\beta_s)dT/dt = -(I_0/2\Delta k_s)[(4\pi/\lambda)(1-R)P]\times \times z\exp(-2\beta z)\delta æ(1+\exp(i\Omega t)) \qquad (4.2.4)$$

$$\Delta\beta_s=\beta_s^{\parallel}-\beta_s^{\perp}, \quad \Delta k_s=k_s^{\parallel}-k_s^{\perp},$$

coefficients of temperature conductivity $\beta_s^{\parallel,\perp}$ are related with coefficients of thermal conductivity $k_s^{\parallel,\perp}$ along orthogonal directions by correlations $k_s=\beta_s/\rho C$, ρ, C is density and specific heat of medium;

b) circular polarization

$$\nabla^2 T - (1/\bar{\beta}_s)dT/dt = -(I_0/2\bar{k}_s)[(4\pi/\lambda)(1-R)P]\times \times z\exp(-2\beta z)\alpha''(1+\exp(i\Omega t)) \qquad (4.2.5)$$

$$\bar{\beta}_s=(\beta_s^{\parallel}+\beta_s^{\perp})/2, \quad \bar{k}_s=(k_s^{\parallel}+k_s^{\perp})/2,$$

Equations (4.2.4, 4.2.5) have exact solution which allows to de-

fine on the basis of wellknown method for PA signal calculation its amplitude and phase characteristics.

Considering practically the most interesting case of thermically thick , but optically transparent sample for a PA signal amplitudes and phase it is easy to obtain following expressions

$$q^{L,C} = \frac{\pi I_0 (1-R) P \delta\alpha_0}{\lambda a_s \sqrt{\beta^4 + 4a_s^4}} G^{L,C} \qquad (4.2.6)$$

$$\Psi = \pi/2 - arctg \frac{\beta^2 + 2a_s^2}{\beta^2 - 2a_s^2}, \qquad (4.2.7)$$

where $G^L = \delta\alpha/\Delta k_s$, $G^C = \alpha''/\bar{k}_s$. As follows from (4.2.6) linear and circular dichroism parameters are directly proportional to a resulting signal amplitude. The degree of incident light polarizations P strongly influences PA response value. A useful signal receives a maximum value in case of full polarizations ($P=1$) of a light beam and decreasing according to linear low in dependence on P tends to 0 in natural polarized light ($P=0$). Phase shift value depends neither on polarization degree, nor on the character of incident radiation polarization but is defined only by correlations for optical absorption $\mu_\beta = (2\beta)^{-1}$ and thermal diffusion $\mu_s = a_s^{-1}$.

Having solved equations (4.2.6), (4.2.7) with regard to parameters desired for $\delta\alpha$, α'', β, it is easy to express them through a PA signal amplitude and phase.

Thus the use of polarized modulation method lets with the help of experimentally measured amplitude q^L, q^C and phase Ψ-characteristics of a PA signal for incident light linear and circular polarization give a full and simple solution to the

problem of definig parameters of absorption β, of linear δæ and circular α" dichroism of uniaxial gyrotropic crystals of middle singonies cut parallel to optical axis.

4.3. PA Transformation in Crystals of Rombic Singony.

Of all crystals possessing optical activity PA effect has been investigated most thoroughly in cubic and uniaxial crystals. For gyrotropic crystals of lower singony specific calculations and experimental investigations have not been conducted up to now as far as we know.

This section is devoted to studying PA transformation in absorbing gyrotropic crystals of rombic singony as well as to finding out possibilities of defining optical parameters of such crystals by PA method.

In PA signal calculation in an examined gyrotropic sample one must take into consideration in general cases anisotropy of optical and thermal properties, however it is too difficult to give a solution of such equation, therefore for simplifying we shall make calculation in plane wave approximation. Let a modulated light wave normally fall on a plane-parallel plate of 222 class crystal, cut perpendicular to axis of 2nd order ($\underline{n} \| \underline{e}_3$, $\underline{e}_3$ is unit vector directed along axis of 2nd order). Using material equation [13] as well as expressions for intensity of electric and magnetic fields of refracted waves [73] it is easy to find energy dissipation

$$Q = \frac{\omega |E_0|^2}{8\pi G(1+\tau_0^2)} [\tau_1 R_1 \exp(-\alpha_1 d) + \tau_2 R_2 \exp(-\alpha_2 d)], \quad (4.3.1)$$

where $R_{1,2} = 1/2 k_s [\underline{e}_{1,2} \varepsilon'' \underline{e}_{1,2} + |k_0|^2 |N_{1,2}| \underline{e}_{2,1} \varepsilon'' \underline{e}_{2,1}]$,

$$G = [1 + k_1'k_2' - k_1''k_2''] + [k_1'k_2'' - k_1''k_2'], \quad \alpha_{1,2} = \frac{4\pi}{\lambda} N_{1,2}'',$$

$$\tau_1 = 1 - 2\tau_0 k_2'' + \tau_0^2 |k_2|^2, \tau_2 = \tau_0^2 - 2\tau_0 k_1'' + |k_1|^2$$

τ_0 is incident light ellipticity, $N_{1,2}$ are complex indices of isonormal waves refraction, $k_{1,2} = k_0 N_{1,2}$, $k_0 = \gamma_0/(\varepsilon_1 - \varepsilon_2)$, $\gamma_0 = \gamma_1 + \gamma_2$. Taking into account expressions for energy dissipation and adopted geometry of interaction as well as neglecting temperature dependence on coordinates x and y, we shall calculate a complex amplitude of temperature field (gas-miorophone method of registration [1]) on the gyrotropic sample-detector gas boundary

$$\theta = \frac{|E_0|^2 \omega}{8\pi(g+1)G(1+\tau_0^2)} \left[R_1 \tau_1 \frac{r_1 - 1}{\alpha_1^2 - \sigma_s^2} + R_2 \tau_2 \frac{r_2 - 1}{\alpha_2^2 - \sigma_s^2} \right].$$

The given expression has been obtained for the case of thermally thick ($exp(-\sigma_s d) = 0$) optically transparent sample ($exp(-\alpha_{1,2} d) \approx 1 - \alpha_{1,2} d$). For the purpose of finding possibilities to define parameters of absorption anisotropy, circular dichroism which define PA signal value an analysis of dependence of θ on ellipticity τ_0 of incident light has been made. At $\tau_0 = 0$ and $\tau_0 = \infty$ expressions for temperature field amplitude look like

$$\theta_{\parallel,\perp} = \frac{|E_0|^2 \omega}{8\pi G(g+1)} R_{1,2} \frac{r_{1,2} - 1}{\alpha_{1,2}^2 - \sigma_s^2}$$

In case of circular polarization of incident light ($\tau_0 = \pm 1$) a resulting signal is defined as follows

$$\theta_{\pm} = \frac{|E_0|^2 \omega}{16\pi G(g+1)} \left[R_1 (1 \mp 2k_2'') \frac{r_1 - 1}{\alpha_1^2 - \sigma_s^2} + R_2 (1 \mp 2k_1'') \frac{r_2 - 1}{\alpha_2^2 - \sigma_s^2} \right]$$

Having done not complex mathematic calculation we find real $Re\theta_{\parallel,\perp}$ and imaginary $Im\theta_{\parallel,\perp}$ parts $\theta_{\parallel,\perp}$. Calculation of phase dif-

ference of signals for incident light orthogonal polarizations $\Delta\varphi=|\varphi_{\parallel}-\varphi_{\perp}|$ shows, that $\Delta\varphi$ is proportional to linear dichroism value $\delta\varkappa=N_2''-N_1''$. When light wave polarization is circular a registered signal is a complex functions of parameters which characterize absorption anisotropy and dichroism as well as thermophysical values which presents difficulties in defining circular dichroism in general form. But when linear birefrigence and dichroism are values of 10^{-2}–10^{-4} order ellipticity of eigenwaves in crystals can be considered equal, i.e. one may assume $k_1=k_2=k$, $N_1=N_2=N$ in all members except exponents [73]. We also suppose a crystal on the given wavelength to be ε-isotropic on linear dichroism $\varepsilon_2''-\varepsilon_1''=0$. In the examined particular case PA signals amplitudes for clockwise ($\tau_0=+1$) and counterclockwise ($\tau_0=-1$) circular polarizations of incident light may be written as follows

$$q_{\pm}=\frac{R_0}{4a_s}(1\mp k'')[(Re\theta_{\parallel}+Re\theta_{\perp})^2+(Im\theta_{\parallel}+Im\theta_{\perp})^2]^{1/2},$$

where $$R_0=\frac{\varkappa_0|E_0|^2\omega}{16\pi k_s G(g+1)}\varepsilon''\left[1+\frac{|N|^2|a_0|^2}{(\varepsilon_1'-\varepsilon_2')^2}\right],$$

$\varkappa_0=\gamma P_0/(\sqrt{2}a_g l_g T_0)$, γ is adiabat index hence follows, that

$$k''=\frac{|q_+-q_-|}{2(q_++q_-)}.$$

On the other hand within the limits of adopted approximations $k''\simeq\alpha_0''n'/(\varepsilon_1'-\varepsilon_2')$. Thus, measurements of PA signals amplitudes $q_{\pm}$ lets us find gyration tensor components α'' considering that birefrigence $(\varepsilon_1'-\varepsilon_2')$ is known.

5. PIEZOPHOTOACOUSTIC SPECTROSCOPY OF GYROTROPIC CRYSTALS.

The effect of amplitude-modulated optical radiation on piezoelectric ceramics leads, as shown in [74], to induction in the latter of low-frequency sound signal, the sample under investigation being simultaneously a detector of PA signal as well. An interest to the investigation of PA transformation in piezocrystals is accounted for the possibility of implementation of different mechanisms in acoustic wave generation. Except conventional thermal there are, as shown in [75,76,8], concentration-deformation mechanism of generation in piezosemiconductors where sound excitation results from electrical potential which is connected with concentration change of electric charge free carriers. In [77,78] a theory of linear and nonlinear generation of sound fields due to inverse piezoeffect has been developed.

It is known as well [10], that piezoelectrical characteristics exhibit only noncentralsymmetrical crystals, many of them having stimulated gyrotropy (Faraday effect) [3]. In this connection consider PA transformation characteristics in naturally gyrotropic piezoelectric crystals of different symmetry classes when thermal mechanism of excitation of thermoelastic waves is considered to be principle.

5.1. Piezophotoacoustic crystal spectroscopy of higher and middle singonies.

For the description of PA transformation process relationship of Dyugamel-Neumann is used [79]

$$\sigma_{ij}=c^{E}_{ijkl}u_{kl} - e^{T}_{ijm}E_{m} - \lambda^{E}_{ij}\theta, \qquad (5.1.1)$$
$$D_{i}=e^{T}_{ijk}u_{jk} + \varepsilon^{S}_{ij}E_{j} + P^{S}_{i}\theta,$$

where c^E_{ijkl}, e^T_{ijm} are the tensors of elasticity coefficients and piezoelectric constants, P^S_i are the piroelectric coefficients, λ^E_{ij}, ε^S_{ij} - are the tensors of temperature tensions and dielectric permeability, indexes T, E, S mean, that tensor components are taken at constant temperature, electric field and deformation correspondingly.

Expression for PA signal difference corresponding to right and left ellipcityoal polarized light waves.

Type of boundary condit.	Boundary conditions	Crystals of class 23
1	$\sigma(0)=0$ $\sigma(l)=0$	$\Delta V_1=-h_0[V_0-ktg\frac{kl}{2}(B_+(exp(-\alpha_+l)+1)-$ $-B_-(exp(-\alpha_-l)+1))]$
2	$\sigma(0)=0$ $U(l)=0$	$\Delta V_2=-h_0[V_0-ktgkl(B_+-B_-)-$ $\frac{coskl-1}{coskl}(A_+exp(-\alpha_+l)-A_-exp(-\alpha_-l))]$
3	$\sigma(0)=0$ $U(l)=0$	$\Delta V_3=-h_0[V_0-ktgkl(B_+exp(-\alpha_+l)-B_-exp(-\alpha_-l))$ $+\frac{coskl-1}{coskl}(A_+-A_-)]$
4	$U(0)=0$ $U(l)=0$	$\Delta V_4=0$
		Crystals of class 3, 4, 6
1-3		$\Delta V'_i=-\Delta V_i+\Delta V'_4, \quad i=1,2,3$
4	$U(0)=0$ $U(l)=0$	$\Delta V'_4=\frac{P^S_3}{\varepsilon^S_{33}}[\alpha_-^{-1}E_-(exp(-\alpha_-l)-1)-$ $-\alpha_+^{-1}E_+(exp(-\alpha_+l)-1)]$

At incident amplitude-modulated light wave propagation of arbitrary polarization along direction [110] of absorbing cubic crystal of class 23 relations (5.1.1) in matrix terms take the form

$$\sigma_6=c_{44}^E u_6 - e_{14}^T E_3 - \lambda_1^E \theta, \qquad (5.1.2)$$
$$D_3=e_{13}^T u_6 + \varepsilon_{14}^S E_3.$$

In the case when radiation propagates along the axis of the highest symmetry coinciding with direction [001] of uniaxial piezoelectric crystals of class 3, 4, 6 the following expressions can be derived from (5.1.2)

$$\sigma_3=c_{33}^E u_3 - e_{33}^T E_3 - \lambda_3^E \theta, \qquad (5.1.3)$$
$$D_3=e_{33}^T u_3 + \varepsilon_{33}^S E_3 + p_3^S \theta,$$

which in [74] are used for PAE calculation in nongyrotropic piezoceramic materials. Periodic component of a temperature field in (5.1.2), (5.1.3) is gained from the solution of nonuniform thermal equation for gyrotropic sample (see e.g. [23,32])

$$\theta(z,t) = (U_1 exp(-\sigma_s z) - E_+ exp(-\alpha_+ z) - E_- exp(-\alpha_- z)) exp(i\Omega t). \qquad (5.1.4)$$

In formula (5.1.4) the following notation are introduced

$$E_{\pm} = \frac{A\alpha_{\pm}}{\alpha_{\pm}^2 - \sigma_s^2}, \quad A = \frac{c\sqrt{\varepsilon^T} n^2 |E|^2 (1\pm\tau)^2}{\sqrt{2} k_s |n_0+n|^2 (1+\tau^2)}, \quad \alpha_{\pm} = \frac{4\pi}{\lambda}\left[\frac{\varepsilon''}{2\sqrt{\varepsilon^T}} \pm \gamma''\right],$$

$n_0=(n_+ + n_-)/2$, $n_{\pm}=\sqrt{\varepsilon}\pm\gamma$ are the complex refraction indexes of isonormal waves, U_0 is the constant defined by crystal parameters.

Making use of the equation of elastic medium movement and relations (5.1.2)-(5.1.4) we can obtain relations for potential difference (see Table), occurring in piezoelectric samples at

different boundary conditions [80]: at free ($\sigma(0)=0$, $\sigma(l)=0$), clamped ($U(0)=0$, $U(l)=0$) and alternately loaded ($\sigma(0)=0$, $U(l)=0$ or $\sigma(l)=0$, $U(0)=0$) crystal boundaries. In the table the following notations are used $V_0=A_+[exp(-\alpha_+ l)-1]-A_-[exp(-\alpha_- l)-1]$, $A_\pm=\alpha_\pm E_\pm/(\alpha_\pm^2+k_\pm^2)$, $B_\pm=\alpha_\pm^{-1}A_\pm$, $h_0=h\lambda_{11}^E/c_0$, $c_0=c_{44}^E+(e_{14}^T)^2/\varepsilon_{11}^S$, $h_{14}^T=e_{14}^T/\varepsilon_{11}^S$, k is the wave number of elastic wave, l is the sample length. Note that in the expressions for crystals 3,4,6 instead of value h_0, $h_0'=h'\lambda_0'/c_0'$ will be used, where $h'=e_{33}^T/e_{33}^S$, $\lambda_0'=h'p_3^S-\lambda_{33}^E$, $c_0'=c_{33}^E+(e_{33}^T)^2/\varepsilon_{33}^S$.

Numerical analysis of obtained relations shows that for low modulation frequencies approximately up to 10 kHz there is no essential amplitude difference of PA signals at alternate clamping of front and rear sample surfaces. In the region of kilohertz (over 100kHz) and megahertz modulation frequencies of incident radiation clamping of front crystal boundary of class 23 results in appearance of resonance phenomena (see Fig.15) similar to early discovered at PAE investigation in thermally thick objects with piezoelectric detection of resulting signal [41] Resonance curve character, as it seen from Fig.15, depends largely on geometric dimensions of piezoelectrics. At mechanically clamped sample boundaries PA response in cubic piezocrystals is equal to 0, and in crystals of class 3,4,6 contribution to the value of PA signal is fully determined by value of piroelectric coefficients. The fact that, in uniaxial crystals piezoelectrics the resonance effects are less pronounced, is connected with competing effect of piroelectric sample characteristics on acoustic resonances, stimulated in the first place by piezoeffect value

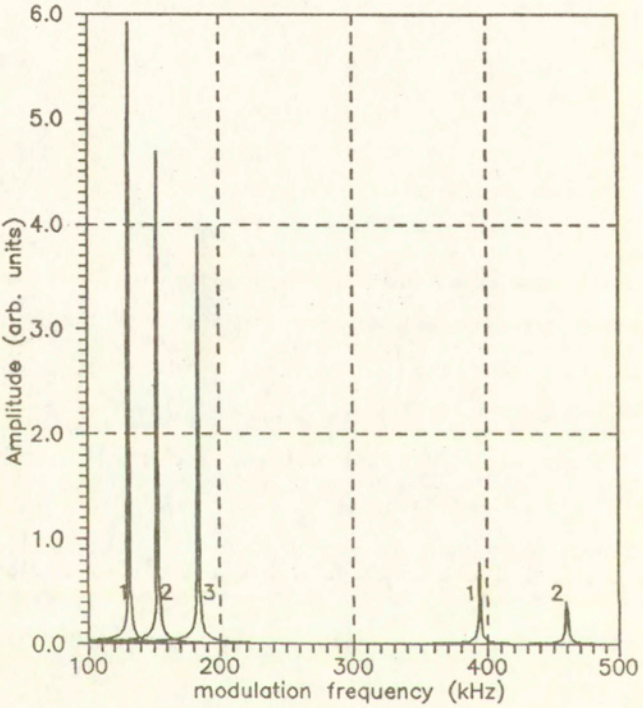

Fig.15. The dependence of PA signal amplitude difference (τ=-1) on the modulation frequency of incident radiation for gyrotropic crystal $Bi_{12}GeO_{20}$ at boundary conditions: $\sigma(l)$=0, $\sigma(0)$=0, 1-l=0.005m, 2-l=0.01m, 3-l=0.015m.

and crystal geometry.

Note, that the results obtained by resonance PA transformation can be used for increasing the resolution of PA spectroscopy and for determining the absorption parameters ε'' and the parameters of circular dichroism γ'' of gyrotropic piezoelectrics.

5.2. Formation of photoacoustic response in nonlinear piezoelectric crystals.

As shown in [8] the presence of nonlinear piezoelectric properties in crystals can lead to a number of peculiarities in the process of PA transformation. In this connection investigation of PA transformation in gyrotropic nonlinear piezoelectric crystals of different symmetry classes is a matter of interest.

Modulated absorption of radiation normally incident on absorbing gyrotropic piezocrystal causes thermooptical generation of elastic waves and through piezoeffect (linear, nonlinear or their combination) leads to the potential difference on the boundaries of a crystal. Basing on the expression for energy dissipation in units of volume [23], containing explicit dependence on ellipticity τ of incident light, from the solution of nonuniform thermal equation we may find a component of temperature field in the crystal under investigation

$$\theta(x,t) = (V_0 exp(-\sigma_s x) - E_+ exp(-\alpha_+ x) - E_- exp(-\alpha_- x)) exp(i\Omega t), \quad (5.2.1)$$

where notations adopted in [80] are used.

Properties of piezoelectric crystals will be described with the help of relations of nonlinear crystal acoustics [81]

$$\sigma_{ij}=c^{E}_{ijkl}u_{kl}+(1/2)c^{E}_{ijklmn}u_{mn}u_{kl}-(1/2)e^{T}_{mijkl}E_{m}u_{kl}-e^{T}_{mij}E_{m}-$$
$$-(1/2)f_{mnij}E_{n}E_{m}-(1/2)e^{T}_{mijkl}u_{kl}E_{m}-\lambda^{E}_{ij}\theta, \qquad (5.2.2)$$
$$D_{m}=e^{T}_{mij}u_{ij}+(1/2)e^{T}_{mijkl}u_{ij}u_{kl}+(1/2)f_{mnij}E_{n}u_{ij}+\varepsilon^{S}_{mn}E_{n}+$$
$$+(1/2)\varepsilon^{(S)}_{mnp}E_{p}E_{n}+(1/2)f_{mnkl}u_{kl}E_{n}+P^{S}_{m}\theta,$$

containing expressions for $\theta(t)$. In (5.2.2) nonlinear characteristics of medium are determined by tensors c^{E}_{ijklmn} of nonlinear elastic constants, e^{T}_{mijkl} of nonlinear piezoelectric coefficients, $\varepsilon^{(S)}_{mnp}$ of quadratic dielectric permeability, f_{mnkl} of electrostriction coefficients. To make calculations, more particular consider case of propagation of amplitude modulated light beam along angle bisectrix, formed by directions [010] and [110] of cubic piezocrystal of classes 23, $\bar{4}3m$. Then from (5.2.2) it follows assuming that $\sigma=\sigma_{12}+\sigma_{22}$,

$$\sigma=c^{E}_{22}u_{2}+c^{E}_{66}u_{6}+(1/2)c^{E}_{626}(2u_{2}u_{6}+u^{2}_{6})-e^{T}_{36}E_{3}-$$
$$-(1/2)e^{T}_{326}E_{3}(u_{2}+u_{6})-(1/2)f_{32}E_{3}E_{2}-\lambda^{E}_{1}\theta, \qquad (5.2.3)$$
$$D_{3}=e^{T}_{36}u_{6}+e^{T}_{326}u_{2}u_{6}+\varepsilon^{S}_{3}E_{3}+f_{32}u_{2}E_{3}.$$

Assuming $e^{T}_{36}=0$, from (5.2.3) we can get relations valid for crystal of class 432. In the case of uniaxial crystals of class 3, 4, 6, 3m, 4mm, 6mm when radiation propagates along the axis of highest symmetry expressions (5.2.2) take the form

$$\sigma_{3}=c^{E}_{33}u_{3}+(1/2)c^{E}_{333}u_{3}u_{3}-e^{T}_{33}E_{3}-(1/2)f_{33}E_{3}E_{3}-\lambda^{E}_{3}\theta, \qquad (5.2.4)$$
$$D_{3}=e^{T}_{33}u_{3}+(1/2)e^{E}_{333}u_{3}u_{3}+\varepsilon^{S}_{33}E_{3}+(1/2)\varepsilon^{S}_{33}E_{3}E_{3}+P^{S}_{3}\theta.$$

Having done the linearization of relations (5.2.3) and (5.2.4) according to [82] and making use of elastic medium move-

Expressions for potential difference occurring in non linear piezocrystals at different boundary conditions

Boundary conditions	Crystals of class 23, $\bar{4}3m$, 432
1, 2, 3	$V_i = \frac{a(e_{36}^T + e_{326}^T u_0)}{2\varepsilon_3^S} \frac{\lambda_1}{a_1} V_i^{(1)} + \frac{(e_{36}^T + e_{326}^T u_0)b + E_0 f_{32} a}{2\varepsilon_3^S} \frac{\lambda_2}{a_2} V_i^{(2)} + V_4, \quad i=1,2,3$
4	$V_4 = const$
	Crystals of class 3, 4, 6, 3mm, 4mm, 6mm
1, 2, 3	$V_i = \frac{\hbar\lambda_0}{c_0} V_i^{(0)} + V_4, \quad i=1,2,3$
4	$V_4 = \frac{P_3^S}{\varepsilon_3^S} \left[\frac{V_0}{\sigma_s}(exp(-\sigma_s l)-1) - \frac{E_+}{a_+}(exp(-a_+ x)-1) - \frac{E_+}{a_+}(exp(-a_+ x)-1) \right.$

ment equation we can easily get expressions for potential occurring in nonlinear piezocrystals calculated at different boundary conditions [83,84]: 1- free ($\sigma(0)=0$, $\sigma(l)=0$), alternately loaded 2-($\sigma(0)=0$, $u(l)=0$), 3-($\sigma(l)=0$, $u(0)=0$) and clamped ($u(0)=0$, $u(l)=0$)boundaries of crystal sample (see Table).

Note that for crystals 3m, 4mm, 6mm, $\bar{4}3m$ in expressions

(5.2.5) and (5.2.6) $E_+=E_-=E$, $\alpha_+=\alpha_-=4\pi/\lambda(\varepsilon''/2\sqrt{\varepsilon'})$. Values $V_1^{(1,2)}$ are determined by thermal, acoustic and geometric crystal parameters and are not quoted because of awkwardness of expressions.

Analysis of expressions received shows that PA signal amplitude in cubic crystals largely depends on parameter of absorption and relation of values of linear and nonlinear piezoelectric effects and in uniaxial crystals of classes in question it is determined also by the value of piroelectric coefficients. For cubic crystals of class 432 in which linear piezoeffect is prohibited by crystal symmetry, resulting PA signal is fully determined by component value of nonlinear piezoeffect e^T_{326}, what makes it possible to determine the value of quadratic piezoeffect by experimental measurement of PA response amplitude. It is not difficult to show that in some special cases measurement of amplitude difference of PA signals corresponding to clockwise and counterclockwise circular polarizations of incident light permits on the basis of expressions (5.2.6), (5.2.5) to determine circular dichroism parameter of gyrotropic nonlinear piezocrystals. At high modulation frequencies of incident radiation (>500kHz) resonance phenomena have been discovered in crystals of class 432 (see Fig.16), similar to early described in linear piezoelectrics. In this case resonance frequencies are defined from conditions: in the case of free boundaries

$$\cos(k_1 l/2)=0, \quad \cos(k_2 l/2)=0, \tag{5.2.7}$$

at alternative clamping of front and rear boundary

$$\cos(k_1 l)=0, \quad \cos(k_2 l)=0. \tag{5.2.8}$$

Modifying conditions (5.2.7), (5.2.8) we may write

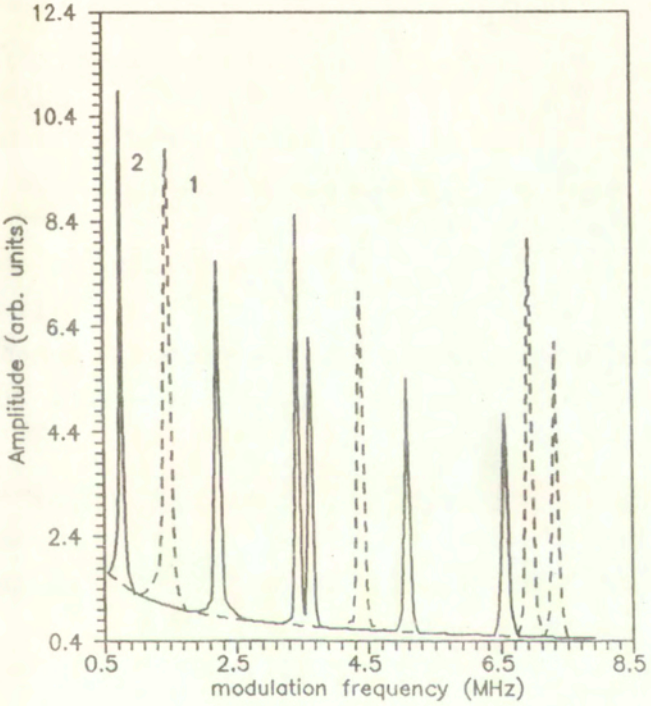

Fig.16. Dependence of PA signal amplitude q on modulation frequency Ω for cubic crystal of class 432, (e^{m}_{326}~100Kl/m, c_s=400J/kg·K, k_s=20W/mK, ρ_s~10^3kg/m^3 at different boundary conditions.) 1-$\sigma(0)=0$, $\sigma(l)=0$, 2-$\sigma(0)=0$, $u(l)=0$ or $u(0)=0$, $\sigma(l)=0$

$$\Omega^{(1)}_{\text{рез}}=(\pi+2\pi k)(1/l)\sqrt{a_1/\rho_s}, \qquad (5.2.9)$$
$$\Omega^{(2)}_{\text{рез}}=(\pi+2\pi k)(1/l)\sqrt{a_2/\rho_s}, \quad k=0,1,\ldots$$

for free crystal faces and

$$\Omega^{(1)}_{\text{рез}}=(\pi/2+\pi k)(1/l)\sqrt{a_1/\rho_s}, \qquad (5.2.10)$$
$$\Omega^{(2)}_{\text{рез}}=(\pi/2+\pi k)(1/l)\sqrt{a_2/\rho_s}, \quad k=0,1,\ldots$$

at clamping of one of the faces.

In (5.2.9), (5.2.10) the following notations are adopted

$a_1=(1/2)c_1a$, $a_2=(1/2)c_1b+c_2a$, $a=1/\cos(22^\circ30')$, $b=1/\cos(60^\circ30')$,

$$c_1=c^E_{66}+2c^E_{626}-2e^E_{326}E_0-(e^T_{326}/\varepsilon^S_3)(E_0f_{32}u_0+2\varepsilon^S_3E_0+f_{32}u_0E_0+e^T_{326}u_0^2),$$

$$c_2=c^E_{22}-2e^E_{326}E_0-(1/2\varepsilon^S_3)f^2_{32}E_0-(e^T_{326}/\varepsilon^S_3)(f_{32}E_0u_0+\varepsilon^S_3E_0).$$

It should be noted that in nonlinear piezocrystal of class 432 there are two main resonance frequencies $\Omega^{(1)}$, $\Omega^{(2)}$. It can be accounted for the fact that nonlinear piezoeffect is caused by two elastic deformations connected with propagation of two elastic waves having different wavelength.

Thus, method of piezophotoacoustic spectroscopy gives possibility of determining tensor components of linear and nonlinear piezoeffects as well as circular dichroism parameter on amplitude characteristics measurement of PA signal.

5.3. PA transformation in layered piezoelectric structures.

Consider PA transformation in nongyrotropic 2-layered sample taking into account the reflection of light waves within layers, assuming that layered sample under investigation is simultaneously a PA signal detector and comprises absorbing cubic crystals of 23 or $\bar{4}3m$ class, cut along the direction [110], coinciding with the propagation direction of amplitude modulated light.

Basing on the Dyugamel-Neuman relations and using the expressions for energy dissipation [52] in the 1-st $Q_1^{\pm}$ and the 2-nd $Q_2^{\pm}$ layers let us determine potential difference $V=V_1+V_2$,

$$V_1=h_1\int_0^{d_1} E_3^{(1)}dx, \qquad V_2=h_2\int_0^{d_1+d_2} E_3^{(2)}dx,$$

developing in piezostructure under boundary conditions[84].

Note that in 2-layered system resonance phenomena can occur, early observed at piezoelectric registration of PA signal in optically opaque objects whose frequencies are determined by the condition [85]

$$\frac{k_{2,1}c_{02,1}}{k_{1,2}c_{01,2}}\cos(k_1d_1)\sin(k_2d_2)+\sin(k_1d_1)\cos(k_2d_2)=0 \qquad (5.3.1)$$

for free and loaded boundaries of 2-layered sample. At alternative clamping of front and rear boundaries resonance condition takes the form

$$\frac{k_{2,1}c_{02,1}}{k_{1,2}c_{01,2}}\cos(k_1d_1)\cos(k_2d_2)+\sin(k_1d_1)\sin(k_2d_2)=0 \qquad (5.3.2)$$

From the conditions (5.3.1), (5.3.2) let us determine resonance frequencies

$$\Omega_{pez}=\frac{\pi kl}{2k_1}\sqrt{\frac{c_{01}}{\rho_1}},\ k=0,1\ldots,\quad d_2=\sqrt{\frac{c_{02}\rho_1}{c_{01}\rho_2}}\,d_1 \qquad (5.3.3)$$

for free and loaded boundaries of the sample

$$\Omega_{pez}=\frac{1}{k_1}\sqrt{\frac{c_{01}}{\rho_1}}\arcsin\left[\frac{\sqrt{c_{01,2}\rho_{1,2}}}{\sqrt{c_{01,2}\rho_{1,2}}+\sqrt{c_{01,2}\rho_{1,2}}}\right]^{1/2} \qquad (5.3.4)$$

$$d_2=\sqrt{\frac{c_{02}\rho_1}{c_{01}\rho_2}}\,d_1$$

at clamping front and rear surface.

As follows from (5.3.1), (5.3.2) in 2-layered gyrotropic structure half-wavelength, quarter-wavelength and mixed resonances are possible while fulfilling certain relationships between sample lengths. The existence of light waves reflection within 2-layered gyrotropic structure essentially influences on the behavior of the amplitude characteristic of PA response (Fig.17) and results in strongly oscillating dependence of the signal value on the thickness of the 1-st layer, caused by multibeam interference of light waves within the layers (Fig.17).

To make clear the influence of spatial dispersion on the mechanism of PA signal formation in thin gyrotropic layers one may choose as absorbing only the first optically active layer with thickness d_1, the second layer with d_2=0,5sm is considered to be transparent and non-gyrotropic. The case under consideration may be experimentally implemented in sputtering of a thin gyrotropic film $Y_3Fe_5O_{12}$ on the crystal of $\bar{4}3m$ class. Confine to modulation frequencies ($\Omega<10^3$Гц) at which acoustical characteristics of absorbing layer up to $d_1=10^{-4}$m can be neglected compared to transparent layer. Numerical analysis of expressions for potential difference V_1^+ has shown that amplitude and phase characteristics dependence of PA response on the value of circular dichroism at different polarizations of incident light at low modulation frequencies is of strongly expressed nonlinear character (see Fig.18 a,b). It should be noted that experimental determination of circular dichroism parameter can be carried out under the influence of external magnetic field on the 2-layered sample under investigation (crystal $Y_3Fe_5O_{12}$ has strong enough Faraday effect).

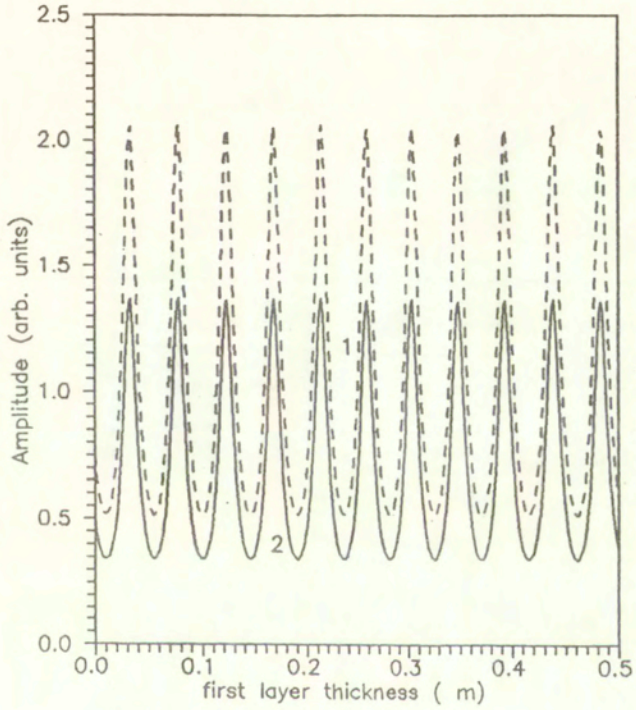

Fig.17. Amplitude dependence of PA signal q on the first layer thickness d_1 taking into account the reflection of light waves in layered structure at different polarizations of incident light: 1-τ=+1, 2-τ=-1.

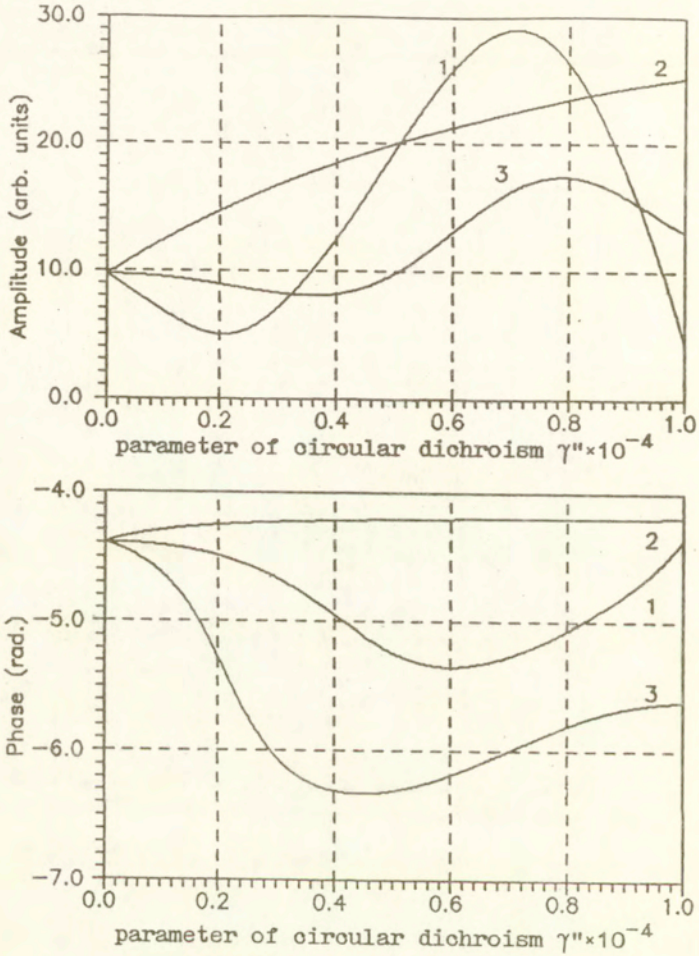

Fig.18. Dependence of amplitude (a) and phase (b) characte ristics of PA response in 2-layered sample (d_1=10mkm, Ω=100Hz) on the value of circular dichroism parameter γ" at different polarizations of incident light: light: 1-τ=+1, 2-τ=-1.

At frequency modulation rise the dependence of amplitude and phase of PA signal at $\tau=\pm 1$ becomes linear (while implementing the special case of thermally thick first layer). In this case as was shown theoretically above for gyrotropic piezocrystal samples the determination of circular dichroism parameter by by experimental measurement of PA signal amplitude and phase difference corresponding to clockwise and counterclockwise polarizations of the incident light. For the thicknesses of layer d_1 of light wave length order the measurements of γ'' value are possible as well at low modulation frequencies, as an important contribution to resulting PA signal is made due to optical characteristics of gyrotropic film.

Thus, the value of circular dichroism parameter essentially influences the behavior of amplitude and phase characteristics of resulting PA signal. Piezophotoacoustic spectroscopy method of 2-layered structures gives possibility of determining γ'' parameter of one of the layers as related to experimental determination of PA spectra corresponding to right and left circular polarizations of the incident light in wide range of thicknesses.

6. PHOTOACOUSTIC SPECTROSCOPY OF CHOLESTERIC LIQUID CRYSTALS.

The laser photoacoustic (PA) technique, being highly sensitive, fast and applicable over a wide spectral range, has produced numerous and original results in liquid-crystal optics [86,89]. In [87,88], for example, the thermal diffusivity D_s, specific heat capacity c_s and thermal conductivity k_s of liquid crystals at the nematic isotropic phase transition were simultaneously measured for the first time by a PA method. Parameters c_s and D_s show a critical change in the phase-transition region, where as the thermal conductivity does not exhibit any critical behaviour. The PA signal as a function of the thermal and mechanical displacement of the acoustic piston was studied in [89] for various modulation frequencies of incident radiation, sample thickness and thermal conductivity. These studies were done for the 4-octyl-4'-cyanobiphenyl liquid crystal. As noted in [89] the experimental results are in good agreement with the theoretical predictions [90,91]. The optical properties of cholesteric liquid crystals (CLC) with a weak temperature dependence of the spiral pitch were studied in [92], where the PA signal dependence on temperature in a selective reflection maximum was found to exist in a narrow temperature range.

Since the PA effect permits one to study various liquid crystal properties [86-89, 92], further development of the theory of thermooptically induced elastic perturbations in such media is required.

6.1. Photoacoustic interaction in cholesteric liquid crystals. Eigenmodes circular polarization rates.

Consider photoacoustic interaction in cholesteric liquid crystals (CLS) having optical anisotropy, characteristic of crystals, and reological peculiarities analogous to liquids [93,94].

We describe PA effect in CLS by the phenomenological material equations [93-97]

$$\underline{D} = \varepsilon(z)\underline{E}, \quad \underline{B} = \underline{H}, \tag{6.1.1}$$

where $\varepsilon(z)=\varepsilon'(z)+i\varepsilon''(z)$ is the complex permeability tensors. Its dependence on the z coordinate is given by

$$\varepsilon(z) = U\varepsilon U^{-1} \tag{6.1.2}$$

where $\varepsilon=\varepsilon'+i\varepsilon''$ is the complex local permeability tensor, imaginary part of which defines absorption, and

$$U = U(z) = \begin{pmatrix} cos(qz) & -sin(qz) & 0 \\ sin(qz) & cos(qz) & 0 \\ 0 & 0 & 1 \end{pmatrix} = exp(qz\underline{c}^{\times}) \tag{6.1.3}$$

is the matrix of rotation by the angle qz around the $\underline{c}$ vector directed along the z axis, $\underline{c}^{\times}$- is the second rank antisymmetric tensor dual to the $\underline{c}$ vector, and q is connected with spiral pitch, related by $h=2\pi/q$.

Consider a ZLC sample of thickness l placed in a vertical PA cell with detecting gas and substrate. A circularly polarized monochromatic electromagnetic wave modulated at frequency Ω falls normally upon CLC surface. Asssuming a wave modulation at polarization (right, left) we shall go on to the case when the right and left circular eigenmodes are excited in the crystal in turn. Resulting rate of circular polarizations takes place in

inequality [93]

$$\frac{\omega^2}{c^2}\Delta\varepsilon^2 \ll q^2, \qquad (6.1.4)$$

where $\Delta\varepsilon$ is anisotropy value. Energy dissipation in the mode under consideration is defined by the ratio

$$Q_{\pm} = \frac{i\omega}{16\pi}(\underline{E}_{\pm}\underline{D}^{*}_{\pm} + \underline{H}_{\pm}\underline{B}^{*}_{\pm} - \text{к.с.}), \qquad (6.1.5)$$

which can be easily transformed with regard to (6.1.1)-(6.1.3) expressions for the semiinfinite CLC fields [96]

$$\underline{E}_{\pm} = U\tilde{\underline{E}}_{\pm} = UE_0\frac{1}{\sqrt{2}}(\underline{a} \pm i\underline{n})exp[i(k_{\pm}z - \omega t)] \qquad (6.1.6)$$

and permeability tensor in covariant form $\varepsilon=\varepsilon_1+(\varepsilon_2-\varepsilon_1)\underline{n}\cdot\underline{n}$ as follows

$$Q_{\pm} = \frac{\omega}{8\pi}\,\bar{\varepsilon}''|E_0|^2 exp(-2k''_{\pm}z), \qquad (6.1.7)$$

where $k_{\pm}=k'_{\pm}+ik''_{\pm} = k_0\sqrt{\bar{\varepsilon}} \pm (q+(k_0^3\Delta\varepsilon^2)/(8q(k_0\sqrt{\bar{\varepsilon}} \pm q)\sqrt{\bar{\varepsilon}}))$ are complex wave numbers of circularly polarized eigen waves [93, 97], $\Delta\varepsilon=(\varepsilon_1-\varepsilon_2)/2$, $\bar{\varepsilon}=(\varepsilon_1+\varepsilon_2)/2$, $\underline{a}$ is unit vector forming the right threa vectors with a director $\underline{n}$ and vector $\underline{c}$, $k_0=\omega/c$ is wave number of electromagnetic wave of ω frequency in vacuum.

For calculation of temperature field redistribution in PA cell it is nesessary to solve by analogy [90] equations for heat conductivity in all the regions.

Assuming temperature continuity and its gradients at the cell boundary and by the PA signal calculation method [90] we obtain for gas pressure in the cell $\Delta P_{\pm}(t)$ following expressions [98]

$$\Delta P_{\pm}(t) = \theta_{\pm}exp[i(\Omega t - \pi/4)], \qquad (6.1.8)$$

where the following notation is used

$$\theta_{\pm} = \frac{\gamma_0 P_0 h_{\pm}}{\sqrt{2} a_g l_g T_0} \times \tag{6.1.9}$$

$$\times \frac{(r_{\pm}-1)(b+1)\exp(\sigma_s l)-(r_{\pm}+1)(b-1)\exp(-\sigma_s l)+2(b-r_{\pm})\exp(-\alpha_{\pm} l)}{(b+1)(g+1)\exp(\sigma_s l)-(b-1)(g-1)\exp(-\sigma_s l)}$$

$h_{\pm} = A_0/(\alpha_{\pm}^2-\sigma_s^2)$, $r_{\pm} = (1-i)\alpha_{\pm}/2a_s$, $A_0 = \lambda\overline{\varepsilon''}|E_0|^2/8k_s c$, $\sigma_s = (1+i)a_s$, $a_j = (\Omega/2\beta_j)^{1/2}$ and $\beta_j = k_j/\rho_j C_j$ are thermal diffusion and temperature conductivity of the j-th material respectively; $b = k_b a_b/k_s a_s$, $b = k_g a_g/k_s a_s$,

$$\alpha_{\pm} = 2k''_{\pm} = \frac{k_0}{\sqrt{\overline{\varepsilon}'}}\left[\overline{\varepsilon}'' \pm \frac{k_0^2 \Delta\varepsilon' \Delta\varepsilon''}{2q(k_0\sqrt{\overline{\varepsilon}'} \pm q)}\right],$$

γ_0 is adiabyt value, P_0 and T_0 are detecting gas initial pressure and temperature.

According to (6.1.9) PA signal value is defined by a CLC anisotropy $\Delta\varepsilon'$, absorption parameters $\Delta\varepsilon''$, $\overline{\varepsilon''}$, thermophysical characteristics of a cell material, modulation frequency Ω, as well as by PA cell geometry.

Investigating the most interesting case of optically and thermally thick sample when a liquid crystal length l is larger than that of thermal diffusion $\mu_s = a_s^{-1}$ and those of optical absorption $\mu_{a\pm} = a_{\pm}^{-1}$, we significantly simplify the correlation

$$\theta_{\pm} = \frac{\gamma_0 P_0 A_0}{\sqrt{2} a_g l_g T_0 (g+1)} \frac{r_{\pm}-1}{\alpha_{\pm}^2 - \sigma_s^2}. \tag{6.1.10}$$

PA signal amplitude

$$q_{\pm} = |\theta_{\pm}| = \sqrt{(Re\theta_{\pm})^2 + (Im\theta_{\pm})^2}$$

in accordance with (6.1.10) is defined by the expression

$$q_{\pm} = \frac{A\Omega^{-1/2}}{\alpha_{\pm}^4 + 4\alpha_s^4}(\alpha_{\pm}^6 + \beta_{\pm} + 8\alpha_s^6)^{1/2}, \qquad (6.1.11)$$

where

$$A = \frac{\gamma_0 P_0 A_0 \beta_s^{1/2}}{\alpha_g l_g (g+1) T_0}, \quad \beta_{\pm} = -2\alpha_s \alpha_{\pm}(\alpha_{\pm}^4 - \alpha_s \alpha_{\pm}^3 - 2\alpha_s^3 \alpha_{\pm} + 4\alpha_s^4).$$

Let us analyse (6.1.11) in some particular cases.

1. If a CLC thermal diffusion length is less than those of optical absorption ($\mu_s < \mu_{a\pm}$) which takes place at little absorption and dichroism, when from (6.11) follows

$$q_+ \simeq q_- \simeq \frac{\chi\pi\varepsilon''|E_0|^2\sqrt{\beta_g}}{2\sqrt{2}\omega p_s C_s}\Omega^{-3/2}, \qquad (6.1.12)$$

i.e. PA signal depends on modulation frequency according to the law $\Omega^{-3/2}$ and the crystal is not sensitive to right and left polarized circular waves

2. In case when a CLC has essential absorption and dichroism ($\mu_s > \mu_{a\pm}$), from (6.1.11) we get different dependence $q_{\pm}$ on frequency Ω

$$q_{\pm} = \frac{\chi\pi\varepsilon''|E_0|^2\sqrt{\beta_s\beta_g}}{2\sqrt{2}k_s\alpha_{\pm}}\Omega^{-1}. \qquad (6.1.13)$$

On calculating difference $\Delta q = |q_+ - q_-|$ it is easily to find explicit expression of relative absorption anisotropy parameter $\Gamma = (\varepsilon_1'' - \varepsilon_2'')/(\varepsilon_1'' + \varepsilon_2'')$ with the help of (6.1.13) in terms of Δq [98]

$$\Gamma = \frac{\sqrt{2}cq(k_0^2\overline{\varepsilon'} - q^2)k_s\lambda}{\pi^2\chi\sqrt{\beta_s\beta_g}\Delta\varepsilon'\overline{\varepsilon'}|E_0|^2}\Omega\Delta q, \qquad (6.1.14)$$

where $\chi = \gamma_0 P_0/[l_g(g+1)T_0]$.

According to expression obtained (6.1.14) experimental measurement of dichroic CLC PA spectra for right and left circular polarization of the incident light lets us define a parameter of relative absorption anisotropy.

6.2 Photoacoustic Response in the CLC samples. Bragg-reflection Region.

Further we shall investigate peculiarities of PA transformation in absorbing CLC for optical radiation frequency range of which coincides with the Bragg reflection region or comes close to its boundary.

We shall describe optical characteristics of absorbing CLC samples on the basis of phenomenological material equations (6.1.1).

Consider a CLC sample of thickness l placed in PA cell with detecting gas and substrate. A circularly polarized monochromatic light modulated at frequency Ω falls normally upon the CLC surface. Let the electric field rotation direction coinside with that of the CLC director vector. For the radiation propagation along the pitch axis, the electric field vector in the coordinate system rotating with director has the form

$$\underline{E} = A_2(\underline{a}+i\gamma_2\underline{b})exp(i(k_2z-\omega t))+A_3(\underline{a}+i\gamma_3\underline{b})exp(i(k_3z-\omega t)), \quad (6.2.1)$$

where $\gamma_{2,3}$, $A_{2,3}$, $k_{2,3}$ are the ellipticities, amplitudes and eigenvectors of the electromagnetic field, respectively, $\underline{a}$ and $\underline{b}$ are the unit vectors of polarization ellipsoid. We use the two wave approximation of diffraction theory [94] in the electric light intensity is assumed to be neglibigle compared with the difracted-wave intensity.

Taking into account the expression for the energy dissipation [4]

$$Q = \frac{i\omega}{16\pi} (\underline{E}\cdot\underline{D}^{*}+\underline{H}\cdot\underline{B}^{*}-\text{K.C.})$$

and (6.1.1) we obtain

$$Q = \frac{i\omega}{8\pi} \underline{E}\varepsilon''\underline{E} \qquad (6.2.2)$$

where the imaginary part of the permetivity tensor presented in a covariant form [3], $\varepsilon''=\varepsilon_1'-2\Delta\varepsilon''\underline{b}\cdot\underline{b}$, $\underline{b}\cdot\underline{b}$ denotes the dyad, and $\Delta\varepsilon''=(\varepsilon_1''-\varepsilon_2'')/2$ describes the CLC absorption anisotropy. Substituting (6.2.1) into (6.2.2), we obtain the expression for the energy dissipation in the Bragg-reflection region [99]

$$Q_1 = A_1+B_1 exp(-2|k_2|z)+C_1 exp(2|k_2|z). \qquad (6.2.3)$$

Outside the Bragg-reflection region the energy dissipation Q has the form

$$Q_2 = A_2+B_2 cos(2k_2z)+C_2 sin(2k_2z). \qquad (6.2.4)$$

The quantities A_i, B_i, C_i (i=1,2) are defined by the optical parameters of the system and the corresponding expressions are given in [100].

One can obtain the thermal distribution in PA cell using the of the heat-conduction equations. In general, solution of the heterogeneous heat-conduction equations with the right-hand side in the form of (6.2.4) is an involved mathematical problem. Therefore to obtain an analytical solutions we restrict ourselves toa particular case. Expanding $cos(2k_2z)$ and $sin(2k_2z)$ in the Bragg-reflection region ($k_2\to 0$), we present (6.2.4) in the form

$$Q_2 = A_2' z^3 + B_2' z^2 + C_2' z + D_2' \qquad (6.2.5)$$

where the constants A_2', B_2', C_2', D_2' are defined by the parameters A_2, B_2, C_2.

Using (6.2.3) and (6.2.6) one obtains from the set of (6.2.5) the gas pressure variation $\Delta P(l)$ inside the cell in the Rosencwaig form:

$$\Delta P(l) = \frac{\gamma_o P_o \theta_o}{\sqrt{2} a_g l_g T_g} \exp(i(\Omega t - \pi/4)), \qquad (6.2.6)$$

where θ_o is the complex amplitude of the temperature field on the sample-detector gas boundary in the Bragg-reflection region [100].

Outside the Bragg-reflection region the temperature field can be presented as follows:

$$\theta_o' = \chi^{-1}[E_4(\exp(\sigma_s l)(b+1) + \exp(-\sigma_s l)(b-1) - 2b) - 2G], \qquad (6.2.7)$$

The notations in (6.2.6), (6.2.7) are the same as in [98]. When the light frquency comes closer to the boundary of the Bragg-reflection region, the complex temperature field amplitudes given by (6.2.6), (6.2.7) approach each other and have the form

$$\theta = \frac{\omega E}{16\pi k_s \sigma_s^2} \chi^{-1}[(\exp(\sigma_s l)(b+1) + \exp(-\sigma_s l)(b-1) - 2b]. \qquad (6.2.8)$$

Using the results obtained we analyse the amplitude q and phase φ dependences on the light frequency ω. For an optically thick CLC sample (l=130μm) the PA signal amplitude increases asymmetrically as the incident-light frequency decreases [99] (see Fig.19). The maximum of the $q=f(\omega)$ curve is caused by the energy dissipation increasing at the region boundary. In this

region, the electromagnetic field eigenwaves are polarized along the absorption-oscillator direction (in this case the latter is directed along the x axis). When the absorption oscillator is directed mostly along the y axis, the maximum of the PA signal amplitude shifts symmetrically to the opposite boundary of the Bragg region.The phase characteristics of the PA signal do not depend significantly on the absorption-oscillator orientation (see Fig.20).

6.3. Influence of temperature on the CLC structure in the PA transformation process.

Note that we ignored the effect of the temperature field on the spatial structure of the crystal. However, the liquid crystals are known to be quite sensitive to temperature variation. For some CLC, an experiment [94,95] gives for the spiral pitch $p \sim 1/T$, where T is the temperature. We assume that the cholesteric phase transition does not occur in the frequency range considered when the absorption oscillator is directed along the x axis ($\varepsilon_1''=3.8\cdot10^{-3}$, $\Delta\varepsilon'=1.4\cdot10^{-3}$). The numerical approximation then gives the dependence of dissipation Q on the temperature T in the form

$$Q(T) = QT^3\xi. \qquad (6.3.1)$$

Here ξ is some experimentally determined constant independent of the incident light frequency ω. For the crystals with y orientation of the absorption oscillator ($\varepsilon_1''=1.0\cdot10^{-3}$, $\Delta\varepsilon'=-1.4\cdot10^{-3}$) the temperature variation of the energy dissipation has the form

$$Q(T) = QT^{-3}\chi. \qquad (6.3.2)$$

For optically thick CLC samples ($l \gg p/\Delta\varepsilon$), the progressive

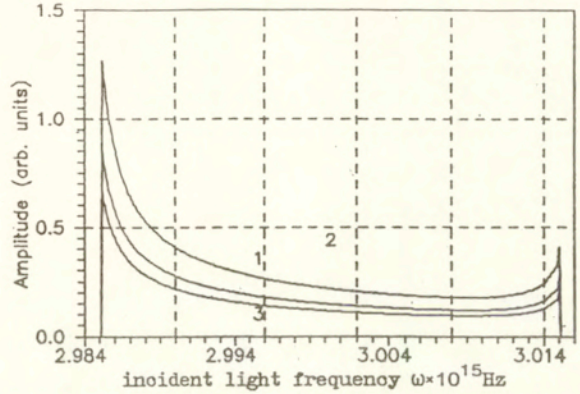

Fig.19. PA signal amplitude from incident light frequency for various light modulation frequencies ($\varepsilon_1''=3.8\cdot10^{-3}$, $\Delta\varepsilon''=1.4\cdot10^{-3}$) The temperature dependence of the CLC pitch is neglected. Modulation frequency Ω (Hz): 1-100, 2-170, 3-240.

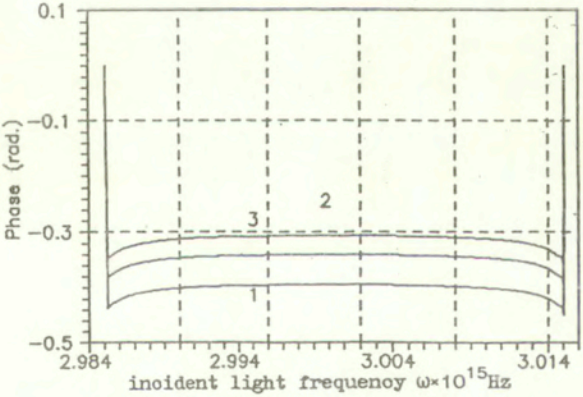

Fig.20. PA signal phase incident light frequency for various light modulation frequencies ($\varepsilon_1''=3.8\cdot10^{-3}$, $\Delta\varepsilon''=1.4\cdot10^{-3}$) The temperature dependence of the CLC pitch is neglected. Modulation frequency Ω (Hz): 1-100, 2-170, 3-240.

approximation method that takes account of Eq. (6.3.1) gives the solution of the nonlinear equation of heat conductivity. The computed complex amplitude of the temperature field at the sample- detector gas boundary has the form [100]

$$\theta=\chi^{-1}E_2[sh\sigma_s l(1+rb)+sh\sigma_s l(r+b)-exp(\alpha l)(r+b)], \qquad (6.3.3)$$

where

$$E_2=\frac{B_1\xi E_1^3}{\alpha^2-\sigma_s^2}, \quad E_1=\sqrt{\frac{\sigma_s^2-\alpha^2}{B_1\xi}}, \quad \alpha=|k_2|.$$

For orystals with $Q=f(T)$ given by (6.2.2) the same method yields

$$\theta'=\chi^{-1}E_2^1[sh\sigma_s l(1-rb)-sh\sigma_s l(r-b)+exp(-\alpha l)(r-b)] \qquad (6.3.4)$$

where the following notation is used

$$E_2'=\frac{B_1\chi\sqrt[3]{E_1'}}{\alpha^2-\sigma_s^2}, \quad E_1'=\sqrt[4]{\frac{B_1\xi}{\sigma_s^2-\alpha^2}}, \quad \alpha=|k_2|/2.$$

We numerically analyzed the dependence of the temperature field amplitudes (6.3.4, 6.3.5) on the incident light frequency for various modulation frequencies. The PA signal amplitude (Fig.21) and phase (Fig.22) vary with temperature owing to the crystal structure change. It is worth emphasizing that the Bragg-reflection region shifts linearly with temperature variation. The PA signal maximum appears for different directions of the absorption oscillator. The maximum is best revealed in crystals with the orientation of absorption oscillator directed along the $x$axis (see Fig.3). Two processes competitively influence the location of the maximum of the PA signal. The first is the PA signal increase, determined by the relative ori-

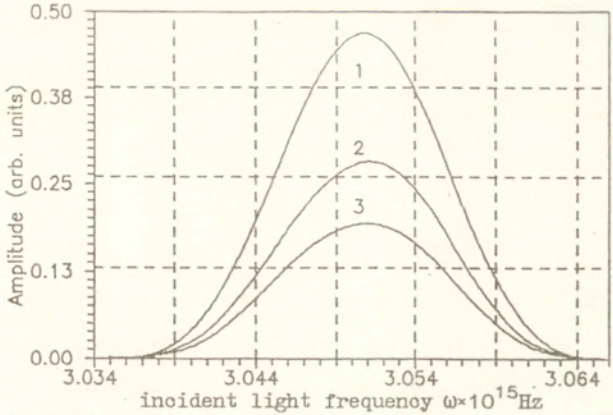

Fig.21. PA signal amplitude vs incident light frequency for various light modulation frequencies ($\varepsilon_1''=3.8\cdot10^{-3}$, $\Delta\varepsilon''=1.4\cdot10^{-3}$) The temperature dependence of the CLC pitch is taken intoaccount. Modulation frequency Ω (Hz): 1-100, 2-170, 3-240.

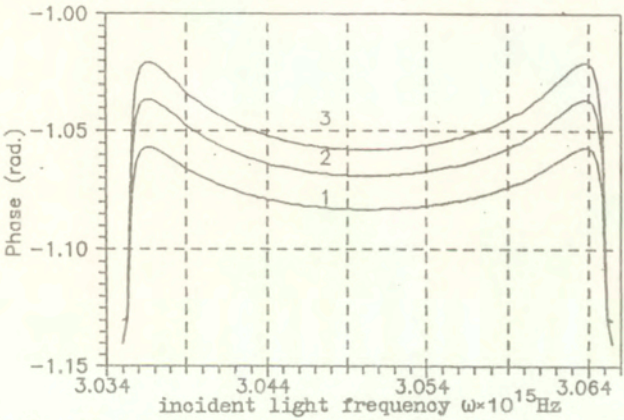

Fig.22. PA signal phase vs incident light frequency for various light modulation frequencies ($\varepsilon_1''=3.8\cdot10^{-3}$, $\Delta\varepsilon''=1.4\cdot10^{-3}$)The temperature dependence of the CLC pitch is taken intoaccount. Modulation frequency Ω (Hz): 1-100, 2-170, 3-240.

entation of the electric field eigenwave and of the absorption oscillator. The second consists of the energy dissipation decrease called forth by the spiral pitch change of CLC due heating liquit crystal and consequent violation of Bragg reflection.

Thus, here the PA transformation is considered for a CLC in the Bragg-reflection region. The asymmetrical increase of the PA signals amplitude is found at the Bragg-region boundary. The influence of the temperature field on the crystal spatial structure was taken into account. This effect gives rise to a shift in the Bragg-region frequency range and to the appearance of the PA signal amplitude in the center of that region for crystals with various directions of the absorption oscillator.

7. PHOTOACOUSTIC SPECTROSCOPY OF NONLINEAR GYROTROPIC CRYSTALS.

7.1. PA transformation in nonlinear gyrotropic crystals of selenite type. Approximation of given field.

Use of a powerful laser radiation allows to expand essentially the field of application of PA method which can be useful while studying non-linear characteristics of a medium. A great number of publications is devoted to the treatment of non-linear processes of sound waves optical generation in liquids and gases [7,2,101]. As for solids, systematic investigations in this field start just now [8,102,103].

The section seeks to describe peculiarities of PA transformation in nonlinear gyrotropic cubic crystals of class 23 as well as to inquire into possibilities of optical parameters determination of such crystals by PA spectroscopy method.

Let intensity modulated circular polarized laser radiation be incident on a nonlinear gyrotropic crystal of length l, cut perpendicular to the axis of the third order [111] and put in a PA cell. In correspondence with [104] along the given direction second gharmonic wave is generated, which has circular polarization with direction opposite to the first harmonic of electric field intensity vector rotation. We will assume, that only second harmonic radiation is being absorbed, and the wave of the main frequency is propagating in the domain of sample transparency. The situation is implemented, e.g., in gyrotropic crystals of selenite type ($Bi_{12}GeO_{20}$, $Bi_{12}SiO_{20}$, Bi_8TiO_{14}), which are transparent for radiation of ruby laser ($\lambda \approx 0{,}694\mu m$), but absorb heavily the second harmonic [105]. Note, that reali-

zation of phase synchronism conditions in gyrotropic crystals of cubic symmetry is possible, as is shown in [104], due to the phenomenon of natural and induced (Faraday effect) optical activity of crystals.

The value of PA signal appearing in the cell due to modulated absorption of double frequency wave is determined by energy dissipation

$$Q_{\pm}(2\omega) = \frac{\omega}{4\pi}|\underline{E}_{\pm}(2\omega)|^2 N''_{\pm}(2\omega) + \frac{i\omega}{2}(\underline{E}_{\pm}(2\omega)\underline{P}^{*}_{\pm}(2\omega) - \text{к.с.}). \quad (7.1.1)$$

Expression for $Q_{\pm}(2\omega)$ is derived from the relation

$$Q = \frac{1}{16\pi}(\underline{E}\cdot\dot{\underline{D}}^{*} + \underline{H}\cdot\dot{\underline{B}}^{*} + \text{к.с.})$$

and material equations [106]

$$\underline{D} = \varepsilon\underline{E} - \frac{\alpha}{c}\frac{d\underline{B}}{dt} + 4\pi\underline{P}, \qquad \underline{B} = \underline{H} + \frac{\tilde{\alpha}}{c}\frac{d\underline{E}}{dt} \quad (7.1.2)$$

describing the characteristics of gyrotropic nonlinear media. In (7.1.1), (7.1.2) $P_i = X_{ijk}E_jE_k$ is the nonlinear polarization of the medium, $\chi_{ijk} = \chi'_{ijk} + i\chi''_{ijk}$ is the complex tensor of quadratic susceptibility, imaginary part of which χ''_{ijk} is responsible for nonlinear absorption, $\varepsilon = \varepsilon' + i\varepsilon''$, $\alpha = \alpha' + i\alpha''$ are the complex tensors of dielectric permeability and optical activity respectively, ε'' determines ordinary absorption, and α' is the circular dichroism, $N''_{\pm}(2\omega) \approx (\varepsilon''(2\omega)/2\sqrt{\varepsilon''(2\omega)}) \pm \gamma''(2\omega)$ are absorption coefficients of circular polarized waves of the second harmonic, $\gamma''(2\omega) = 2\omega\alpha''(2\omega)/c$, c is the velocity of light in vacuum, ω is the cyclic frequency.

Making use of the results obtained on the second harmonic

generation in the approximation of the given field [104,106] and assuming that the conditions of the phase synchronism are fulfilled, one may present energy dissipation of double frequency eigenwaves in the following form

$$Q_{\pm}(2\omega) = (A_{\pm}z^2+B_{\pm}z+C_{\pm})\exp(\alpha_{\pm}z), \qquad (7.1.3)$$

where

$$A_{\pm}=(4\pi/\lambda)^2 D_{\pm}, \quad B_{\pm}=\frac{8\pi N''_{\pm}(2\omega)}{|a_0|^2}D_{\pm}, \quad C_{\pm}=|a_0|^{-2}D_{\pm},$$

$$D_{\pm}=\frac{16\pi\omega n^2 E^4|\chi_{123}|^2 N''_{\pm}(2\omega)}{|N_{\pm}+n_{\mp}|^2(n_{\mp}+n)^4}, \quad a_0=N_0+N,$$

χ_{123} is the component of nonlinear susceptibility tensor in coordinate system with an axis z, directed along the axis of the third order [104], $n_{\pm}$, $N_{\pm}$ are the refractive indexes of circular polarized waves of the main and double frequency, N_0 is the refractive index without taking into account optical activity, E is the electric field intensity of the incident light, $\alpha_{\pm}=(4\omega/c)N''_{\pm}(2\omega)$.

It should be kept in mind, that z in (7.1.3) is negative. Expression (7.1.3) with regard to substitution $a_0=N_0+N \to a_{\pm}=N_{\pm}+N$ (here $N^2_{\pm}=\varepsilon_0\pm\underline{e}\cdot\underline{g}$, $\underline{e}$ is the unit vector of wave normal, $\underline{e}\cdot\underline{g}=g_z$ are the complex vector projections of magnetic gyration on direction z, imaginary part of which g''_z defines magnetic circular dichroism) remains to be valid for magnetoactive media as well.

Energy dissipation $Q_{\pm}(2\omega)$ is included in the thermal conduction equation

$$\frac{d^2T_{\pm}}{dz^2}-\frac{1}{\beta_s}\frac{dT_{\pm}}{dt}=\frac{1}{2k_s}(A_{\pm}z^2+B_{\pm}z+C_{\pm})(1+\exp(i\Omega t))\exp(\alpha_{\pm}z) \qquad (7.1.4)$$

as the density of thermal sources power.

Received equation (7.1.4) differs from the thermal conduction equation corresponding to media with linear dependence of polarization on electric field intensity by summands $A_{\pm}z^2$ and $B_{\pm}z$, the appearance of which is connected with the dependence of second harmonic amplitude on coordinate z, what is valid generally speaking only for non-linear processes in crystals of sufficiently small thickness.

Joint solution of equation (7.1.4) with the set of thermal conduction equations for detector gas and PA cell backing allows to determine complex amplitude of periodical component of a temperature field on the gas-sample boundary

$$\theta_{\pm}=\frac{2(bH_{\pm}-K_{\pm})-(b-1)(G_{\pm}+L_{\pm})exp(-\sigma_s l)-(b+1)(G_{\pm}-L_{\pm})exp(\sigma_s l)}{(b+1)(g+1)exp(\sigma_s l)-(b-1)(g-1)exp(-\sigma_s l)} \qquad (7.1.5)$$

where the following notations are introduced

$$G_{\pm}=-y_{1\pm}=-\chi_{\pm}^{-1}C_{\pm}+2\chi_{\pm}^{-2}(A_{\pm}-\alpha_{\pm}B_{\pm})-8\chi_{\pm}^{-3}\alpha_{\pm}^2A_{\pm},$$

$$H_{\pm}=-(y_{1\pm}+R_{\pm})exp(-\alpha_{\pm}l), \quad L_{\pm}=-q_{\pm}^{0}\sigma_s^{-1},$$

$$K_{\pm}=\sigma_s^{-1}(\alpha_{\pm}R_{\pm}+q_{\pm}^{0}-2y_{3\pm}l)exp(-\alpha_{\pm}l), \quad y_{3\pm}=-\chi_{\pm}^{-1}A_{\pm},$$

$$y_{2\pm}=\chi_{\pm}^{-1}B_{\pm}+4\chi_{\pm}^{-2}A_{\pm}, \quad \chi_{\pm}=\alpha_{\pm}^2-\sigma_s^2,$$

$$R_{\pm}=y_{3\pm}l^2-y_{2\pm}l, \quad q_{\pm}^{0}=y_{2\pm}+\alpha_{\pm}y_{1\pm}, \quad b=\frac{k_b a_b}{k_s a_s}, \quad b=\frac{k_g a_g}{k_s a_s},$$

$\sigma_s=(1+i)a_s$, $a_j=\sqrt{\Omega/2\beta_j}$ is the thermal diffusion coefficient of j-material, indexes b, g refer to the backing and the detector gas respectively.

Making use of (7.1.5) one can calculate the value of the

resulting signal $q_{\pm}=\chi_0((Re\theta_{\pm})^2+(Im\theta_{\pm})^2)^{1/2}$ (here $\chi_0=\gamma_0 P_0/\sqrt{2}a_g l_g T_0$), detected by microphone and its phase $\varphi_{\pm}=-(\pi/4)-arctg(Im\theta_{\pm}/Re\theta_{\pm})$. In most interesting case from practical point of view of thermally thick ($exp(-\sigma_s l)=0$), but optically transparent ($exp(-\alpha_{\pm} l)\tilde{=}1-\alpha_{\pm} l$) sample $\theta_{\pm}\tilde{=}(L_{\pm}-G_{\pm})/(g+1)$ expressions for amplitude and phase have the form

$$q_{\pm}=\left|\frac{\Delta P_{\pm}}{P_0}\right|=\frac{\omega\gamma_0|A_{0\pm}|^2}{\sqrt{2}a_s^2 a_g l_g T_0}\,|\chi_{123}|^2 N''_{\pm}(2\omega)(16k^4\mu_s^4+|a_0|^{-4})^{1/2}, \quad (7.1.6)$$

$$\varphi_0=-(\pi/4)-arctg(a_s^2/4k^2|a_0|^2). \quad (7.1.7)$$

Here $|A_{0\pm}|^2=64\pi n^2E^4/|N_{\pm}+n_{\mp}|^2(n_{\mp}+n_{\pm})^2$; $k=2\pi/\lambda$ is the wave number, $\mu_s=a^{-1}$ is the thermal diffusion length. For magnetoactive media in (7.1.7) substitution should be made of a_0 for $a_{\pm}$ and φ_0 for $\varphi_{\pm}$.

From the given relations (7.1.6), (7.1.7) it follows that PA signal value depends on the modulation frequency of incident light by law $\Omega^{-3/2}$ and is defined generally by incident light power, parameters of linear and nonlinear absorption.

Let us make numerical estimation of relative PA signal amplitude. If the parameters of detector gas are equal T_0=300K, γ_0=1.4, l_g=1sm, they for crystal $Bi_{12}SiO_{20}$ at λ=0.694μm, $\chi'_{123}\tilde{=}5\cdot10^{-8}$ед. CGSE [107], $\varepsilon'(2\omega)$=9.61, $\varepsilon''(2\omega)=1.21\cdot10^{-4}$ [105], $\gamma''(2\omega)\sim10^{-6}$,*) $N''_{\pm}(2\omega)\tilde{=}6.3\cdot10^{-6}$and at modulation frequency of laser radiation Ω=250Hz ($E\sim10^3$V/sm)relation $|\Delta P_{\pm}/P_0|$ will constitute value 10^{-7}. Change of electrical field intensity ($E\sim10^4$V/sm) results in sufficient growth of PA signal amplitude ($|\Delta P_{\pm}/P_0|\sim10^{-3}$).

Note, that maximum PA sound excitation will be reached at implementation of phase synchronism, when wave energy of the main frequency is most effective being pumped on the wave fre-

quency of the second harmonic, which is further effectively being absorbed. As a result the modulation frequency of incident light should be chosen in resonance regime so, that condition $\tau \leqslant \tau_c$ should be satisfied, where τ is the relations of temperature wave propagation to sample surface, making contact with detector gas, to the duration of a single light signal, and τ_c is the relative pulse duration of light impulses. Calculations shows that at thermal conduction coefficient $\beta_s \sim 3 \cdot 10^{-2}$ cal/K·sm^2 and thermal diffusion length changing from 10^{-2} to $1.4 \cdot 10^{-2}$ sm, amplitude modulation frequency lies in the range of values from 600 to 100 Hz.

Received relations (7.1.6), (7.1.7) may be useful at investigation of dissipative characteristics in gyrotropic cubic crystals. Taking into account that real part of the quadric susceptibility tensor for crystals of selenite type is known [105,107], experimental measurement of difference of PA signal relative values $\Delta q_{\pm} = |q_+ - q_-|$ .with regard to (7.1.6) allows to find tensor component of quadric susceptibility χ_{123}, responsible for nonlinear sample absorption, with the help of phase difference calculations of PA signals for magnetoactive media one can find circular dichroism parameter [109]

$$\Delta\varphi = |\varphi_+ - \varphi_-| = arctg\lambda^2 a_s^2 \frac{|a_+|^2 - |a_-|^2}{16|a_+ a_-|^2 + \lambda^4 a_s^4}. \qquad (7.1.8)$$

Taking into consideration that $|a_+|^2 - |a_-|^2 \sim g_z''(2\omega)\varepsilon''(2\omega)/2\varepsilon'(2\omega)$, and $|a_+ a_-|^2 \sim g_z'$, in linear approximation by parameters of magnetic gyrotropy we come we come to final expression according to (7.1.8)

$$g_z''(2\omega) = \frac{2\varepsilon'(2\omega)}{\varepsilon''(2\omega)\lambda^2 a_g^2}(16|a_+a_-|^2+\lambda^4 a_s^4)tg\Delta\varphi.$$

Thus, PA effect in nonlinear naturally or stimulated gyrotropic crystals of selenite type is investigated, condition of mostly effective PA transformation are marked. It is shown that by experimentally measured phase difference of acoustic signal corresponding to clockwise and counterclockwise circular polarizations of incident light one can determine magnetic circular dichroism parameter $g_z''(2\omega)$ at second harmonic frequency. It is ascertained that the measurement of relative PA signal amplitude allows to find tensor imaginary part component of quadric susceptibility χ''_{123}, responsible for nonlinear crystal absorption, assuming that value χ''_{123} is known.

7.2 Thermooptical sound excitation at generation of higher harmonics in piezocrystals.

It is known [105] that there are crystals absorbing second and third harmonic radiation, but which are transparent for the wave of the main frequency. Many of them have piezoelectric characteristics.

Consider a problem on thermooptical sound excitation under the conditions of nonlinear interactions of electromagnetic waves with gyrotropic piezoelectric crystals.

Let circular polarized light wave modulated in amplitude with frequency of Ω propagate along optical axis of uniaxial nonlinear gyrotropic crystal of thickness l. In conformity with [104] along the given direction in crystals of class 3 the second harmonic wave is generated, and in crystal of class 4 the

third harmonic generation occurs, the waves of higher harmonics having circular polarization with direction opposite to the first harmonic rotation direction of electric field intensity vector. We suppose that the frequency of the main radiation lies in the region of crystal transparency, and absorption occurs only at frequency of the second and third harmonic, what results in PA signal.

Basing on the expressions for wave fields of the second and third harmonic $E_{\pm}^{2\omega}$ and $E_{\pm}^{2\omega}$, gained from the solution of electrodynamics boundary task on harmonic generation in the approximation of the given field in [104], making use of relation for energy dissipation $Q_{\pm}$ with clockwise and counterclockwise elliptically polarized waves of the second and third harmonic and considering conditions of phase synchronism to be fulfiled (realization of conditions of phase synchronism in gyrotropic uniaxial crystals is possible as is shown in [104], due to natural and stimulated (Faraday effect) optical activity) one can find energy dissipation of the second harmonic in the following form

$$Q_{\pm} = \left(A_{\pm} z^2 + B_{\pm} z + C_{\pm}\right) e^{-\alpha_{\pm} l}, \qquad (7.2.1)$$

where the following notations are introduced

$$A_{\pm} = A_{O}^{\pm} \frac{4\omega^2}{c^2}, \quad B_{\pm} = \frac{2\omega}{c} \frac{A_{O}^{\pm} N_{\pm}''}{(N_{\pm}'+N)^2+(N_{\pm}'')^2}, \quad C_{\pm} = \frac{A_{O}^{\pm}}{(N_{\pm}'+N)^2+(N_{\pm}'')^2},$$

$$A_{O}^{\pm} = \frac{c\sqrt{\varepsilon'}(8\pi U^2 n^2)^2\left[(\chi'_{111}\mp\chi''_{222})^2+(\chi''_{111}\pm\chi'_{222})^2\right](1\mp\gamma_O^2)\alpha_{\pm}}{\pi(n_{\pm}+n)^4(1+\gamma_O^2)\left[(N_{\pm}'+N_{\pm}^{O'})^2(N_{\pm}''+N_{\pm}^{O''})^2\right]}.$$

Further one can find variable component of temperature fi-

eld in the sample under investigation

$$T(z)= U_0^{\pm}e^{-\sigma_s z}-E_1^{\pm}z^2e^{-\alpha_{\pm}z}-E_2^{\pm}ze^{-\alpha_{\pm}z}-E_3^{\pm}e^{-\alpha_{\pm}z} \qquad (7.2.2)$$

In (7.2.2) it is designated

$$E_1^{\pm}= \frac{A_{\pm}}{\alpha_{\pm}^2-\sigma_s^2}\ ,\ E_2^{\pm}= \frac{B_{\pm}}{\alpha_{\pm}^2-\sigma_s^2}+\frac{4\alpha_{\pm}A_{\pm}}{(\alpha_{\pm}^2-\sigma_s^2)^2}\ ,\ U_0^{\pm}= \alpha_{\pm}E_3^{\pm}-E_2^{\pm}\ ,$$

$$E_3^{\pm}= \frac{C_{\pm}}{\alpha_{\pm}^2-\sigma_s^2}+\frac{2\alpha_{\pm}B_{\pm}-2A_{\pm}}{(\alpha_{\pm}^2-\sigma_s^2)^2}+\frac{8\alpha_{\pm}^2A_{\pm}}{(\alpha_{\pm}^2-\sigma_s^2)^3}$$

Making use of the received expression (7.2.2) and basing on the method of PA signal evaluation in piezoelectric ctystals one can determine potential difference developing by piezoelectic under different boundary conditions [110]

$$V_1^{\pm}= h_0'\left[\frac{1}{k}\,tg(kl/2)(C_1^{\pm}+C_2^{\pm})+V_0^{\pm}\right]+V_4^{\pm}$$

$$V_2^{\pm}= h_0'\left[-\frac{1}{k}C_1^{\pm}tg(kl)-C_3^{\pm}\frac{\cos(kl)-1}{\cos(kl)}+V_0^{\pm}\right]+V_4^{\pm}$$

$$V_3^{\pm}= h_0'\left[-\frac{1}{k}C_2^{\pm}tg(kl)+C_4^{\pm}\frac{\cos(kl)-1}{\cos(kl)}+V_0^{\pm}\right]+V_4^{\pm} \qquad (7.2.3)$$

$$V_4^{\pm}= \frac{P_3^s}{\varepsilon_{33}^s}\left\{\frac{V_0}{\sigma_s}+E_1^{\pm}\left[e^{-\alpha_{\pm}l}\left(\frac{l^2}{\alpha_{\pm}}+\frac{2l}{\alpha_{\pm}^2}+\frac{2}{\alpha_{\pm}^3}\right)-\frac{2}{\alpha_{\pm}^3}\right]-\right.$$

$$\left.-E_2^{\pm}\left[e^{-\alpha_{\pm}l}\left(\frac{l}{\alpha_{\pm}}+\frac{1}{\alpha_{\pm}^2}\right)-\frac{1}{\alpha_{\pm}^2}\right]-\frac{E_3^{\pm}}{\alpha_{\pm}}\left[e^{-\alpha_{\pm}l}-1\right]\right\}$$

In (7.2.3) notations coinside with those adopted in [110].

Note, that expressions for potential difference (7.2.3) occuring at absorption of clockwise and counterclockwise cir-

cular polarized second harmonic of the main radiation keeps its form at calculation of PA signal at the second and third harmonic frequency in crystals of class 4, taking into account substitution in $E_1^{\pm}$, $E_2^{\pm}$, $E_3^{\pm}$ constants $A_{\pm}$, $B_{\pm}$, $C_{\pm}$ correspondingly for $A_{\pm}^{'}$, $B_{\pm}^{'}$, $C_{\pm}^{'}$ (see [110]).

To make clear the influence of optical characteristics of gyrotropic crystal on the mechanism of PA signal formation consider several particular cases. In the region of low modulation frequencies of incident light ($\Omega<300$ Hz) the length of generated sound wave Λ is essentially larger then the thickness of layer l ($\Lambda>>l$), that's wy we can neglect sample acoustic characteristics up to $l=0.5$ sm. Relations (7.2.5) in this case are esntially simplified $V_1^{\pm} = V_2^{\pm} = V_3^{\pm} = h_0^{'} V_0^{\pm} + V_4^{\pm}$ and resulting signal will be defined by optical and thermal ctystal parameters. The numerical analysis of the expressions received shows that the dependence of PA signal amplitude on the thickness has a pronounced maximum (Fig.23) caused by the energy dissipation growth due to increasing of second harmonic generation effectiveness on the given thickness of a crystal with subsequent absorption. The increasing of bulk absorption coefficients results in displacement of a signal maximum to small sample thickness, what is connected with decreasing of optical absorption length $\mu_{\alpha} = 1/\alpha^{(2\omega)}$. Phase of PA response doesn't undergo so essential change. At clamped crystal boundaries the PA signal formation is realized through the mechanism of piroelectric effect. Dependence of amplitude-phase characteristics of PA signal on the thickness of crystal sample has certain peculiarity, manifesting in flash of amplitude and phase on the same thickness of the crys-

tal [110]. This is connected with nonlinear character of thermal discharge in the sample at light absorption at the second harmonic frequency. The change of a bulk absorption coefficient doesn't lead to the displacement of signal "maximum", as optical absorption length μ_a remains larger than the thickness of a crystal, i.e. case of opticaly transparent sample is being realized.

7.3. PA spectroscopy in nonlinear crystals with centralsymmetrical paramagnetical phase.

The authors [111] investigated possibility of nonlinear effects in magnetically ordered crystals when crystal structure has inversion center, and magnetic one has no such center. The interest to such crystals may be explained by the fact that in the paramagnetic state of the crystals with inversion center dipole approximation doesn't assume the existence of the effects of optical activity and second harmonic generation. However, at appierence of magnetic structure one can assume that effects mentioned above become possible, they may be caused by a magnetic alignment or an external magnetic field. In [112] second harmonic generation was experimentally investigated in the central symmetrical crystals, ferrite-garnets, which were placed in external magnetic field. The sample under investigation was an epitaxial film of yttrium ferrite-garnet substituted for *Bi* of the composition $Y_{2,5}Bi_{0,5}Fe_5O_{12}$ of thickness 4,8mkm, wich was grown on the backing $Y_3Fe_5O_{12}$ with orientation [111]. Transparent along the pump wavelength (λ = 1064nm) sample had a considerable absorption in the visible range at the frequency of the

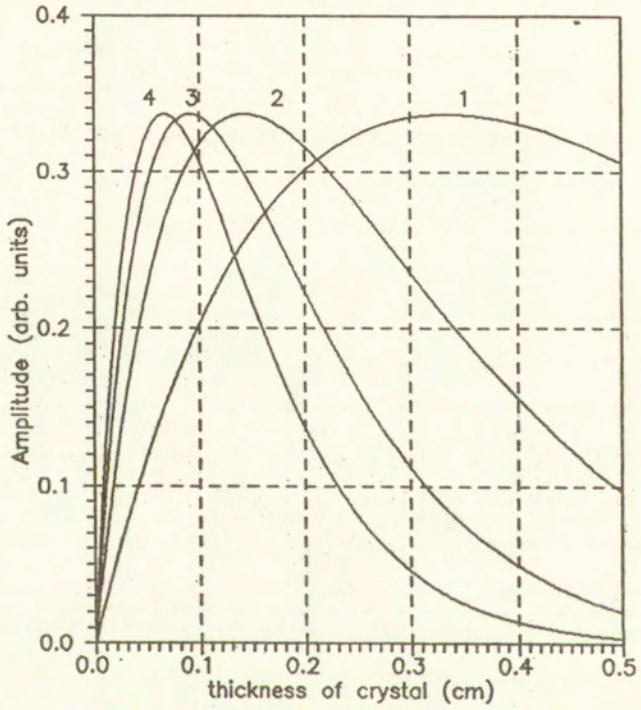

Fig.23. Dependence of PA signal amplitude q on the thickness of crystal l at different values of absorption coefficient at second harmonic frequency ($\alpha_+^{2\omega}$): 1-$3\cdot10^2$, 2-$7\cdot10^2$, 3-$1.1\cdot10^3$, 4-$1.5\cdot10^3$.

second harmonic (optical density of the epitaxial film was about 0.6 for λ=632nm [112]). All that makes it possible to apply method of PAS for investigation of film dissipative properties.

Let laser beam intensity modulated with the frequency Ω be normally incident on a nonlinear central symmetrical crystal of class m3m of thickness d, cut perpendicular to the axis of the third order [111], placed in a gas-microphone cell [44], which is placed in an external magnetic field . According to [111,112] along the direction of propagation generation of the second harmohic wave will occur, which being intensively absorbed causes initiating a PA signal. Using the results of the boundary task solution of second harmonic generation in the approximation of given field [111] and assuming that the conditions of phase synchronism are satisfied we can present energy dissipation for double frequency waves in the following form

$$Q_{\pm} = \left(A_{\pm} z^2 + B_{\pm} z + C_{\pm}\right) e^{-\alpha_{\pm} l} , \qquad (7.3.1)$$

where

$$A_{\pm} = \frac{\omega^2}{c^2} A_0^{\pm 2}, \quad B_{\pm} = \frac{2\omega}{c} A_0^{\pm 2} \frac{Rn'' - Tn'}{R^2 - T^2} , \quad C_{\pm} = A_0^{\pm 2} |n(2\omega)|^2,$$

$$A_0^{\pm 2} = \frac{32\omega^2 n^2 |\chi|^2 |n(2\omega)|^2 (1 \mp \gamma_0)^2 N_{\pm}''(2\omega)}{(n_0+n)^2 (S^2+L^2)(1+\gamma_0^2)} ,$$

$$R = 2(n'^2 - n''^2) + g' + 2Nn', \quad T = 4n'n'' + g'' + 2Nn'', \quad L = 4n'n'' + g'' + 2n_0 n'',$$

$$S = 2(n'^2 - n''^2) + g' + 2n_0 n', \quad |\chi|^2 = \chi_{111}'^2 + \chi_{111}''^2,$$

$$N_{\pm}''(2\omega) = \frac{1}{2}\varepsilon'' \pm g'', \quad \alpha_{\pm} = \frac{4\pi}{\lambda}\left[n'' \pm \frac{g''n' - g'n''}{n'^2 - n''^2}\right] ,$$

The rest of notations corresponds to those adopted in [111].

The joint solution of a set thermal conduction equations for the detector gas , sample (taking into account (7.3.1)) and backing makes it possible to determine complex amplitude of a temperature field on the sample-gas boundary [113].

$$\theta^{\pm} = \frac{(F_2^{\pm}-F_1^{\pm})e^{-\sigma_s l}(b-1)+(F_2^{\pm}+F_1^{\pm})e^{\sigma_s l}(b+1)-2(bF_3^{\pm}+F_4^{\pm})}{(b+1)(g+1)\exp(\sigma_s l)-(b+1)(g+1)\exp(-\sigma_s l)} \qquad (7.3.2)$$

Here the following notations are used

$$F_1^{\pm}= -E_3^{\pm}, \quad F_2^{\pm}= r^{\pm}E_3^{\pm}-\sigma_s^{-1}E_2^{\pm}, \quad F_3^{\pm}= -\left(E_1^{\pm}l^2+E_2^{\pm}l+E_3^{\pm}\right)e^{-\alpha_{\pm} l},$$

$$F_4^{\pm}= r^{\pm}E_1^{\pm}l^2e^{-\alpha_{\pm} l}+\left(r^{\pm}E_2^{\pm}-2\sigma_s^{-1}E_1^{\pm}\right)le^{-\alpha_{\pm} l}+\left(r^{\pm}E_3^{\pm}-\sigma_s^{-1}E_2^{\pm}\right)e^{-\alpha_{\pm} l},$$

$$E_1^{\pm} = \frac{A_{\pm}}{\alpha_{\pm}^2-\sigma_s^2}, \quad E_2^{\pm} = \frac{B_{\pm}}{\alpha_{\pm}^2-\sigma_s^2}+\frac{4\alpha_{\pm}A_{\pm}}{(\alpha_{\pm}^2-\sigma_s^2)^2},$$

$$E_3^{\pm} = \frac{C_{\pm}}{\alpha_{\pm}^2-\sigma_s^2}+\frac{2\alpha_{\pm}B_{\pm}-2A_{\pm}}{(\alpha_{\pm}^2-\sigma_s^2)^2}+\frac{8\alpha_{\pm}^2A_{\pm}}{(\alpha_{\pm}^2-\sigma_s^2)^3}$$

The numerical analysis of amplitude and phase characteristics of PA response, performed for crystal $Y_{2,5}Bi_{0,5}Fe_5O_{12}$, showed that the amplitude dependence on the thickness of crystal sample has a pronounced peak value caused by the effectiveness of excitation (and therefore absorption) of the second harmonic wave at a certain thickness. Variation of the magnitude of circular dichroism parameter changes absolute value of the signal amplitude and slightly effects on the behaviour of its phase (Fig.24a,b).

Considering most interesting special case in practical aspects of thermally thick ($\exp(-\sigma_s l) = 0$) and optically transpa-

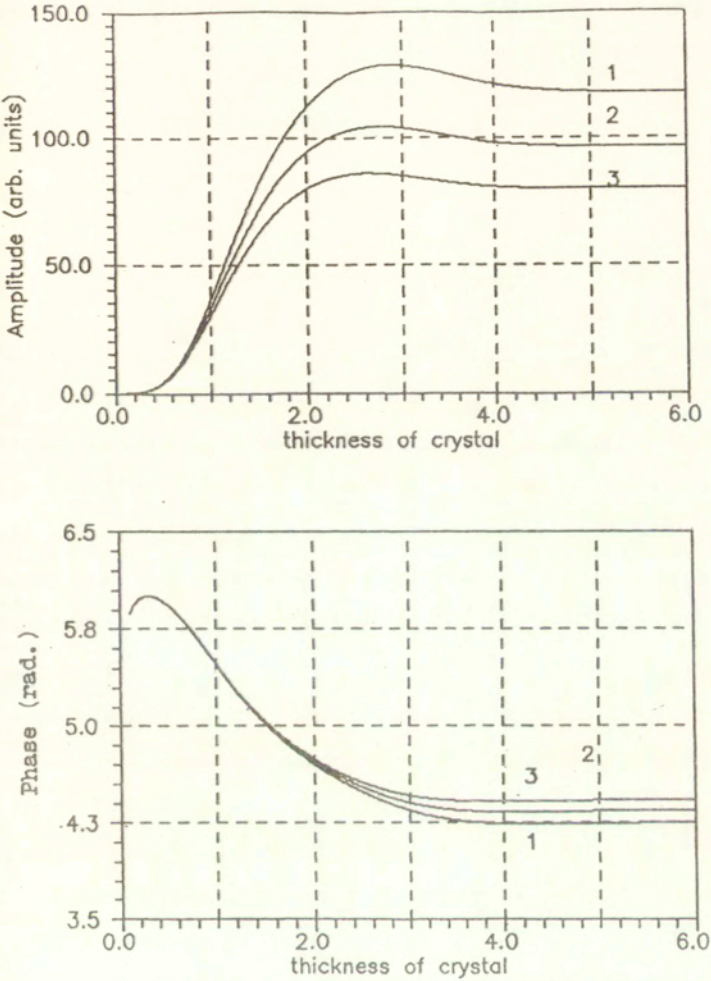

Fig.24. Dependence of PA response amplitude (a) and phase (b) (τ=-1) on the thickness of crystal sample at different values of magnetic circular dichroism parameter g'': 1-1.0·10^{-5}, 2-3.0·10^{-5}, 3-5.0·10^{-5}.

rent ($\exp(-\alpha l) = 1 - \alpha l$) sample expression (7.3.2) is essentially simplified and its amplitude takes the form

$$q^{\pm} = \varkappa_0 \frac{\omega^2}{c^2} A_0^2 |\chi|^2 N''_{\pm}(2\omega) \frac{(1 \mp \gamma_0)^4}{(1 + \gamma_0^2)^2} \qquad (7.3.3)$$

where

$$A_0^2 = \frac{32\omega W^2 n^2 |n(2\omega)|^4}{\alpha_s^4 (n_0 + n)^2 (S^2 + L^2)} ,$$

Received relations (7.3.3) can be used at investigation of dissipative characteristics of a crystal sample. Assuming ,that the real part of magnetoelectric tensor with quadric susceptibility χ'^2_{111} is known, experimental measurement of amplitude difference of PA signals $\Delta q = |q^+ - q^-|$ corresponding to the clockwise and counterclockwise circular polarizations of incident light with regard to (7.3.3) gives the possibility of estimating of imaginary part of qudric susceptibility component tensor χ''_{111}, and calculation of phase difference of PA signals $\Delta\varphi = |\varphi_+ - \varphi_-|$ permits to find circular dichroism parameter.

As far as PA signal emerges due to light absorption at double frequency, which is generated under magnetic ordinary of the crystal, i.e. under magnetic phase transitions of the type $\bar{3}m1' \longleftrightarrow \bar{3}'m'$, $m3m \longleftrightarrow \bar{3}m'$, $m3m \longleftrightarrow m\bar{3}\bar{m}'$ it makes possible to determine a point of magnetic phase transitions by a PA method.

8. PHOTODEFLECTION SPECTROSCOPY OF THE MOVING GYROTROPIC MEDIA.

A method of photodeflection spectroscopy is widely applicable at optic investigation of thermophysic, acoustic, nonlinear characteristics of different media and materials [114,115]. We have reviewed some cases with fixed samples [115] as well as with moving samples[116]. An impulse variant of photodeflection spectroscopy is proposed in [117] for the investigation of semiconductor energy transfer process, as well as for the measuring of main thermal and electronic parameters of Si samples. Authors [118] have developed a similar method of thermal lens, being successfully applied for studying of gyrotropic media with circular dichroism bands. They have also developed a new ultrasensitive circular dichroism spectropolarimeter based on the thermal excitation in signal medium by two light beams with right and left circular polarization.

The aim of the part is to considered a photodeflection spectroscopy method for the investigation of optical characteristics of the absorbing gyrotropic moving media.

Let us assume that amplitude-modulated laser beam with the frequency $\Omega=2\pi\nu$ influences isotropic-gyrotropic absorbing moving sample, its characteristics being described as material equations.

Similar [116] let us discuss interaction transversal geometry of excitating and probing beams in which probing beam is perpendicular to excitation beam. A velocity vector of translation motion of the gyrotropic sample coinides with the direction of Ox axis. Due to the modulated absorption of falling on the sample

radiation, in the former temperature distribution being established, which can be defined by solving a differential equation:

$$\Delta T - \frac{1}{\beta_s}\frac{dT}{dt} = -\frac{1}{2k_s}Q(r,t)f(t) + V_x\frac{dT}{dx} \qquad (8.1)$$

where $Q=Q_+ + Q_-$, $Q_\pm$ is the velocity of energy dissipation of circular polarized isonormal waves, $f(t)=1/2(1+exp(i\Omega t))$ is the modulating function, Ω is the modulating frequency, t is time of radiation excitation on the sample, V_x is x-component of the translation motion velocity. Basing on [4,32] for energy dissipation of Gaussian beam of a zero-orded mode we can express:

$$Q_\pm = \frac{cn_1^2|E|^2(1\pm\tau_0)^2}{2\lambda|n_0+n_1|^2(1+\tau_0^2)}\left(\frac{\varepsilon''}{2\sqrt{\varepsilon'}}\pm\gamma''\right)exp(-\alpha z)exp\left[-\frac{x^2+y^2}{a^2}\right], \qquad (8.2)$$

In (8.2) a,τ_0 is the radius and incident beam elipticity, $\alpha_\pm = 4\pi/\lambda(\varepsilon''/2\sqrt{\varepsilon'})$. The rest signs coincide with the signs accepted in [32].

Solution of the thermal conductivity equation (8.1) is defined as

$$T(x,y,z,t)=\int_{-\infty-\infty}^{+\infty+\infty+\infty+\infty}\int\int\int_{0\ 0}Q(\xi,\eta,\mu,\tau)G(\xi,\eta,\mu,\tau)d\xi d\eta d\mu d\tau \qquad (8.3)$$

demanding the fulfillment of standard boundary and initial conditions. Here $G(\xi,\eta,\mu,\tau)$ is Green function

$$G=\frac{\theta(t)}{8\rho C_p\pi^{\frac{3}{2}}(\beta_s(t-\tau))^{\frac{3}{2}}}\times exp\left[-\frac{(x-(\xi+V_x(t-\tau)))^2}{4\beta_s(t-\tau)}\right]\times$$

$$exp\left[-\frac{(y-\eta)^2}{4D_s(t-\tau)}\right]\times exp\left[-\frac{(z-\mu)^2}{4D_s(t-\tau)}\right], \qquad (8.4)$$

satisfying the equation

$$\Delta G - \frac{1}{\beta_s}\frac{dG}{dt} = -\frac{1}{2k_s}\delta(x-\xi,y-\eta,z-\mu)\delta(t-\tau) + V_x\frac{dG}{dx},$$

$\theta(t)$ is Heaviside unit step function. Taking into account substitution (8.4),(8.2) into (8.3) and sequential integral calculation on spatial variables for temperature field distribution in absorbing gyrotropic flowing sample moving with the velocity V_x it is easy to derive [118]

$$T(x,y,z,t)= \frac{cn_1^2|E|^2}{4\lambda\pi\ \rho C_p|n_0+n_1|^2(1+\tau_0^2)} \times ((1+\tau_0)^2\times$$

$$\times(\varepsilon''+2\gamma''\sqrt{\varepsilon'})\times\int_0^t \frac{1+\cos(\omega\tau)}{a^2+8\beta_s(t-\tau)} \times exp\left[-\frac{2(x-V_x(t-\tau))^2}{a^2+\beta_s(t-\tau)}\right]\times$$

$$\times exp\left[-\frac{2y^2}{a^2+\beta_s(t-\tau)}\right]\times exp\left[-\alpha_+(z+\alpha_+\beta_s(t-\tau))\right]+$$

$$+(1-\tau_0)^2\times(\varepsilon''-2\gamma''\sqrt{\varepsilon'})\times\int_0^t \frac{1+\cos(\omega\tau)}{a^2+8\beta_s(t-\tau)} \times$$

$$\times exp\left[-\frac{2(x-V_x(t-\tau))^2}{a^2+\beta_s(t-\tau)}\right]\times exp\left[-\frac{2y^2}{a^2+\beta_s(t-\tau)}\right]\times$$

$$\times exp\left[-\alpha_-(z+\alpha_-\beta_s(t-\tau))\right], \qquad (8.5)$$

The use of (8.5) makes it possible to obtain the value of probing beam deflection:

$$\Phi_{\pm}^T(x,z,t)= \frac{1}{n_{\pm}} \frac{dn_{\pm}}{dT} \int \frac{dT_{\pm}(x,y,z,t)}{dx}\, dy \qquad (8.6)$$

Ratio (8.6) is taken for the most interesting case of circular polarization of the incident beam ($\tau_0=\pm1$), which will be treated further.

Basing on the obtained expressions (8.5),(8.6) numerical

calculation of temperature field distribution and probing beam deflection angles is made, their value being analyzed in dependence upon modulated frequency $F=\Omega/2\pi$, flow velocity V_x, generated coordinate x/a and interaction radiation time t. As in [116] asymmetric delay of temperature field enhances while movement velocity is increasing (Fig. 25) and absolute value of the temperature distribution peak decreases simultaneously.

The dependence of deflection angles upon fixed coordinate at zero-order movement velocity possesses antisymmetry (Fig. 26a), and for right and left circular polarized excited beam it differs slightly by the value which is proportional to the circular dichroism parameter value. With the increasing of the moving medium velocity the magnitude of deflection angles increases to peak value (V_x= 0.004 m/s in the presen case) and then decreases roughly in exponent (Fig. 27). The difference of angles $\Phi_{\pm}$ for orthogonal circular polarization in the peak point also recluse maximum value. As it was expected the velocity increasing leads to symmetry loss of deflection angles coordinate dependence (Fig. 26b.c), their magnitude being oscillated by the law, which is similar to harmonic one from the modulation frequency of the excitation beam (Fig. 28). The dependence $\Phi_{\pm}$ on circular dichroism parameter has a linear character and while the movement velocity is increasing absolute value Φ decreases, deflection angle of line $\Phi_{\pm}=\Phi_{\pm}(\gamma'')$ changes relatively abscissa axis what can be explained by temperature field spreading in a sample volume on the fixed modulation frequency. Frequency increase at $V_x=const$ also leads to signal fall due to thermal inertia display.

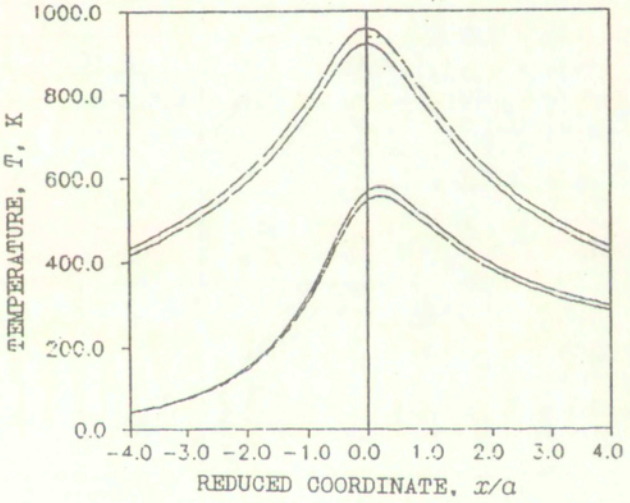

Fig.25. Dependence of temperature on reduced coordinate

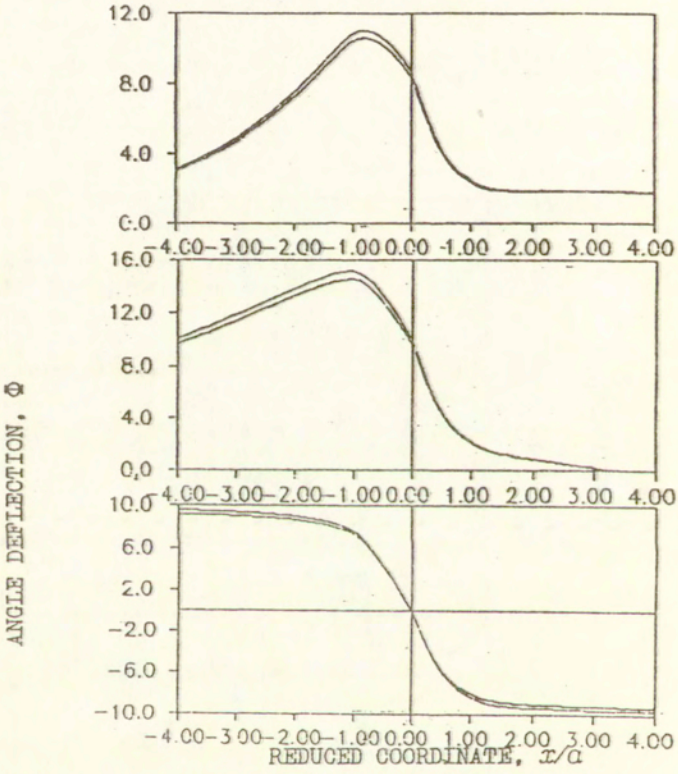

Fig 26.Dependence of deflection angle on coordinate.

Thus while measuring circular dichroism spectra by photodeflection method it is necessary to optimize according to the velocity value V_x, modulation frequency Ω, interaction geometry and its coordinate.

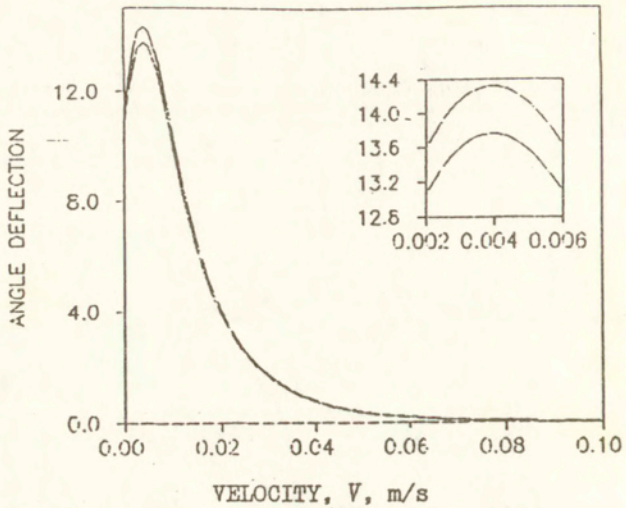

Fig.27. Dependence of deflection angle on velocity.

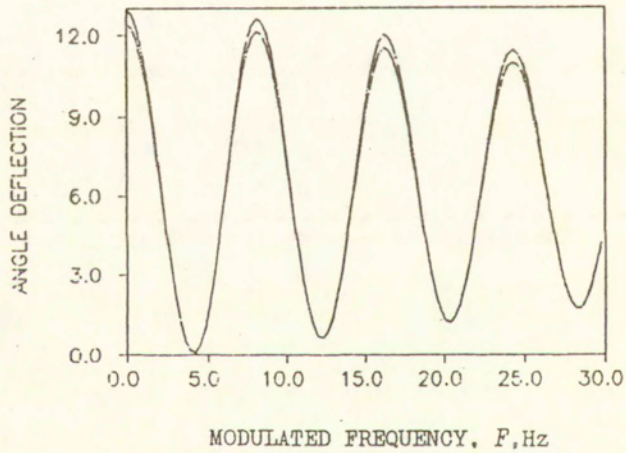

Fig.28. Dependence of deflection angle on modulated frequency.

9. THERMOELASTIC EXCITATION OF SOUND WAVES IN ACOUSTIC GYROTROPIC CRYSTALS.

The influence of modulated optical radiation on absorbing condensed media results in their periodic heating accompanied by the sound waves excitation. This phenomenon is well-known in optics and was named photoacoustic effect [1,2]. It has found wide application and has become the basis of modern perspective field - photoacoustic spectroscopy and microscopy.

It is natural to expect that a thermal mechanism of sound waves generation is quite possible in acoustically absorbing media because sound dissipation, accompanied by heat exchange and if the process is periodical results in thermoelastic oscillations excitation.

Investigation of a "soundacoustic effect" in elastic media was first reported in [119], where it was shown that the resulting signal value is directly proportional to the tension square on an acoustic emitter and inversely proportional to modulation frequency of an emissive sound wave. It is still worth to note that only qualitative dependence of tension on a registering piezodetector on temperature field distribution in the sample under investigation has been established in theoretical part of the paper [119] based on the solution of thermal conductivity equation. Besides that in investigating processes in elastic dissipative media calculation of acoustic gyrotropy effects [120,121] may be very significant, in particular, the circular dichroism phenomena [122], conditioned by absorption coefficients difference in isonormal elastic waves.

That paper investigated peculiarities a thermal mechanism of

exciting elastic waves in acoustically gyrotropic absorbing media with subsequent piezoelectric detection of a generating signal.

We shall proceed from the well-known correlation [122]

$$\gamma_a = s_{a\beta}\sigma_\beta + r_{a\beta,n}\nabla_n\sigma_\beta \qquad (9.1)$$

between elastic deformations tensors γ_{ij} and tensions σ_{ij}. In (9.1) $s_{a\beta}=s'_{a\beta}+is''_{a\beta}$ and $r_{a\beta,n}=r'_{a\beta,n}+ir''_{a\beta,n}$ are complex tensors of medium elastic characteristics with common matrix notation, $s''_{a\beta}$ taking into account ordinary absorption, $r''_{a\beta,n}$ is acoustic circular dichroism.

Let an intensity modulated sound beam with Gaussian amplitude distribution

$$\underline{u} = (\underline{u}_+ + \underline{u}_- + \underline{u}_0)exp[-r^2/w_0^2] \qquad (9.2)$$

with two transverse $\underline{u}_\pm=(1\mp\tau)\underline{e}_\pm uexp[ik_\pm z]/\sqrt{2(1+\tau^2)}$ and one longitudinal $\underline{u}_0=\underline{e}u^0exp[ik_0z]$ components propagate along a crystalographic axis which is a 2nd or 4th order rotation one in a 23 or 423 class absorbing acoustically gyrotropic crystal contacting a piezodetector. Following notation is used here: w_0- radius of a sound beam cross-section; $k_\pm=\omega/\lambda_{44}\pm0,5\rho\omega^2r_{543}$, $k_0=\omega/\sqrt{\lambda_{12}+2\lambda_{44}}$- wave numbers of right and left circularly polarized transverse and longitudinal plane monochromatic waves respectively [81,122]; $\underline{e}_\pm=(\underline{a}\mp i\underline{b})/\sqrt{2}$; $\underline{a},\underline{b},\underline{c}$- unit orts of repart coordinate system; τ is ellipticity; $\lambda_{a\beta}=s^{-1}_{a\beta}/\rho$- tensor of modulated elasticity [33]; ρ is density of medium.

Thermal sources conditioned by transformation of energy into that thermal springing up inside an absorbing medium cause modulated thermoelastic tensions leading to a specters of acoustic waves forming a resulting signal detecting signal value is pro-

portional to eigenwaves energy dissipation, defined by the expression [122]

$$Q = \sigma_{ik} - \frac{d\gamma_{ik}}{dt} \qquad (9.3)$$

We assume that the density of energy in the medium is small and non-linear effects are negligible. A line over expression (9.3) is a time mean. Using correlations (9.1)-(9.3) and neglecting one in comparison with members of order $r^2 exp[-2r^2/w_0^2]/|k_{\pm}|^2 w_0^4$, we represent energy dissipation $Q=Q_+ + Q_- + Q_0$ in linear approximation $r''_{54,3}$, λ''_{44} by the following expressions:

$$Q_\nu = \Phi_\nu exp[-\alpha_\nu z - 2r^2/w_0^2],\ \nu = +,-,0;$$

$$\Phi_{\pm} = \rho\omega^2 \sqrt{\lambda'_{44}}\,\alpha_{\pm}(1\mp\tau)^2|u|^2/4(1+\tau^2),$$

$$\Phi_0 = 0{,}5\rho\omega^2\sqrt{\lambda'_{12}+2\lambda'_{44}}\,\alpha_0|u^0|^2; \qquad (9.4)$$

$$\alpha_{\pm} = -\lambda''_{44}\omega/(\lambda'_{44})^{1,5} \pm \rho\omega^2 r''_{54,3},\ \alpha_0 = -(\lambda''_{12}+2\lambda''_{44})/(\lambda'_{12}+2\lambda'_{44})^{1,5}.$$

Formulal (9.4) define density of thermal sources power of thermal conductivity equation

$$\nabla^2 T - \frac{1}{\beta_s}\frac{dT}{dt} = -\frac{Q}{2k_s}(1+exp(i\Omega t)); \qquad (9.5)$$

$$k_s\frac{dT}{dz} = h_1 T,\ z=0;\ k_s\frac{dT}{dz} = -h_2 T,\ z=l;$$

which lets us find temperature field distribution in gyrotropic plane parallel plate at boundary conditions of third kind. In (9.5) β_s and k_s are a sample temperature and heat conduction coefficients, h_1, h_2 are heat exchange coefficients on the front and back surface of the plate respectively, Ω is modulation frequency of the sound beam. Sound energy absorbed by the medium is transformed into that of thermoelastic oscillations detected by a

piezoelectric. For calculation of potential difference at the piezodetector edges we shall use the methods in [27]. It is worth noting that thermoelastic oscillations generation effect appears owing to low sound absorption modulation frequency (in [119], for example, modulation frequency Ω was changed in range from 10 to 10^3Hz). This circumstance lets us neglect gyrotropy influence on detected sound waves propagation, as acoustic activity significantly displays only at megahertz and gygahertz frequencies [120,121]. Calculation gives the following expression for a resulting signal $V=V_+ + V_- + V_0$, induced in a piezotransformer at $z=l$:

$$V_\nu = K_\nu(3J_\nu - 2J_\nu^0) \tag{9.6}$$

and at $z=0$:

$$V_\nu = -K_\nu(3J_\nu - J_\nu^0) \tag{9.7}$$

In (9.6), (9.7) the following notations are used:

$$K_\nu = C_\nu(\tau)B_\nu, \quad D=(1+g)(1+b)exp(\sigma_s l)-(1-g)(1-b)exp(-\sigma_s l),$$

$$C_\nu = \frac{\pi e_{31}^P L a_t (3\lambda'_{12}+2\lambda'_{44}) w_0^2 \Phi_\nu}{2k_s \varepsilon_{33}^P S \alpha_\nu (\lambda'_{12}+2\lambda'_{44})}, \quad B_\nu = \frac{\alpha_\nu}{(\alpha_\nu^2-\sigma_s^2)\sigma_s D l};$$

$$e_{31}^P = e_{31} - e_{33}c_{13}^E/c_{33}^E, \quad \varepsilon_{33}^P = \varepsilon_{33} - e_{33}^2/c_{33}^E, \quad r_\nu = \alpha_\nu/\sigma_s;$$

$$g = \frac{h_1}{k_s\sigma_s}, \quad b = \frac{h_2}{k_s\sigma_s}, \quad \sigma_s = (1+i)a_s;$$

$$J_\nu = (g+r_\nu)[(b-1)F(\sigma_s l)exp(-\sigma_s l) + (b+1)F(-\sigma_s l)exp(\sigma_s l)] +$$

$$+ (r_\nu - b)exp(-\alpha_\nu l)[(1+g)F(\sigma_s l) - (1-g)F(-\sigma_s l)] - \alpha_\nu^{-1} D\sigma_s F(-\alpha_\nu l);$$

$$J_\nu^0 = (g+r_\nu)[(b-1)F^0(-\sigma_s l) + (b+1)F^0(\sigma_s l)] + r_\nu^{-1} DF^0(-\alpha_\nu l) +$$

$$+ exp(-\alpha_\nu l)(r_\nu - b)[(1-g)F^0(-\sigma_s l) - (1+g)F^0(\sigma_s l)];$$

$F(p)=exp(p)+(1-exp(p))/p$, $F^{0}(p)=1-exp(p)$,

e_{31}, e_{33}, ε_{33} and c_{13}^{E}, c_{33}^{E} are piezoelectric modules tensors components, dielectric permeability and coefficient of elasticity of a detector material; L and S is thickness and area of a piezodetector; $a_s=\sqrt{\Omega/2\beta_s}$ and a_t are thermal diffusion and a sample thermal expansion coefficients.

The obtained general expressions in (9.6), (9.7) allow us to calculate a resulting signal amplitude and phase but are very cumbersome, therefore let us turn to investigating some particular cases.

Consider frontal distribution of a piezoelectric detector ($z=0$) with regard to the sample under investigation, which thermally thick ($exp(-\sigma_s l)=0$, $exp(-\alpha_\nu l)=1-\alpha_\nu l$). We shall neglect heat exchange on a plate surface ($g=b=0$). Let a propagating in the medium transverse sound beam be linearly polarized ($\tau=0$, $C_+(0)=C_-(0)=C$). Then the resulting signal q ($q_\nu=\sqrt{(Re V_\nu)^2+(Im V_\nu)^2}$) will be defined by the correlation

$$\Delta q = q_+ - q_- = \frac{2C\alpha\lambda''_{44}\omega}{\alpha_s^2(\lambda'_{44})^{1.5}}, \qquad (9.8)$$

hence follows inversely proportional dependence q on modulation frequency Ω of an initial sound beam, which coincides with the results of paper [119].

In the case of circular polarization of a transverse component of a sound beam ($\tau=\pm 1$, $C_{\pm}(\mp 1)=2C$) the resulting signal amplitude is expressed by the formula

$$q_{\pm} = \frac{2C\alpha_{\pm}}{\alpha_s^2} \qquad (9.9)$$

Calculating on the basis (9.9) signals amplitude difference $\Delta q=q_+-q_-$ one can clearly express a parameter of acoustic circular dichroism $r''_{54,3}$ through Δq

$$r''_{54,3}=\alpha_s^2\Delta q/4C\rho\omega^2. \qquad (9.10)$$

Thus, for example, it to take $r''_{54,3}=1{,}5\cdot10^{-23}m^3/H$, signals amplitude difference $|\Delta q|$, registered by a piezodetector made of transverse isotropic ceramics CTS-4 ($S=0{,}1sm^2$, $L=1{,}8\cdot10^{-2}sm$), which were excited by circularly polarized sound beam of $10^{-3}W$ power and frequency 1GHz ($w_0=0{,}1sm$) in the sample of α-quartz (for transverse sound waves, propagating along the axis of third order in a crystal of 32 symmetry class, with the frame of adopted approximations all the above stated can be considered remaining in force) of 2,5sm thickness at modulation frequency $\Omega=10Hz$ will amount $1{,}6\cdot10^{-4}$. For a longitudinal sound amplitude signal value q_0 is defined by the expression

$$q_0=\frac{C_0\alpha_0}{\alpha_s^2} \qquad (9.11)$$

Thus, experimental measurements of a resulting signal amplitudes for various polarizations of an initial sound beam let us in accordance with (9.8)-(9.11) define absorption value λ''_{44} and the parameter of acoustic circular dichroism $r''_{54,3}$ of the elastic medium, which has spatial disperse.

10. INSTRUMENTATION FOR EXPERIMENTAL INVESTIGATION OF GYROTROPIC MEDIA

Experimental investigations of gyrotropic media properties conducted collectively by Gomel University and IFTR will be carried out on measurement stands in IFTR.

The measuring set-up consists of optical and electronic units (Fig. 29). The optical unit comprises the light source, monochromator and chopper. Broken lines in Fig. 29 present a block scheme of the electronic unit designed in IFTR, comprising photoacoustic cell and electronic circuitry.

Apparatus for photoacoustic spectroscopy is designed in single-beam or double-beam versions. In the IFTR design a single-beam principle was adopted. The principle of operation is as follows: a xenon lamp with power in the range of the several hundred watts and a broad radiation spectrum is used as a light source for excitation of tested sample. Light beam formed in the optical system is directed to the monochromator, where the exciting signal of required wavelength is selected. Monochromatic light beam passes through the chopper, where is periodically choppered. Choppering frequency is adjustable and settable within a wide range. Its value is displayed on a digital display. Light pulses are introduced into the measuring cell and, acting on tested sample, cause photoacoustic effect. Ther acoustic wave generated in the cell is detected by means of acoustic transducer, such as a condenser or a piezoelectric microphone. The apparatus is designed for operation with both types of transducers. Next, the electric signal is amplified in the

preamplifier. The low noise preamplifier level matches high output impedance of the transducer to the input of the rest of the complete system. This signal is next sent to the amplifying-filtering channel. Amplifier features gain control for matching to signal level. High- and low-pass filters are intended for suppression of noise and interference signals below and above detection frequency.

The synchronous detector with an integrator are used for separation of usable signal with an amplitude small with respect to spurious background. The detector generates a product of instantaneous value of measured signal and reference signal value, being the representation of light modulation waveform in the chopper.

Multiplication function of above signals could be represented by means of equation

$$u = k \cdot A \cos\omega t \cdot B \cos(\omega t + \phi)$$

where: $A \cos\omega t$ - reference signal,

$B \cos(\omega t + \phi)$ - measured signal,

K - factor of proportionality.

From this multiplication one obtains the sum of time-independent component proportional to cosine of phase shift between measured and reference signals and the component being the second harmonic of measured signal. This second component is eliminated by means of filtering action of integrator cascaded with phase detector.

Reduction of the influence of spurious signals is carried out in the integrator by means of compression of frequency band of those signals, Δf_n. Effective band Δf_n is related to time

constant of the integrator with relation

$$\Delta f_n = 1/(4\tau_i)$$

where τ_i - time constant of the integrator. Then for τ_i equal 1 s Δf_n = 1/4 Hz.

Very high selectivity of the system results from this relation and enables in practice to measure the signal of the order of 60 dB below noise level. Additionally results of measurements are averaged in result of the high time constant of the integrator. Averaged signal voltage value is applied to a digital voltmeter and to an output amplifier, where the measured signal is summed with light wavelength markers. The total signal is applied to output with connected X-T plotter.

Technical data of the electronic unit:

Maximum gain - 100 dB, that is equivalent to 2 μV at input for full span indication of the digital voltmeter.

Frequency range - measurement within 6 Hz up to 200 kHz range.

Limit frequency for:

a) high-pass filter 6 Hz up to 384 Hz adjustable in octave bands and 50 kHz, 100 kHz and 150 kHz;

b) low-pass filter 20 Hz up to 1280 Hz adjustable in octave bands and 20 kHz.

Permissible signal-to-noise ratio at input - 40 dB.

Output of measured signal to the plotter and output of the signal prior to detector for displaying the waveform on the oscilloscope.

The idea of the new model of photoacoustic spectrometer with digital data processing is shown on Fig. 30. The optical transmitter and acoustic receiver units of this spectrometer are similar to the previous spectrometer. The difference lies only in the signal processing block.

In this model the data processing block is composed of following units:

- A/D converter,
- multiplexer,
- parallel interface,
- microcomputer IBM-PC compatible,
- graphics printer and plotter as data display units.

The principal features of the digital data processing system are as follows:

- Computes FFT spectra with conveniently selectable analysis parameters;
- Computes the principal wide band signal parameters; RMS, Average, Peak Value, Crest Factor, Form Factor;
- Time history presentation available similarily to the storage scope with selectable time scale;
- Linear or logarithmic spectrum amplitude scales;
- 80 dB spectrum dynamic range;
- Spectrum comparison facility: with earlier current spectrum as well as with preset reference spectrum;
- Special cursor facility allowing exact amplitude, wavelength or time reading;
- Advanced statistical signal analysis procedures available;

- Three-dimensional presentation of spectra sequence, i. e. visualisation of spectra changes as function of time;

- Spectrum zooming facility;

- Data display by the monitor, graphics printer or plotter;

- Can be user operated as well as automatically controlled by preset control procedures;

- Measurement reports available on request.

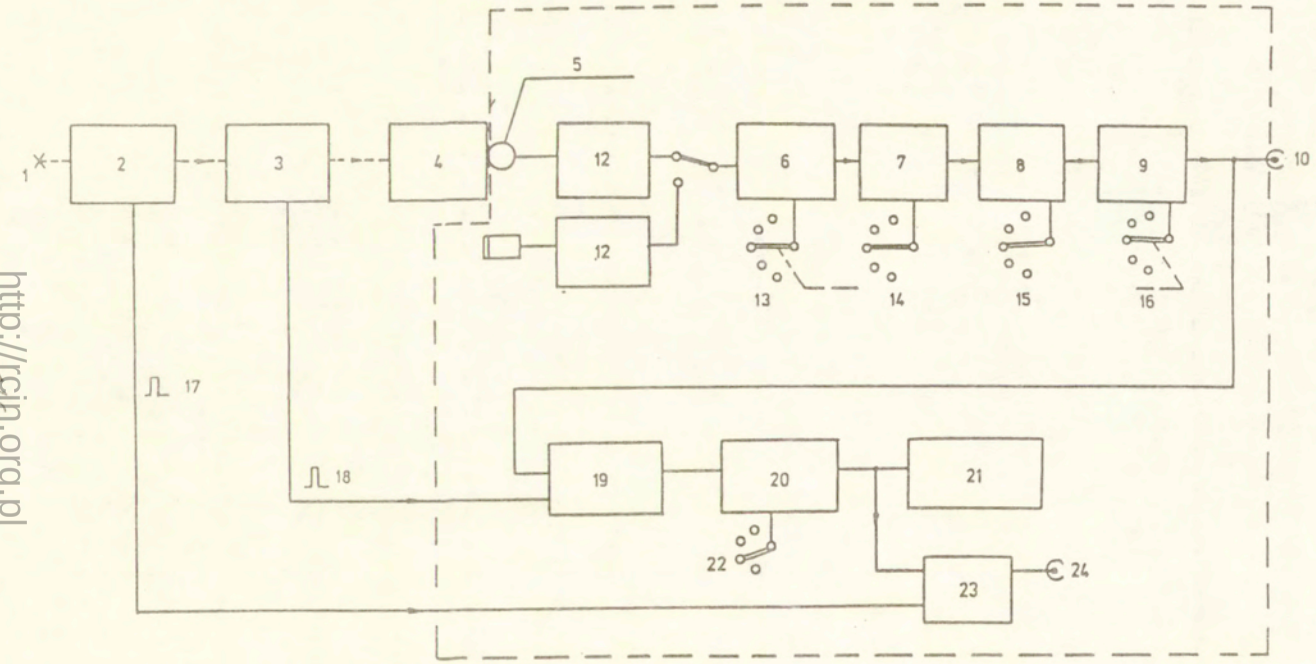

Fig. 29. Apparatus set for measurement of PA effect. *1* — light source; *2* — monochromator; *3* — chopper; *4* — measuring cell; *5* — microphone; *6* — amplifier; *7* — high-pass filter; *8* — low-pass filter; *9* — amplifier; *10* — output to oscilloscope; *11* — piezoelectric head; *12* — preamplifier; *13* — gain; *14* — high limit frequency; *15* — low limit frequency; *16* — gain; *17* — light wavelength markers; *18* — synchronizing pulses; *19* — synchronous detector; *20* — integrator; *21* — digital voltmeter; *22* — time constant; *23* — mixer; *24* — output to plotter

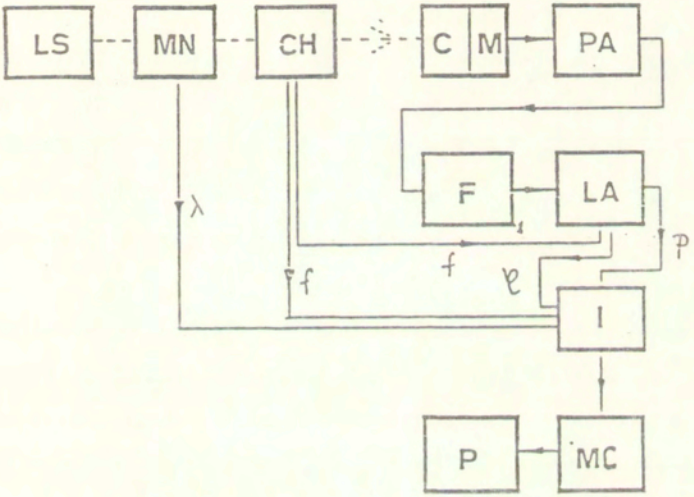

Fig. 30. Block diagram of the PA spectrometer with digital signal processing: LS - light source, MN - monochromator, CH - chopper, C - PA cell, M - microphone, PA - preamplifier, F - filters, LA - lock-in amplifier, I - computer input devices, MC - microcomputer, P - plotter, λ - wavelength, f - frequency, ϕ - phase shift of PAS signal, p - sound pressure (PAS)

CONCLUSION

Data given in the review form from our point of view a complete notion about the state of theoretical photoacoustics of gyrotropic media. Just recently considerable growth of experimental development in photothermodeflectional spectroscopy of media with spatial dispersion takes place. Attained accuracy of measurement of circular dichroism parameter - 10^{-7} of optical density, tracking concentrations of object, decreasing to 10^{-9}M [1819] etc, makes it possible to assert, that method of up-to-date photoacoustical spectroscopy is one of the most sensitive and selective spectroscopy methods. Out looks for its development may be connected with investigation of new nonthermal processes of sound wave generation, for example in gyrotropic semiconductors due to inverse piezoeffect [8] or by means of concentration-deformation mechanism [75].

Development of complementary to already existent and considered to be good methods of photoacoustic signal registration, for example based on the investigation of possibilities of combining photoacoustic spectroscopy of gyrotropic media with reflection ellipsometry.

A number of important practical photoacoustic tasks in optics and acoustics of gyrotropic media is to be solved. We imply here research of photoacoustic transformation in magnetoactive crystal plates, in homogeneous layers and films, linear and nonlinear conductors with magnetic circular dichroism, magnetic liquids, gyrotropic planal and nonuniform waveguides etc.

Till now problems of impulse laser photoacoustical and photodeflectional spectroscopy of naturally gyrotropic and magneto-

active moving or static media. A matter of principle is account of effects of acoustical space dispersion under laser excitation of supershort sound impulses when space extent of picosecond acoustic response can coinside by order with characteristic size of crystal lattice cell.

In conclusion let us draw attention to the fact that we have mentioned only some problems on photoacoustics of gyrotropic media demanding quicker solution. Growing interest to the study of dichroic media by photoacoustic methods, marked stimulation of research allows to make well founded conclusion that photoacoustical, acoustical, thermal methods would give many original and useful results while investigating interaction of radiation with absorbing gyrotropic media.

REFERENCES

1. Rosencwaig A. Photoacoustics and Photoacoustic Spectroscopy-N.Y.1980-309 P.

2. Zharov V.P., Letokhov V.S. Laser acousto-optical spectroscopy M.Science, I984,-320 P.

3. Fedorov F.I. Theory of Gyrotropy Minsk.Science and Technics I976,-456 P.

4. Bokut' B.V., Serdyukov A.N., Shepelivich V.V. Phenomenological Theory of Absorbing Optically Active Media // Opt. and Spectr.I974.v.37.NI.P.I20-I24.,

5. Vellyuz L., Legrane M., Grozhan M. Optical Circular Dichroism M. Mir. I967.-3I8 P.

6. Kizel V.A., Burkov V.I. Gyrotropy og Crystals M.Science.I980,-304 P.

7. Lyamshev L.M. Laser Thermooptical Excitation of Sound M.Science.I989,-238 P.

8. Gusev V.E., Karabutov A.A. Laser acousto- optics M.Science. I99I,-304 P.

9. Mityurich G.S., Zelyony V.P., Serdyukov A.N. Photoacoustic transformation in gyrotropic media at interaction of two light beams// Proc. 5th Spring School on Acousto-Optics and Applications, SPIE, 1992, p.309-318

10. Landau L.D., Liphshits E.M. Electrodynamics in Continuous Media. M.Science.I982,-624 P.

11. Bokut' B.V., Serdyukov A.N., To the PhenomenologicalTheory of Natural Optical Activity //J. of Exp.and Theor.Phys.I97I.v.6I.N5.P.I808-I8I3

12. Bokut' B.V., Girgel S.S. Electromagnetic Waves in Magnetoregulated Crystals with Natural Optical ActivityOpt. and Spectr.I980.v.49.N4.P.738-74I.

13. Agranovich V.N., Ginsburg V.L. Crystalo-optics with Regard to Spatial Dispersion and Theory of Excitons .M.Science I979,-432 P.

14. Bokut' B.V., Mityurich G.S. Determination of Optical Parametersfor Absorbing Gyrotropic Crystals by Photoacoustical Method// Crystallography.I987,v.32,N4,P.962-966.

15. Fournier D., Boccara A.C., Badoz J. Dichroism measurements in photoacoustic spectroscopy .Appl.Phys.Lett.1978.v.32.N10.P.640-642

16. Fournier D., Boccara A.C., Badoz J. Photothermal deflection Fourier transform spectroscopy: a tool for high sensitivity absorption and dichroism measurements// Appl.Opt. 1982.v.21.N1.P.74-76.

17. Ferguson A.I., Ironside C.N. Picosecond photoinduced dichroism detected by photothermal deflection// Proc. SPIE.Int.Soc.Opt.Conf.1983.v.369.P.374-378.

18. Tran C.D., Xu M. Ultrasensitive thermal lens-circular dichroism spectropolarimeter for small volume sample//Rev.Sci.Instrum.1989.v.60.N10.P.3207-3211.

19.Tran C.D., Analytical thermal lens spectrometry: past,present and future prospects.-Springer Series in Optical Soiences.,v.69.,Editor:D.Bicanic. Photoacoustic and Photothermal Phenomena 3. Springer -Verlag.Berlin, Heidelberg.1992.P463-473.

20. Palmer R.A., Roak J.C., Robinson J.C. Photoacoustic detection of natural circular dichroism in crystalline transition metal

complexes//ACS Symp.Ser.: Stereochem.Opt.Act.Transition Met.Comp. 1980.v.119.P.375-395.

21.Howell T.L .Photoacoustic detection of natural circular dichrosm in Solids//In: Topical meeting on photoacoustical spectroscopy .Ames.Iowa.1979.P.Th A3.

22. Willson P.H., Imhof R.E., Birch D.G.S., Webb J.F. Opto-thermal investigation of dichroic materials//Springer Series in Optical Sciences , v.62, Photoacoustic and Photothermal Phenomena 2.Editors: J.C.Murphy, J.W.Maclachan-Spicer, L.Aamodt, B.S.H.Royce. Springer-Verlag Berlin, Heidelberg,1990.P.322-325.

23. Mityurich G.S. Photoacoustical Effect in Optical Activity media //Proc.Acad.Science BSSR.1982.v.26.N5.P.414-417.

24. Tranter K.J. Integration Transformations in Mathematical Physics M.State Techn.Publish.1956-204 P.

25. Mityurich G.S., Starodubtsev E.G. Characteristic Properties of Photoacoustical Signal Formation in Gyrotropic Layer// Opt. and Spectr.1993.v.75.N4.P.789-794.

26. Farrow M.M., Burnham R.K., Auzauneau M., Olsen S.L.,Purdie N., Eiring E.M., Piesoelectric detection of photoacoustic signal// Appl.Opt.1978.v.17.N7.P.1093-1098.

27. Jackson W., Amer N.M. Piezoelectric photoacoustic detection: Theory and experiment//Appl.Opt.1980.v.51.N6.P.3343-3353.

28. Rosencwaig A., Willis J.B. Photacoustic absorption measurements of optical materials and thin films//J.Appl.Phys.1980.v.51.N8.P.4361-4364.

29. Busse G., Rosencwaig A. Thermal wave piezoelectric microphone detection for nondestructive evaluation: a comparison//J.Photoacoust.1982-1983.v.1.N3.P.365-369.

30. Nelson E.T., Patel C.K.N. Response of piezoelectric transducers used in pulsed optoacoustic spectroscopy//Opt.Lett.1981.v.6.N7.P.354-356.

31. Tronconi A.L., Amato M.A., Morais P.C., Neto K.S.Simple model for measurements of the photoacoustic signal by a piezoelectric detector in the microwave region//J.Appl.Phys.1984.v.56.N5.P.1462-1464.

32. Mityurich G.S., Shalupaev S.V. Piezoelectric Detection of Photoacoustical Signal in Gyrotropic Media// J.Th.Ph.1987.v.57.N1.P.114-117.

33. Sirotin Yu.I., Shaskolskaya M.P. The Fundamentals of Crystallophysics M.Science.1979.-640 P.

34. McDonald F.A., Wetsel G.S.Jr. Generalized theory of the photoacoustic effect//J.Appl.Phys.1978.v.49.N4.P.2313-2322.

35. McDonald F.A. Photoacoustic determination of small optical absorption coefficients: extended theory//Appl.Opt. 1979.v.18.N9.P.1363-1367.

36. Strashilov V.L., Konstantinov L.L., Ivanov O. Topographic studies by using a combined photo-acoustoelectric method//Appl.Phys.1987.v.B43.N1.P.17-21.

37. Vinokurov S.A. Non-contact Acousto-Optical Method with Signal Piezoelectric Registration // Letters in J.Th.Ph. 1988.т.14.в.1.с.34-36.

38. Vinokurov S.A. Potentialities of a New Non-Contact Acoust-Optical Method for Signal Piezoelectric Registration// Opt. and Spectr.1988.v.64.P.473-475.

39. Mandelis A., Siu E.K.M., Combined photoacoustic and photoconductive spectroscopic investigation of nonradiative

recombination and electronic transport phenomena in crystalline n-type CdS. 1.Experiment//Phys.Rev.B.1986.v.34.N10.P.7209-7211.

40. Zelyony V.P., Mityurich G.S. Combined Method for Registration of Photoacoustical Signal in Isotropic Media // Letters to J.Th.Ph.1990.v.16.P.44-49.

41. Gulyaev Yu.V., Morosov A.N., Raevsky V.Yu. Photoacoustical Spectroscopy of Optical Non-Transparent Objects with Piezoelectric Detection //Acoust.J.1985.v.31.P.469-474.

42. Matyska S., Matyskova E., Sladky P. Tree dimensional thermoacoustic theory for stratified media a cylindrical photoacoustic cell//Czech. J.Phys.1985.v.B35.N3.P.433-441.

43. Sidorenkov V.V., Tolmachev V.V. Tunnel Interference Effect in Metalic Films // Letters in J.Th.Ph.1989.v.15.P.34-37.

44. Cahen D. Photoacoustic cell for reflection and transition measurements//Rev.Sci.Instrum.1981.v.52.N9.p.1306-1310

45. Fujii Y., Moritani A., Nakai J. Photoacoustic spectroscopy theory for multi-layered samples and interference effect//Jap.J.Appl.Phys.1981.v.20.N2.p.361-367.

46. Helender P., Lundstrom J., Mc Queen D. Photoacoustic study of layered samples//J.Appl.Phys.1981.v.52.N3.p.1146-1151.

47. Morita M. Theory and experiments on the photoacoustic effect in double-layer solids//Jap.J.Appl.Phys.1981.v.20.N5.p.835-842.

48. Mandelis A., Siu E., Ho S. Photoacoustic spectroscopy of thin silicon dioxide films grown on (100) crystalline silicon substrates: A thermal interferometric techniques complementary to optical interferometry//Appl.Phys.A.1984.v.A33.N3.p.153-159.

49. Tilgner R.,Baumann T., Beyluss M. On the influence of thin absorber layers in thermal wave applications//Can.J.Phys. 1986.v.64.N6.p.1287-1290.

50. Campbell S.D., Yee S.S., Afromovitz M.A. Applications of photoacoustic spestroscopy to problems in dermatology reseaarch//IEEE Trans. Biomed. Eng.1979.v.BME-26.N4.p.220-227.

51. Gedrowits Ya.Ya. Photoacoustics and Related Methods Riga.I987-302 P.

52. Mityurich G.S., Sviridova V.V., Serdyukov A.N. Photoacoustic Spectroscopy in Gyrotropic Layered Samples // J.Appl.Spectr.I990.v.54.N4.P.6II-6I7.

53. Coldwell D.T., Eyring H. The theory of optical activity//N.-Y.1971.244p.

54. Eritsyan O.S. Optical Problems of Electrodynamics of Gyrotrpioc Media // U Ph N.I982.v.I38.N4.P.645-674.

55. Hilo N.A., Serdyukov A.N. Electromagnetic Wave Passing through Gyrotropic Layer in a Magnetic Field // J.of Appl.Spectr.I976.v.25.P.169-171.

56. Eremenko V.V., Kharchenko F.N., Litvinenko Yu.G., Nauchenko V.V. // Magnetooptics and spectroscopy of Antiferromagnetics Kiev.Scientific Thought.I989-262 P.

57. Mityurich G.S. Interaction of Electromagnetic Waves with Absorbing Gyrotropic Crystals Diss.of Cand.of Phys.-Math.Sc. Minsk.I984.-I42 P.

58. Mityurich G.S. Photoacoustic Effect in Magnetoactive Media Theses of Papers of 12 All-Union Conference on Acoustoelectrics and Quantum Acoustics Saratov. I983.Part I.P.266-267.

59. Saxe J.D., Foulkner T.R., Richardson F.S. Photoacoustic detection of circular dichroism // Chem.Phys.Lett.1979.v.68.N1. P.71-75.

60. Girgel S.S., Sviridova V.V., Serdyukov A.N. // Proc. of All-. Union Conference "Wave and diffraction-90" M.I990.v.2.P.78-8I.

61. Mityurich G.S., Girgel S.S., Sviridova V.V., Serdyukov A.N. Photoacoustic Transformation in Magnetoactive ε-isotropic Crystals // Proc. "Ultrawave and Laser Methods for Non-Destructive Control", Kiev.1991.P.32-34.

62. Bely V.N., Serdyukov A.N. Linear Influence of Magnetic Field on Optical Activity // Crystallography.I974.T.I9.N6.C.I279-I280.

63. Markelov V.A., Novikov M.A., Turkin A.A. Experimental Observation of a New Non-Reciprocal Magneto-Active Effect // Letters to JThPh.I977.v.25.N9.P.404-407.

64. Mityurich G.S., Philipov V.V. Polarization Reciprocity of Gyrotropic Media // Crystallography. I984.v.29.N5.P.837-840.

65. Mityurich G.S., Zelyony V.P., Sviridova V.V., Serdyukov A.N. Photoacoustic method of the determination of amplitude non-reciprocalness in gyrotropic media// Second Int. Congress on Recent Developments in Air- and Structure-Borne Sound and Vibration. March 4-6. Ausburn.USA.P.845-846.

66. Aamodt L.C., Murphy J.C. Thermal effects in materials with continuously varying otical and thermal properties in one dimension// Can.J.Phys.1986.v.64.p.1221-1229.

67. Iravani M.V., Nikoonahad M. Photothermal wave in anisotropic media//J.Appl.Phys.1987.v.62.N10.P.4065-4071.

68. Lu Yang-Feng Transform of dynamic heat equation in anisotropic media and its application in laser-induced temperature rise//Appl.Phys.Lett.1992.v.61.P.2482-2484.

69. Kaldybaev K.A., Konstantinova A.F., Perecalina Z.B., Grechushnikov B.N., Kalinkina I.N. Optical Activity and Circular

Dichroism of Benzyle // Crystallography.I978.v.23.N4.P.779-787.

70. Vodopyanov K.L., Kulevsky L.A., Malyutin A.A. Properties of Good Quality Modulators with Partial Polarizers // Quantum Electr. I982.v.9.NII.P.2280-2288.

71. Bokut' B.V., Mityurich G.S., Shepelevitch V.V. Absorbing Gyrotropic Crystal in the System of Arbitrary Oriented Elliptical Polarizers // Crystallography. I985.v.30.N3.P.43I-436.

72. Mityurich G.S. Determination of the parameters are absorbtion an dichroism for cristals of midlle synqonies by photoacoustic methods//crystallography. 1991.v36.N1.P.212-213.

73. Konstantinova A.F., Okorochkov A.I., Philipov V.V. Light Passing through Absorbing Optically Active Crystals of Rombic Syngony // Crystallography. I983.v.28.N5.P.845-849.

74. Wetsel G.C.Jr. Photoacoustic effect in piezoelectric ceramic//J.Opt.Soc.Am.1980.v.70.N5.P.471-474.

75. Deev V.N., Pyatakov P.A. Photoacoustic Effect in Photo-conductivity Piezoelectrics //JThPh.I986.v.56.NIO.P.I909-I9I5.

76. Kozlov A.I., Plesky V.P. Excitation Of Acoustic Waves in the Dember Field with Laser Generation of Electronic Doorway Pairs in Piezosemiconductors //Acoust.J.I988.v.34.N4.P.663-666.

77. Gusev V.E., Makarova L.N. Influence of Surface Recombination on Laser Generation of Acoustical Impulses in Piezoelectrics // Acoust.J.I99I.T.37.N4.P.670-68I.

78. Gusev V.E., Makarova L.N. Non-Linear Conditions for Excitation of Longitudinal Acoustical Impulses by Supershort Laser Action in Piezoelectrics //Acoust.J.I992.v.38.N4.P.683-692.

79. Novatsky V. Theory of Elasticity M.Mir.I975-872 P.

80. Mityurich G.S., Zelyony V.P. Photoacoustical Transformation in Gyrotropic Piezoelectric Crystals // Letters to JThPh.1988. v.I4.N20.P.I879-I883.

81. Lyamov V.E. Polarization Effects and Anisotropy of Interection - Acoustic Waves in Crystals M.MGU Publ.I988.-223 P.

82. Parton V.E., Kudryavtsev B.A. Electromagnetic Elasticity of Piezoelectric and Electroconductive Bodies M.Science.I988.-620 P.

83. Mityurich G.S., Zelyony V.P. Thermooptical Excitation of Sound in Non-Linear Piezoelectrics// Crystallography.1991. v.36.N5.P.I250-I253.

84. Mityurich G.S., Zelyony V.P., Serdyukov A.N. Theory of photoacoustic effect in linear and nonlinear gyrotropic piezoelectric crystals //Physical Acoustics. Edited by O.Leroy and M.A.Breaseale . Pergamon Press. New York.1991. P.517-521

85. Mityurich G.S., Zelyony V.P., Serdyukov A.N. Piezophoto-acoustic spectroscopy of gyrotropic layered structures// Photoacoustic and Photothermal Phenomena. Springer Verlag. Berlin-Heidelberg.1991.P.

86. Louis G., Peretti P., Mangeot B., Billard J. Photoacoustic detection of phase transitions in 4-octyl-4'-cyanobiphenil//Mol. Cryst. Liq.Cryst.1985.1985.v.122 p.261-267

87. Marinelli M., Zammit U., Scudieri F., Martellucci S., Bloisi F., Vicari L. Simultaneous heat capacity and thermal diffusivity photoacoustic measurement at liquid-crystal phase transitions// Nuovo Cim.1987.v.9.N7.P.885-862

88. Marinelli M., Zammit U., Scudieri F., Martellucci S. Photoacoustic analysis of first and high-order phase

transitions in 8CB liquid crystal//J.Phys.D.1987.v.20.p.1045-1048

89. Louis G., Peretti P., Mangeot B., Billiard J. Study of thin smectic A samples by a photoacoustic technique//Can.J.Phys.1986. v.64.p.1230-1233

90. Rosencwaig A., Gersho G. Theory of photoacoustic effect with solids//J.Appl.Phys.1976.v.47.N1.P.64-69

91. McDonald F.A., Wetsel G.C.Jr. Generalized theory of the photoacoustic effect//J.Appl.Phys.1978.v.49.N4.p.2313-2322

92. Hadj-Sahraoni A., Louis G., Peretti P., Billard J. Optical properties of cholesteric liquid crystals// Photoacoustic and photothermal phenomena: Proc.5th Int.Top.Meet.,Heidelberg.27-30 July.1987.p.160-161

93. de Zhen P. Physics of Liquid Crystals M.Mir.1977.-400 P.

94. Belyakov V.A., Sonin A.S. Optics of Cholesteric Liquid Crystals M.Science.1982.-360 P.

95. Kats E.N. Optical Properties of Liquid Cholesteric Crystals// JThPh.1970.v.59.N5(II).P.1854-1861.

96. Bely V.N., Serdyukov A.N. Theorry of Propagation of Electromagnetic Waves in Twisted Crystals//Prac. Acad. Science BSSR.1974.v.18.N5.P.402-404.

97. Semchenko I.V., Serdyukov A.N. Influence of Molecular Gyrotropy on Light Propagation in CLC //Prac. Acad. Science BSSR. 1982.v.26.N3.P.235-237.

98. Mityurich G.S., Semchenko I.V. Photoacoustical Interaction in CLC// Proc. Acad. Science BSSR.1983.v.27.N.7.P.609-612.

99. Mityurich G.S., Zelyony V.P., Semchenko I.V., Serdyukov A.N. Investigation of cholecteric liquid crystals in the Bragg reflection region by photoacoustic method// Ultrasonics

International-91: Confer.Proc.1-4 July 1991. P.147-151

100. Mityurich G.S., Zelyony V.P.,Semchenko I.V., Serdyukov A.N. Photoacoustic Spectroscopy in Holesteric Liquid Crystals//Opt.and Spectr.1992.v.72.N2.P.428-433.

101. Lyamshev L.M., Naugolnyh K.A. Optical Generation of Sound. Non-Linear Effects// Acoust.J.1981.v.27.N5.P.641-668.

102. Avanesyan S.M., Gusev V.E., Zhdanov V.V. and others Non-Linear Conditions for Optical Excitation of Relay Waves in Silicon, Thermoelastic and Concentration-Deformation mechanisms// Letters to JThPh.1986.v.12.N17.P.1067-1071.

103. Conghuan Du. Nonlinear theory of photoacoustic effect//11 международный симпозиум по нелинейной акустике: Тез.докл.Новосибирск.1987.т.1.с.350-354.

104. Bokut' B.V., Serdyukov A.N. Light Waves Frequency Transformation in Optically Active Media //J. Appl. Spectr.1974.т.12.N1.с.65-71

105. Batog V.N., Burkov V.I., Kizel V.A. Non-Linear Optical Properties of Monocrystals of Sillenite Type // Crystallography 1971.v.16.N5.P.1044-1045.

106. Bokut' B.V., Serdyukov A.N., Fedorov F.I. Electrodynamics of Optical Active Media // Preprint og IPh Acad. Science BSSR.Minsk. 1970.-36 P.

107. Blistanov A.A., Bogdarenko V.S., Perelomova N.V. and others Acoustic Crystals. Directory .M.Science.1982.632 P.

108. Burkov V.I., Kargin Yu.F., Kisel V.A. and others. Circular Dichroism in the Regions Conditioned by Vacancies in Crystals of Sillenite Type//Letters to JthPh.1983.v.38.N7.P.326-328.

109. Mityurich G.S. Photoacoustic Transformation in Non-Linear

Crystals of Sillenite-Type.//JThPh.1989.v.59.N9.P.118-122.

110. Mityurich G.S., Zelyony V.P., Serdyukov A.N. Photoacoustic transformation in nonlinear gyrotropic piezoelectric crystals//Proc.6th Inter .Conf."Acoustoelectronics'93" Sept.19-25.Varna.Bulgaria.1993.p.46

111. Girgel S.S., Demidova T.V. Electromagnetic Waves Frequency Transformation in Crystal with Central Symmetric Paramagnetic Phase//Opt. and spectr. 1987.v.62. N1.P.101-104.

112. Aktsipetrov O.A., Braginsky O.V., Esikov D.A. Non-Linear Optics of Gyrotropic Media: GVG in Rare Earth Ferrit-Garnets// Quantum Electr.1990.v.17.N3.P.320-324.

113. Mityurich G.S., Zelyony V.P., Demidova T.V., Serdyukov A.N. Photoacoustic transformation in nonlinear crystals with central symmetrical paramagnetic phase//Ultrasonics International'93 Confer. Proc. 6-8 July.Vienna.Austria.1993.P.54.

114. Boccara A.C., Fournier D., Badoz J. Thermooptical spectroskopy: Detection by the "mirage" effect// Appl.Phys.Lett. 1980.v. 36.N2.p.130-132

115. Jackson W.B., Amer N.M., Boccara A.C., Fournier D. Photothermal deflection spectroscopy and detection//Appl.Opt.1988.1981.v.20.N8.p 1333-1344

116. Vyas R., Monson B., Nie Y-X., Gupta R. Continuous wave photothermal deflection spectroscopy in a flowing medium//Appl.Opt.1988.v.27.N18.p.3914-3920

117. Zuev V.V., Mechtiev M.M., Muchin D.O., and others Impulse Photodeflection Spectroscopy of Semiconductors: Theory and Experiment. // Preprint 031-90 .M.MIFI.1990.-23 P.

118. Mityurich G.S., Astakhov P.V. Photodeflection spectroscopy of the flowing gyrotropic media//Proc.5th. Spring School on Acousto-Optics and Applications. SPIE v. 1844 (1992) p. 300-308.

119. Ringermacher H.I., Heyman I.S. Observation of a sono-acoustic effect using piezoelectric thermo-acoustic detection//Ultrasonics Symp. Proc. Chikago.Oct.14-16.1981.New York.1981.v.1.p.840-843

120. Andronov A.A. Natural Rotation of Sound Polarization Plane// Izvestiya Vusov. Radiophysics.I960.v.3.N4.P.645-649.

121. Bryksina M.F., Esayan S.H., Lemanov V.V. Investigation of Acoustic Activity in Crystals by the Bragg Light Dispersion Method//Letters to JThPh.I977.v.25.NII.P.5I3-5I6.

122. Serdyukov A.N. Circular Dichroism in Acoustics of Crystals with Spatial Dispersion// Crystallography.I977.T.22.N3.C.459-462.

123. Mityurich G.S. Shalupaer S.V.Generation of thermoelasticity waves of sound beams in absorbing acoustic gyrotropic media.//Proc. Acad. Sci. BSSR.1987.V.31.N6. P.515-518.

124. Motylewski J., Ranachowski J., Rzeszotarska J., [In:] Selected methods for liquids and polymers investigation, p. 183, IFTR, Warsaw 1979 (in Polish).

125. Motylewski J., Ranachowski J., Rzeszotarska J., [In:] Electrical and acoustic methods for dielectric materials investigation, p. 205, IFTR, Warsaw 1980 (in Polish).

126. Motylewski J., Ranachowski J., Investigation of physical and chemical properties of materials by means of photoacoustical and acoustoelectrical spectroscopy, IFTR Reports No. 37, Warsaw 1983 (in Polish).

127. Motylewski J., Ranachowski J., Photoacoustic spectroscopy as a method in biological investigations, Archives of Acoustics 8 (1-2), 51 - 56 (1984).

128. Adamczyk E., Ranachowski J., Rzeszotarska J., Photoacoustic spectrometer PAS 10, Nauch. Apparat. 2, 2, 3 - 14 (1987).

129. Motylewski J., Photoacoustic spectrometer with digital data processing, Proc. of 4th Spring School on Acoustooptics and Applications, Gdansk 1989, pp. 377 - 382, World Scientific Publishing Co., Singapore 1990.

130. Malecki I., Ranachowski J., Rzeszotarska J., Photoacoustic and photothermal spectroscopy, Proc. of 4th Spring School on Acoustooptics and Applications, Gdansk 1989, pp. 175 - 192, World Scientific Publishing Co., Singapore 1990.

131. Ranachowski J., Motylewski J., Rzeszotarska J., Opydo W., Photoacoustic cells for liquids and solids investigation, Proc. SPIE vol. 1844 Acousto-Optics and Applications, pp. 271 - 276 (1992).

132. Motylewski J., Marasek K., Time-frequency analysis of pulsed photoacoustic signals, Proc. SPIE vol. 1844 Acousto-Optics and Applications, pp. 265 - 270 (1992).

ACKNOWLEDGEMENTS

The authors wish to express their thanks to Prof. A. N. Serdyukov for helpful comments on first chapter of this review. Special thanks are due V. P. Zelyony, E. G. Starodubtsev, P. V. Astakhov from Photoacoustic Spectroscopy Laboratory in Gomel State University for creative cooperation in obtaining presented results, and I. W. Yefremchenko, I. M. Akulov, E. A. Rachragovich for skilful assistance in the preparation of this paper. Finally, our thanks go to J. Rzeszotarska and E. Adamczyk from IFTR Warsaw for their help during the measuring stands design.